Endurance Array Site Characterization:
Oceanographic and Environmental Constraints

Control Number: 3205-00007

Version: 1-02

Date: February 25, 2011

Prepared by: E. Dever, C. Risien, J. Barth, and R. Collier

Document Series:

CGSN Endurance Array Site Characterization	document control #
Endurance Array Site Characterization: Bathymetric Surveys.	3205-00006
Endurance Array Site Char.: Oceanogr. and Environ. Constraints	**3205-00007**
Endurance Array Site Characterization: Site Design	3205-00022

Coastal and Global Scale Nodes

Ocean Observatories Initiative

Woods Hole Oceanographic Institution
Oregon State University
Scripps Institution of Oceanography

Revision History

Version	Description	Originator	ECR No.	Release Date
1-02	Initial Release	E. Dever	1303-00217	25 Feb 2011

Table of Contents

List of Figures

List of Tables

CGSN Site Characterization: Endurance Array

1. Scope

This document series describes surveys to determine the conditions on the sea floor and surrounding environment of the OOI's Endurance Array coastal observatory (Figure 1). This document #3205-0007 “Endurance Array Site Characterization: Oceanographic and Environmental Constraints”, combined with document, #3205-0006 “Endurance Array Site Characterization: Bathymetric Surveys”, which describes the seafloor features surveyed as part of a significant new OOI-funded effort, form the input for the final site design of the Endurance Array (#3205-00022), describing the locations and infrastructure at these sites that have been designed to be in place for the next decades of this Pacific North West Coastal Observatory.

2. Overview

The Endurance Array is a multi-scale array utilizing fixed and mobile assets to observe cross-shelf and along-shelf variability in the coastal upwelling region of the Oregon and Washington coasts, while at the same time providing an extended spatial footprint that encompasses a prototypical eastern boundary current regime and overlaps the RSN cabled infrastructure. In order to provide synoptic, multi-scale observations of the eastern boundary current regime, two cross-shelf moored array lines, each with three instrumented sites, are supplemented by six gliders patrolling the coastal region. The Endurance Array is composed of two lines of moorings: **the Oregon Line** (also called the Newport Line) and **the Washington Line** (also known as the Grays Harbor Line). See Figure 1, Figure 2 and Figure 3 as well as Table 1 and Table 2 below.

Table 1. OR Endurance Array Candidate Locations – December, 2010.

OR Inshore	(CE01IS)	uncabled	44° 39.00'N – 124° 06.00'W	(nominal 25m)
OR Shelf	(CE02SH)	cabled	44° 37.97'N – 124° 18.21'W	(nominal 80m)
primary node	(PN1D)	cabled	44° 41.48'N – 124° 27.42'W	(nominal 113m)
OR Offshore	(CE04OS)	cabled	44° 22.49'N – 124° 57.76'W	(nominal 585m)

Table 2. WA Endurance Array Candidate Locations – December, 2010.

WA Inshore	(CE06IS)	uncabled	47° 08.00'N – 124°17.13'W	(nominal 25m)
WA Shelf	(CE07SH)	uncabled	46° 59.17'N – 124°33.98'W	(nominal 80m)
WA Offshore	(CE09OS)	uncabled	46° 51.50'N – 124°58.00'W	(nominal 570m)

The final locations and infrastructures at these sites will be discussed in the Site Design document of this series (3205-00022).

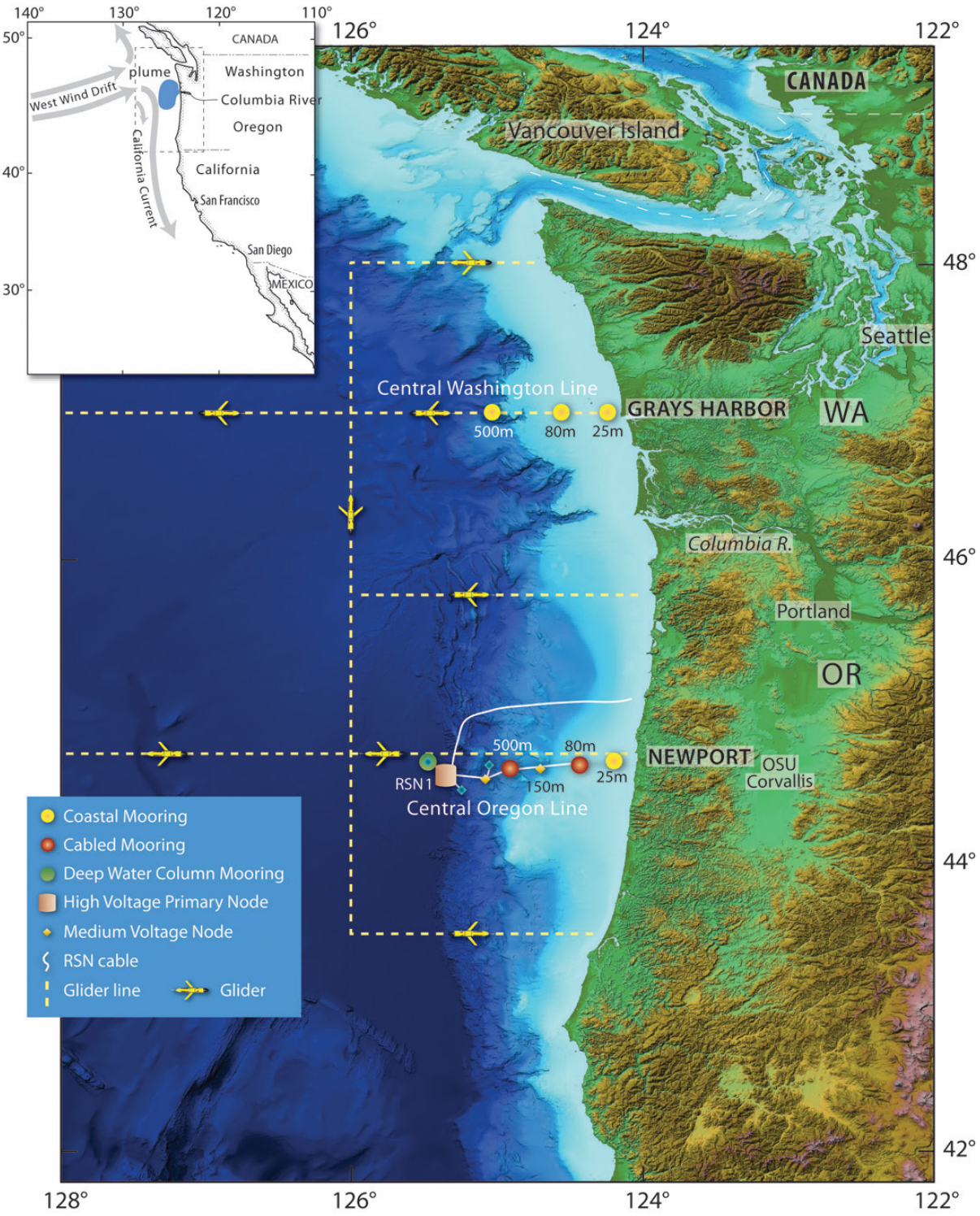

Figure 1. Plan view map of the Endurance Array, including the *nominal* locations of the Oregon and Washington Lines (final locations vary). Also shown are the connection to the RSN cabled infrastructure (at the 80 m and 500 m sites) and regional coverage provided by six gliders.

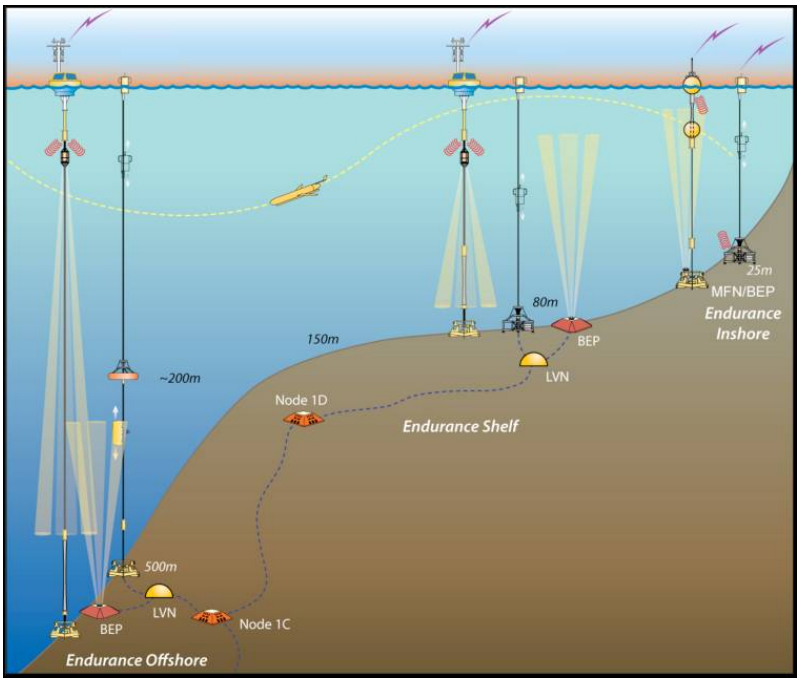

Figure 2. Endurance OR cross-section, including cabled infrastructure.

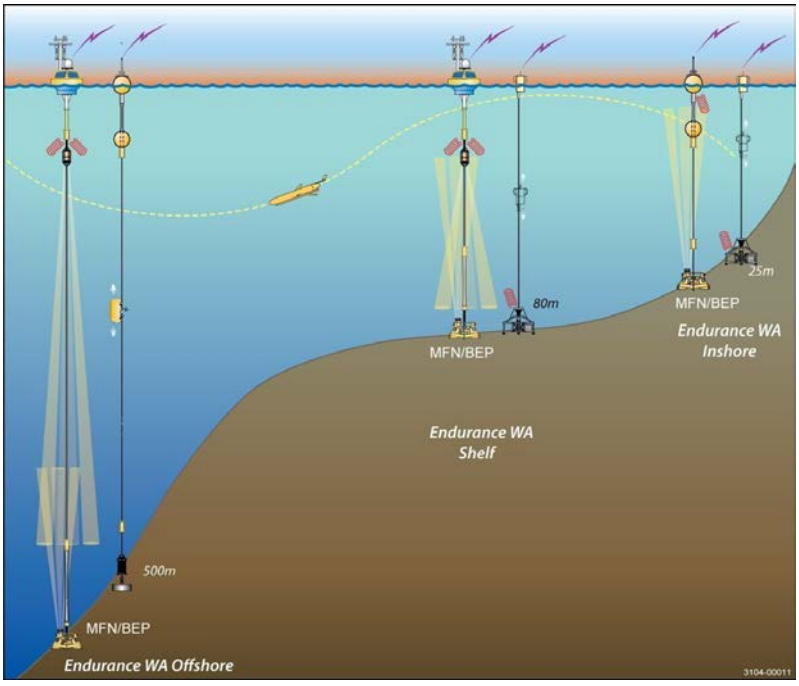

Figure 3. Endurance WA cross-section (no cabled infrastructure).

3. Oceanographic and Environmental Constraints

3.1. Oceanographic Conditions

3.1.1 Overview

The region offshore of Oregon, Washington and British Columbia contains the northern portion of the California Current System (CCS), the eastern boundary current of the North Pacific subtropical gyre. The ocean off the Pacific Northwest (PNW) responds to physical forcing events occurring on a wide range of spatial and temporal scales. Water and suspended material are transported eastward by the North Pacific Current (West Wind Drift) which splits to contribute to both the CCS to the south and to the subpolar gyre to the north (Figure 1, Appendix B). These large-scale currents are modulated by climate variability, in particular on decadal (10-40 years) time scales, with profound consequences for the local and global ocean ecosystem (Figures 5 and 6, Appendix B). The continental margin – the region from the coast out over the continental shelf and slope and into the adjacent deep ocean as far as coastal water properties extend – off the PNW is also strongly influenced by dynamic interannual variability (1-3 years) (Figure 7, Appendix B). Interannual variations in the coastal ocean wave guide and atmospheric teleconnections originating in the equatorial Pacific can also have dramatic consequences for the local ocean ecosystem.

The coastal oceans off the Pacific Northwest are prototypical wind-driven upwelling and downwelling ecosystems with strong seasonal variations in flow direction and primary productivity. Local production during the spring and summer is fueled by the upwelling of deep, nutrient-rich water during wind events lasting 2-20 days (the “weather band”) (Figure 2, Appendix B). Flow-topography interaction (Figure 8, Appendix B) and the influence of buoyancy input from the two major freshwater inputs to PNW waters, the Columbia River (Figures 3 and 9, Appendix B) and flow through the Strait of Juan de Fuca (primarily the Fraser River) also influence currents.

The regional oceanography of the PNW continental margin is influenced by the bifurcation of the North Pacific Current, and by the seasonally varying, strong north-south boundary currents: the California Current, the California Undercurrent and the Davidson Current (Figure 1, Appendix B). The California Current is a surface-intensified, equatorward current that can reach speeds of 0.5–1.0 m s^{-1} and extends into the water column down to 500–1000 m. The California Undercurrent is a subsurface poleward current with a core at 200 m and an average speed of 0.15 m s^{-1}. The Davidson Current is a strong (up to 1 m s^{-1}) poleward, surface-intensified flow found over the continental shelf and slope in winter. The eastern boundary currents exhibit variability from the 2–5-day event time scale through the seasonal scale to interannual (El Niño/La Niña) and interdecadal [Pacific Decadal Oscillation (PDO)] scales. The California Undercurrent extends along the upper continental slope of the entire US west coast and is relatively difficult to observe given its subsurface nature. This large-scale feature transports warm, high-salinity, nutrient-filled water and planktonic organisms hundreds to thousands of kilometers along the coast (Collins, et al, 2000). The undercurrent transport responds to interannual variability (Huyer et al., 2002) and provides a portion of the high-nutrient source water that is upwelled seasonally onto the continental shelves. In spite of these important attributes, long term (> a few months) measurements in the undercurrent are almost nonexistent.

Wind forcing also has important effects on the Washington and Oregon shelves. The wind-driven ocean response includes cross-shelf Ekman transport and the resulting along-shelf transport and upwelling. Current velocities over the shelf are polarized in the along-shelf direction. The weaker cross-shelf current velocities exhibit responses that mainly depend on the surface and bottom Ekman transport as well as a noisy and unpredictable interior cross-shelf component (Smith, 1981).

Moored oceanographic time-series have been acquired on the Oregon and Washington shelves on many occasions since the early 1970's. Most time-series have been acquired during the spring and summer upwelling seasons. Historical programs include Department of Energy sponsored programs along the Washington coast (Hickey, 1989) and the Coastal Upwelling Ecosystems Analysis (CUEA) program along the Oregon coast (Halpern et al., 1974; Smith, 1981). Much of the digitized data from these deployments is inaccessible, but summary statistics and plots of the data are available in technical reports and journal articles (Hickey, 1989; Smith, 1981) Some of the more recent time series include the NSF-funded Coastal Advances in Ocean Transport (COAST) and River Influences on Shelf Ecosystems (RISE) time series, and the NOAA/NSF-funded Ecology and Oceanography of Harmful Algal Blooms program (ECOHAB).

The COAST moorings included measurements made over the Oregon shelf north of the Newport line in a variety of water depths. Data as well as the data report are available online at http://damp.coas.oregonstate.edu/coast/moorings.shtml and http://damp.coas.oregonstate.edu/coast/moorings/coast01_mooring_report.pdf respectively. The RISE moored measurements included measurements made at 80 m water depth off Grays Harbor in the spring and summer and 2005 and 2006. Data are available online at http://www.ocean.washington.edu/rise/data.html. The ECOHAB moored measurements http://coast.ocean.washington.edu/ECOHAB_Data_rep/ECOHABa-1.htm include data from 2003 – 2006 over the Washington shelf near Grays Harbor and elsewhere. The NANOOS NH-10 mooring has been in operation since mid-2006. A subset of the NH-10 dataset is available at http://www.nanoos.org/nvs/. The locations of the COAST, RISE, ECOHAB, NANOOS NH-10, and GLOBEC moorings are shown in Figure 4. The mean for May – October 2005 and 2006 at the RISE Grays Harbor mooring is shown in Figure 5. During these months this location experiences southerly flow throughout the water column. Current velocities of approximately 9 cm s^{-1} are observed at 2.5 m decreasing to about 1 cm s^{-1} at 65.5 meters.

Despite the repeated process studies, few long-term (single or multi-year) time-series exist. Moreover, most moored time-series have been acquired over the mid-shelf with relatively little data acquired over the inner-shelf (water depth < 35 m or so) or over the slope (water depth > 200 m). One exception is the GLOBEC moored Acoustic Doppler Current Profiler data acquired by Mike Kosro off of Newport Oregon at the proposed Endurance 80 m mid-shelf site since October 1997 (http://bragg.coas.oregonstate.edu/NH10/). Near the same site, current meter data have also been acquired since July 2006 as part of the NOAA-funded Northwest Association of Networked Ocean Observing Systems (NANOOS) program (http://www.nanoos.org/). Figure 6 shows the mean flow for July 2006 through February 2010 at NH-10. This location experiences, on average, southerly flow throughout the water column. Current velocities of approximately 14 cm s^{-1} are observed at 10 m decreasing to 3.5 cm s^{-1} at depth.

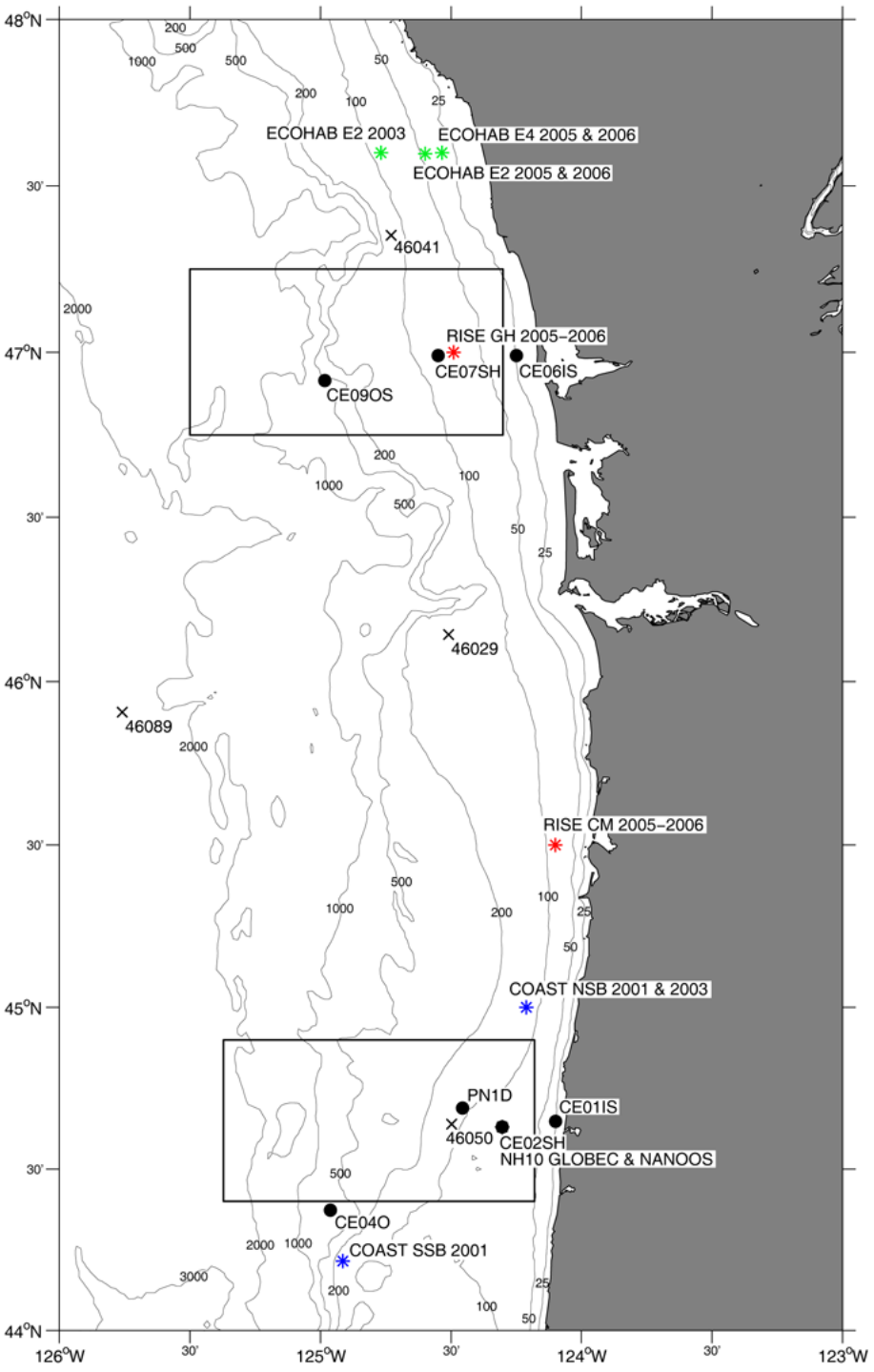

Figure 4. Locations of the NH-10, RISE, COAST, ECOHAB and proposed OOI moorings, as well as the bounding boxes for the Newport and Grays Harbor hydrographic lines.

3.1.2 Current Profiles

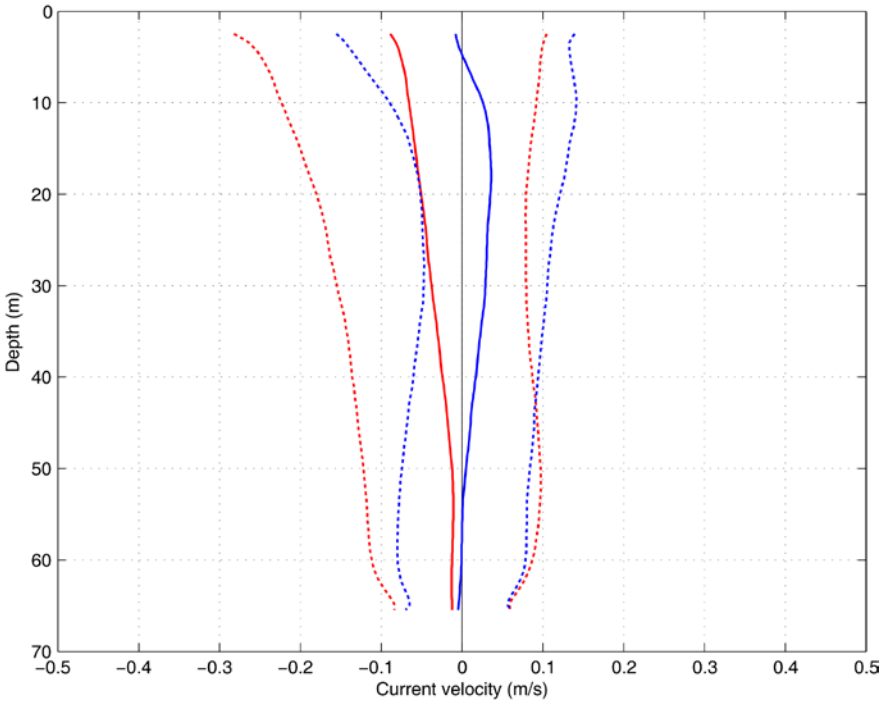

Figure 5. Mean flow for May – October 2005 and 2006 (solid lines) plus and minus one standard deviation (dotted lines) at the RISE Grays Harbor mooring in the eastward (blue) and northward (red) directions.

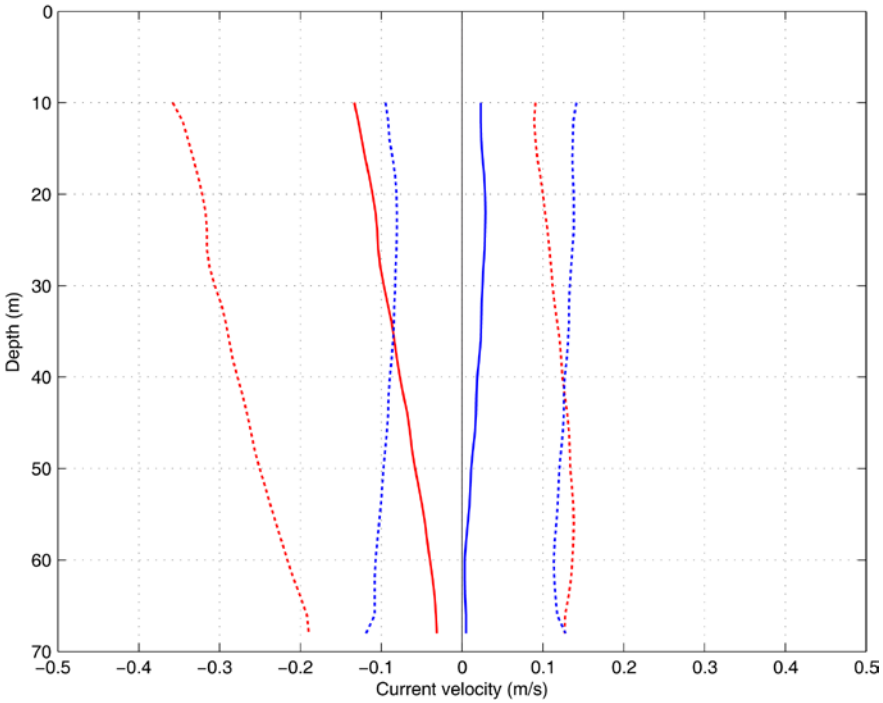

Figure 6. Mean flow for July 2006 – February 2010 (solid lines) plus and minus one standard deviation (dotted lines) at the NH-10 mooring in the eastward (blue) and northward (red) directions.

3.1.3 Tidal Variability

The existing current profiles are more than sufficient to characterize barotropic tidal variability over the shelf. Internal tidal variability is much more local and difficult to predict. However, data assimilating models exist for the Oregon shelf (Kurapov et al, 2003).

The narrowness of the Oregon coastal shelf (30–50 km wide) ensures that the internal tide retains its energy as it moves towards the coast, increasing spatial and temporal variability in currents, mixing, and productivity. The maximum M2 tidal current can be 15 cm s^{-1} or more, while barotropic currents are typically about 5 cm s^{-1} or less (Hayes and Halpern 1976; Torgrimson and Hickey 1979; Erofeeva et al. 2003). Internal tides in coastal waters exhibit spatial variability on the kilometer scale and temporal variability on the scale of days. The high variability may be due to the spring–neap cycle, changes in the stratification, or changes in low-frequency background currents resulting from surface heat flux or wind forcing. Strong vertical mixing near the coast can cause the baroclinic tidal current to lose strength (Hayes and Halpern 1976). This causes significant seasonal variation, with internal tides becoming much weaker in winter (Erofeeva et al. 2003).

3.1.4 Spatial and Temporal Scales in Frontal Regions

In the CCS, ocean fronts on the scale of 20 -100 km are typically associated with wind-driven coastal upwelling and downwelling (Barth, 1994). Beyond the region directly influenced by coastal upwelling lies the Coastal Transition Zone (Brink and Cowles, 1991), a region inhabited by long filaments of cold water that often originate closer to the coast and, in some cases, originate at coastal capes that may serve as upwelling centers. These features filaments, which can have 50- to 300-km length scales and 4- to 18-week temporal scales (Keister and Strub, 2008), possess frontal boundaries that separate them from the surrounding offshore waters. Castelao et al. (2006) show that SST fronts reveal the seasonal evolution of coastal upwelling, as well as meanders and filaments that are often linked with irregularities in coastline geometry. These authors find that winter is characterized by low frontal activity along the US west coast with fronts first appearing close to the coast during spring, particularly south of Cape Blanco, where upwelling favorable winds are already persistent. Frontal activity continues to increase during summer, especially between Monterey Bay and Cape Blanco, extending more than 300 km from the coast. During fall, the weakening of upwelling favorable winds leads to a gradual decrease in frontal activity (Castelao et al., 2006).

Near the coast in shallow water where the influence of bottom topography may be strong, fronts can be associated with major bathymetric features, particularly along the continental margin (Holladay and O'Brien, 1975). In addition, small scale fronts may be associated with estuarine/river discharge (Kilcher and Nash, 2010).

Recently, the role of tidally generated internal bores and nonlinear internal waves, on material transport, mixing and the subsequent ecosystem response has become apparent (Klymak and Moum, 2003; Figs. 13 and 14, Appendix B).

3.1.5 Stratification

3.1.5.1 Climatological profiles

So as to characterize stratification in the vicinity of the Endurance array monthly climatalogical profiles of physical oceanographic variables were downloaded from the World Ocean Atlas (WOA). Gridpoints at which profile data are available are spaced at 1 degree in both latitude and longitude. WOA profiles used for this evaluation are centered at 47°N, 124.5°W and 44.5°N, 124.5°W. In the vicinity of the Grays Harbor hydrographic line (Figure 7) and the Newport hydrographic line (Figure 8) the water column is most stratified, on average, in August, and least stratified in February. Comparing WOA hydrographic profiles from these two months for the Grays Harbor and Newport hydrographic lines shows that most of the annual variability occurs in the upper 50 m. At the surface, the temperature change is about +6 (+5.5) °C and the salinity change is about +0.7 (-0.3) PSU from February to August for the Grays Harbor (Newport) hydrographic lines. Monthly profiles of potential temperature, salinity, and potential density at 47°N, 124.5°W and 44.5°N, 124.5°W are plotted in Figure 9 and Figure 10, respectively. The climatology suggests that temperature inversions are common in the upper 100 m off Oregon and Washington from January through March. Additional discussions of seasonal stratification over the Oregon and Washington shelves are contained in Landry & Hickey (1989).

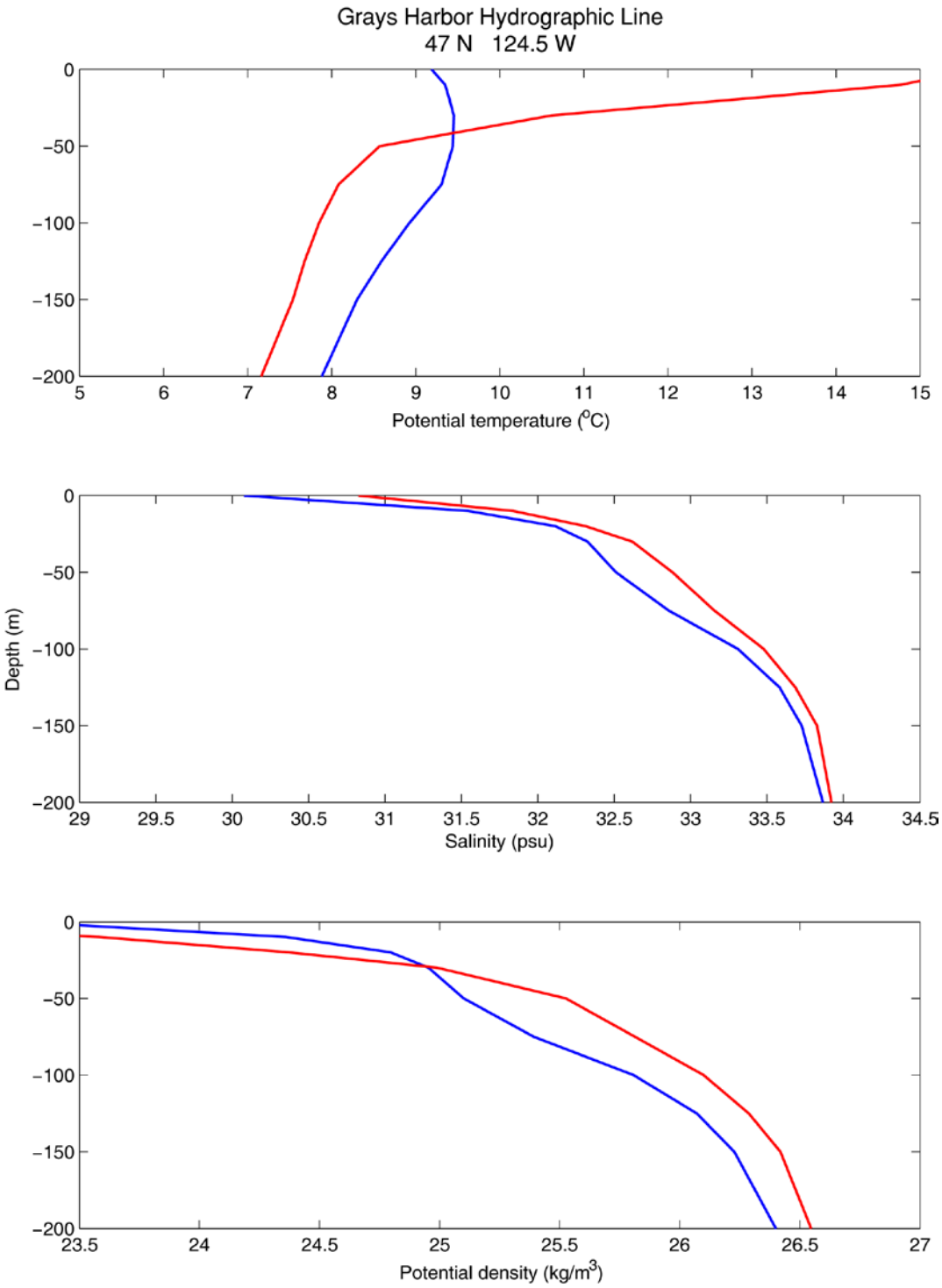

Figure 7. Climatological hydrographic profiles for February (blue) and August (red) from the World Ocean Atlas at 47°N, 124.5°W.

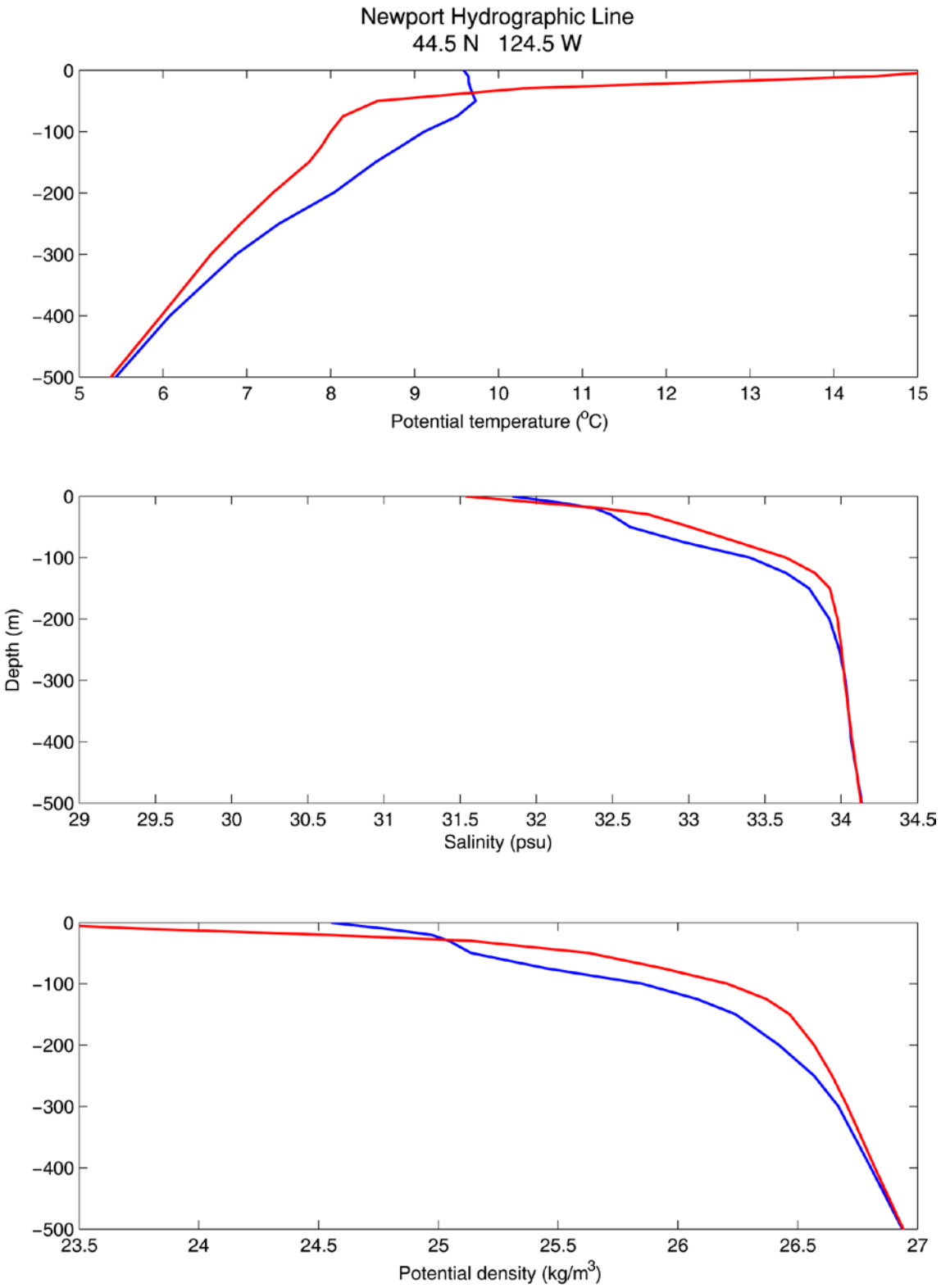

Figure 8. Climatological hydrographic profiles for February (blue) and August (red) from the World Ocean Atlas at 44.5°N, 124.5°W.

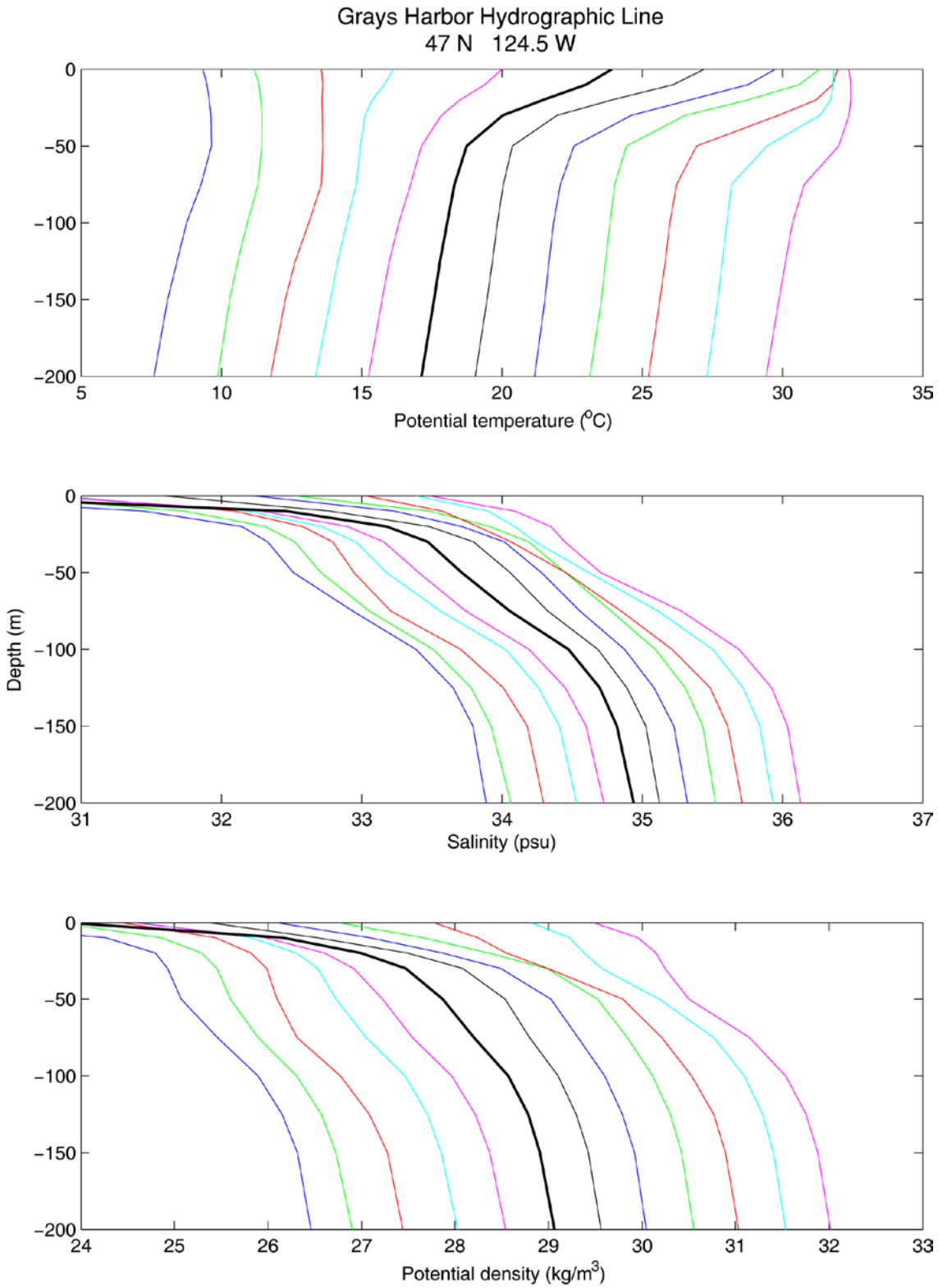

Figure 9. Climatological profiles of (top) potential temperature, (center) salinity, and (bottom) potential density for 47°N, 124.5°W. One profile is plotted for each month, with January on the left. The x-axis labels correspond to the June profiles (bold, black lines), with each successive month offset by 2°C (*top*), 0.2 psu (*center*), and 0.5 kg/m^3 (*bottom*).

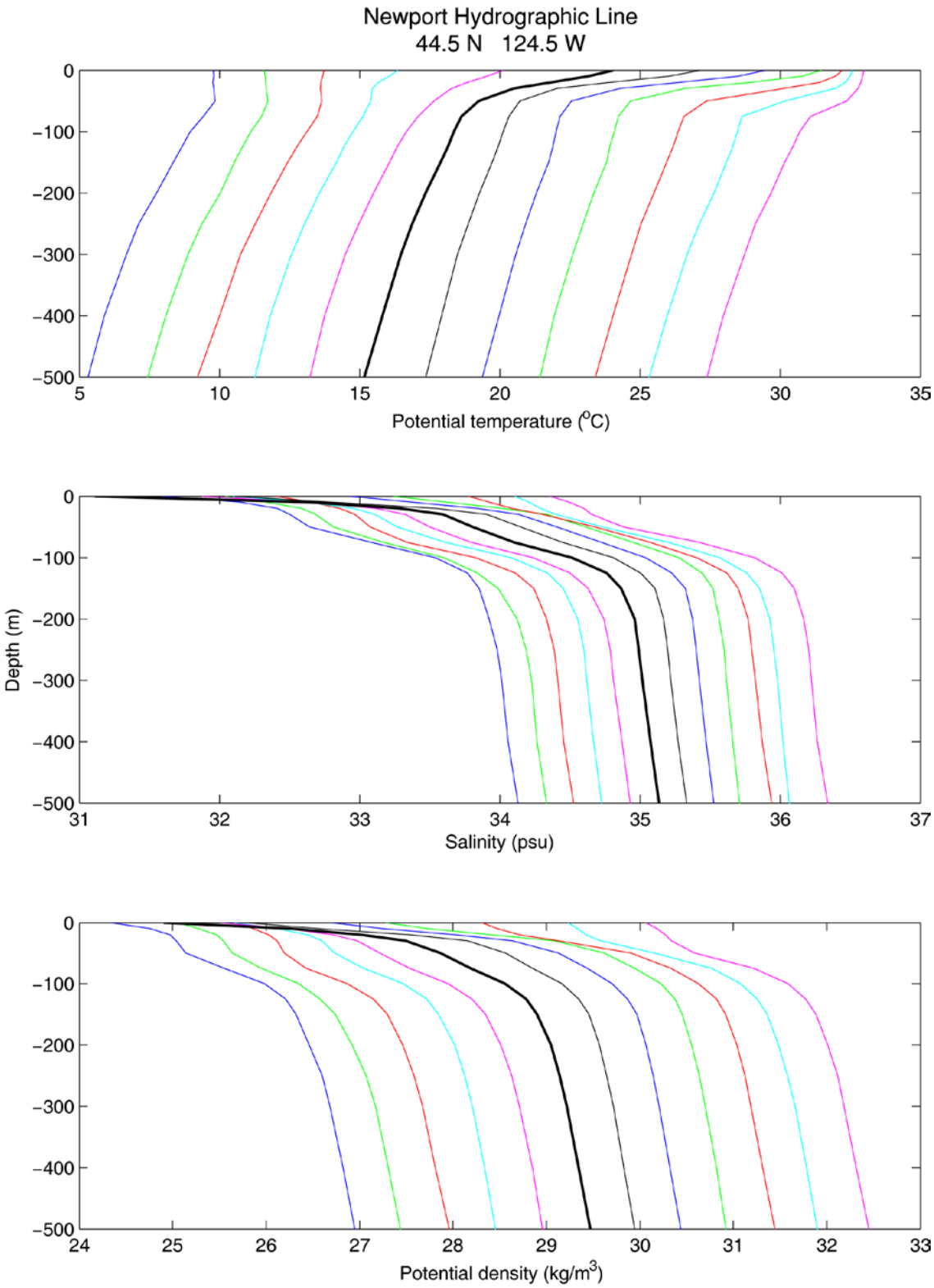

Figure 10. Climatological profiles of (top) potential temperature, (center) salinity, and (bottom) potential density for 44.5°N, 124.5°W. One profile is plotted for each month, with January on the left. The x-axis labels correspond to the June profiles (bold, black lines), with each successive month offset by 2°C (top), 0.2 psu (center), and 0.5 kg/m^3 (bottom).

3.1.5.2 Interannual and decadal variability

Changes in the physical and biological properties of the California Current System (CCS) occur on time scales that range from seasonal (described above) to interannual (e.g., Chelton, 1982; Huyer and Smith, 1985; Strub and James, 2002; Huyer, 2003; Legaard and Thomas, 2006), to decadal (McGowan et al., 1996, 1998; Mantua et al., 1997; Di Lorenzo et al. 2008). On interannual time scales of 5-7 years the CCS is primarily influenced by the El Niño-Southern Oscillation (ENSO). During El Niño events the upper water column typically warms by 1.5°C and the thermocline strengthens and deepens (Figure 11) (McGowan et al. 1998). These changes reflect weaker coastal upwelling, less wind mixing, and a compensating adjustment in alongshelf transport that results in less southward flow, which leads to further warming. In addition, during certain events coastally trapped Kelvin waves, which may be connected to equatorial Kelvin waves, also contribute to a depressed thermocline (Schwing et al., 2005). These physical changes to the CCS act to reduce nutrient input to surface waters and lower plankton biomass (Kahru and Mitchell 2000; Bograd and Lynn 2001), and alter production and distribution of many important fish stocks and marine mammals (Chavez et al. 2002; and papers therein). During La Niña events the response is reversed but weaker, and SST anomalies are typically cooler by 1°C (McGowan et al. 1998).

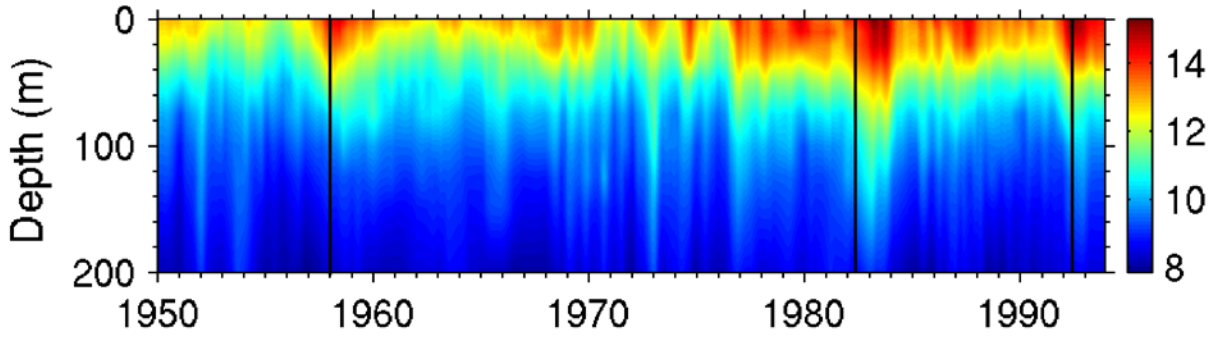

Figure 11. Monthly time series of 0-200 m temperatures from a 1° box centered at 36.5°N, 123.5°W. Vertical lines mark the approximate times that the El Niño events of 1957-58, 1982-83 and 1991-92 impacted the California Current. Figure reproduced and edited from Schwing et al. [2005].

CCS variability on the scale of decades is associated with changes in phase of the Pacific Decadal Oscillation (PDO; Mantua et al. 1997) and the North Pacific Gyre Oscillation (NPGO; Di Lorenzo et al. 2008). The PDO and NPGO are the two dominant modes sea surface temperatures (SST) and sea level height (SSH) variability (Chhak et al., 2008) in the north Pacific and are forced by changes in the Aleutian Low (AL) and the North Pacific Oscillation (NPO) (Mantua et al., 1997; Di Lorenzo et al. 2008; Chhak et al., 2008) respectively.

Shifts in the PDO and the NPGO can significantly impact the CCS. For example during the period 1976–1977 the PDO shifted from its cool (negative) phase to its warm (positive) phase (Mantua et al., 1997). This shift resulted in the CCS becoming warmer and more stratified, causing upwelling to be less effective (McGowan et al., 2003). Di Lorenzo et al. (2008) show that interannual and decadal variations of salinity, nutrient upwelling, and surface chlorophyll-a in the Northeast Pacific, including the CCS, are associated with changes in the NPGO.

3.1.5.3 Short-term variability

Over the continental shelf, wind forcing and river buoyancy influences stratification in well-known ways.

Over the Washington shelf, the year round influence of the Columbia River is strongly felt on stratification. In the classical view, poleward winter winds lead to onshore Ekman transport and poleward along-shelf transport. This traps the Columbia River plume closely along the Washington coast, making it relatively thick and identifiable at Grays Harbor and further north. The Grays Harbor 25 m site is expected to be strongly influenced by the Columbia River plume during poleward winds in winter. In summer, predominantly upwelling favorable winds cause offshore Ekman transport. Equatorward wind-driven current also carry the plume south. Because the plume is not trapped to the coast, it is relatively thin. Recently Hickey et al. (2005, 2008) have reexamined this classical view of the Columbia River plume using modern data and models. They find that wind variability on synoptic meteorological time scales causes the plume to change direction resulting in older plume water becoming cut off from recent plume water by reversals in wind forcing. During poleward wind events in summer the thick poleward tending plume is seen off Grays Harbor. During equatorward wind events, the thin offshore, southward plume is seen.

At the Endurance array off central Oregon, the bidirectional, highly variable Columbia River plume can have a strong impact on the coast and shelf processes (García Berdeal, et al., 2002). Buoyant river input occurs primarily in the winter as a result of smaller Oregon coastal rivers. While the precise effect of these rivers on the stratification is not well described in the literature, evidence for the influence of Yaquina River on the inner shelf is visible in Figure 12, which shows that during periods of significant rainfall, for example 1-10 January 2010, salinity levels decrease in the Yaquina Bay, as measured by LOBO (Land/Ocean Biogeochemical Observatory) and a corresponding decrease in salinity is observed by the ISMT1 buoy.

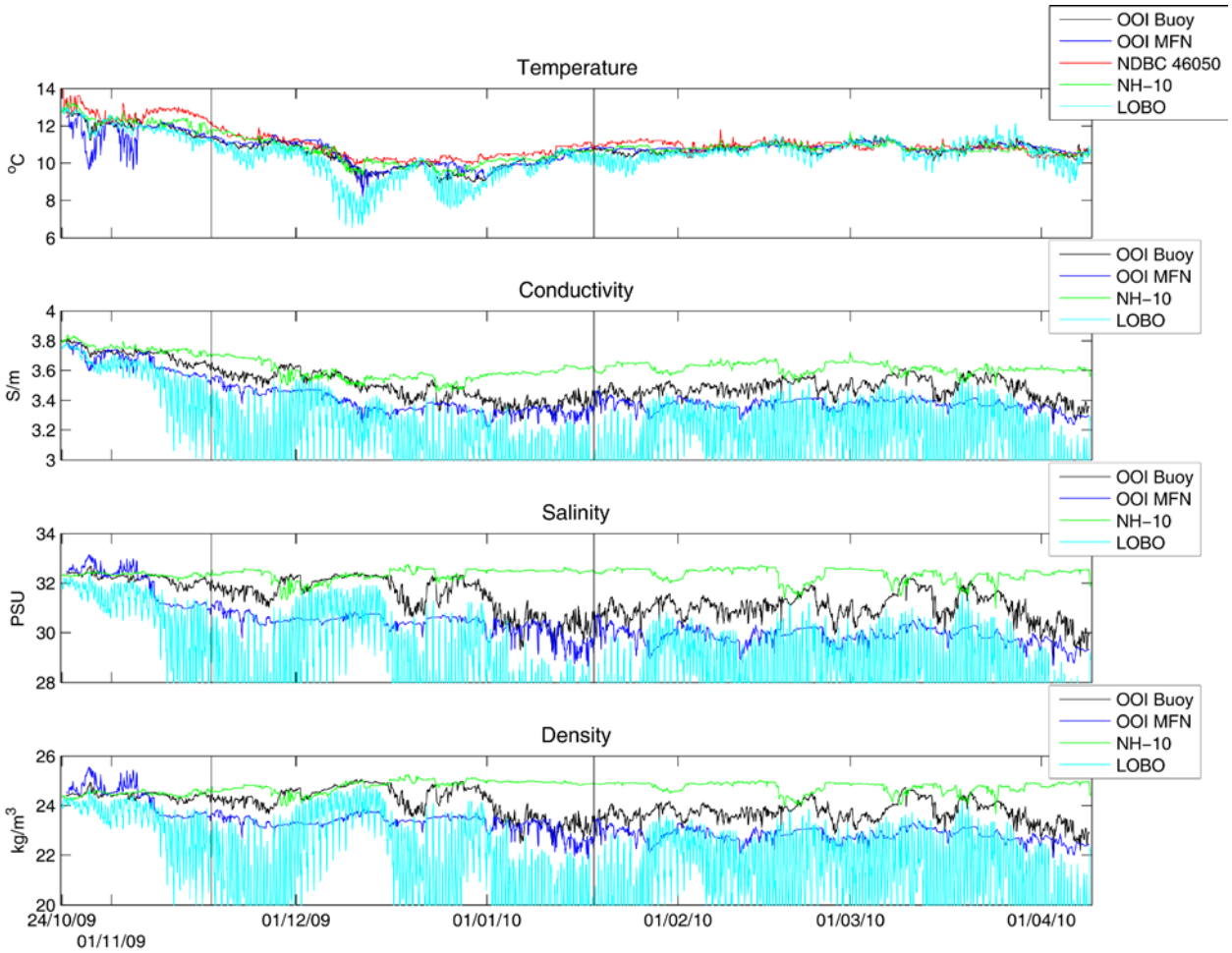

Figure 12. Hourly averaged temperature and conductivity observations (upper two panels) and derived salinity and density (lower two panels), recorded at 46050 (note that there is no conductively sensor on 46050), NH-10, and the ISMT1 25 m and LOBO, which is located in the Yaquina Bay at 44.6294°N 124.0415°N) sites for the period 24 October 2009 – 8 April 2010.

3.2. Climatological Conditions

3.2.1 Historical Wind Data

Wind forcing over the Oregon and Washington shelf is well described by historical National Data Buoy Center (NDBC) measurements. Dorman and Winant (1995) summarize NDBC data along the US west coast acquired through 1990. They characterize the Oregon Washington coast as a distinct region of meteorological forcing along the US west coast. Within this region, monthly mean winds are equatorward (upwelling favorable) in summer and poleward through the winter months with a weak (close to zero) annual mean. However, traveling cyclonic and anticyclonic systems produce synoptic variability and wind reversals throughout the year. Summary statistics of meteorological variability (mean, standard deviations, principal axes, probability density functions etc.) of winds, air and sea temperatures are also presented in this work.

NDBC stations 46050, and 46029 provide a source for average wind speed and direction measurements at a temporal resolution of 10 minutes in the vicinity of the Endurance Array. Maximum gust speed and direction are also recorded. At the time of this writing, data are available, with occasional gaps, during the periods: Nov 1991 – Dec 2010 (46050); March 1984 – Dec 2010 (46029).

Scatterometer measurements made from satellites are a second source for information on wind speed and direction near the Grays Harbor and Newport lines. The Climatology of Global Ocean Winds (COGOW) provides a convenient interface for accessing historical wind data derived from NASA's QuikSCAT scatterometer. Data are available at a spatial resolution of 0.5°of latitude/longitude, and daily temporal resolution. The data used here correspond to a 0.5° x 0.5° grid cell centered at 44.75° N, 124.25° W. Each daily value represents an average of measurements made in the bracketing 3-day interval. Data are available for the period Aug 1999 – Nov 2009.

Wind speed records from both buoys and the satellite observations are strongly correlated (Figure 13), suggesting that, at temporal scales longer than a day, statistics from any of the sources would accurately characterize climatological wind conditions at the Endurance site.

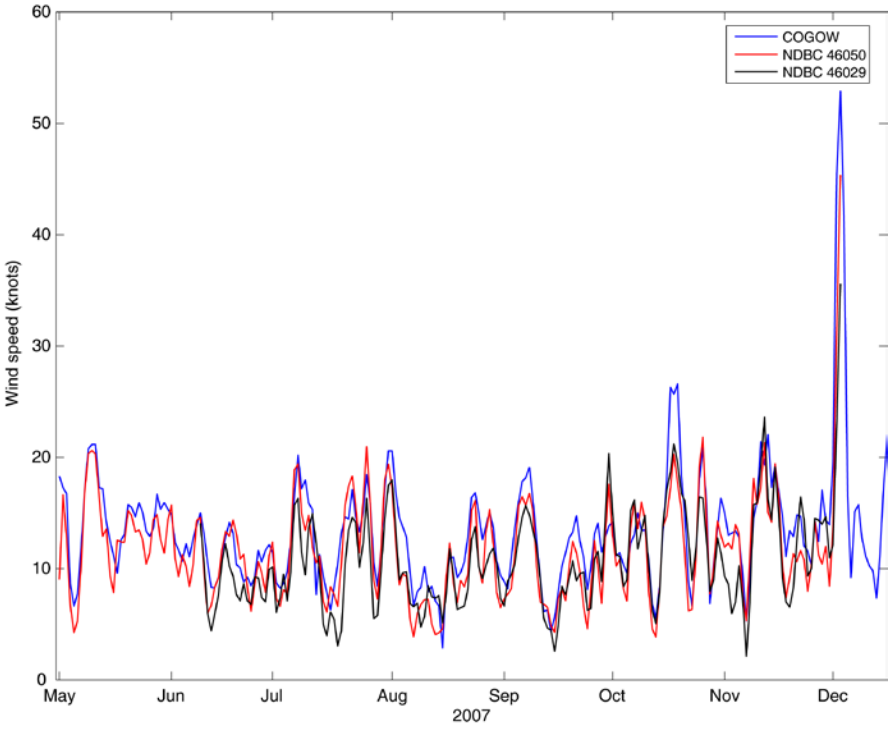

Figure 13. Wind speed measurements from two NDBC buoys and COGOW (Risien and Chelton 2006), a wind product based on NASA's QuikSCAT scatterometer, during a 8-month period in 2007. The buoy data were filtered with a 3-day running mean for consistency with the satellite data product. Note that the two NDBC buoy records end on 3 December 2007 as both buoys broke free from their moorings during the Great Coastal Gale of 2007. This event is described in detail in Section 3.3.1.

Using NDBC 46050 and 46041 to characterize the site, Figure 14 shows that average wind speed has a distinct seasonal cycle, increasing from about 7 kt in August to 14 kt in

January. Wind speed extremes are more variable. Extremes of approximately 25 to 42 kt are found in all months, and extremes of approximately 30 to 42 kt in all months except July.

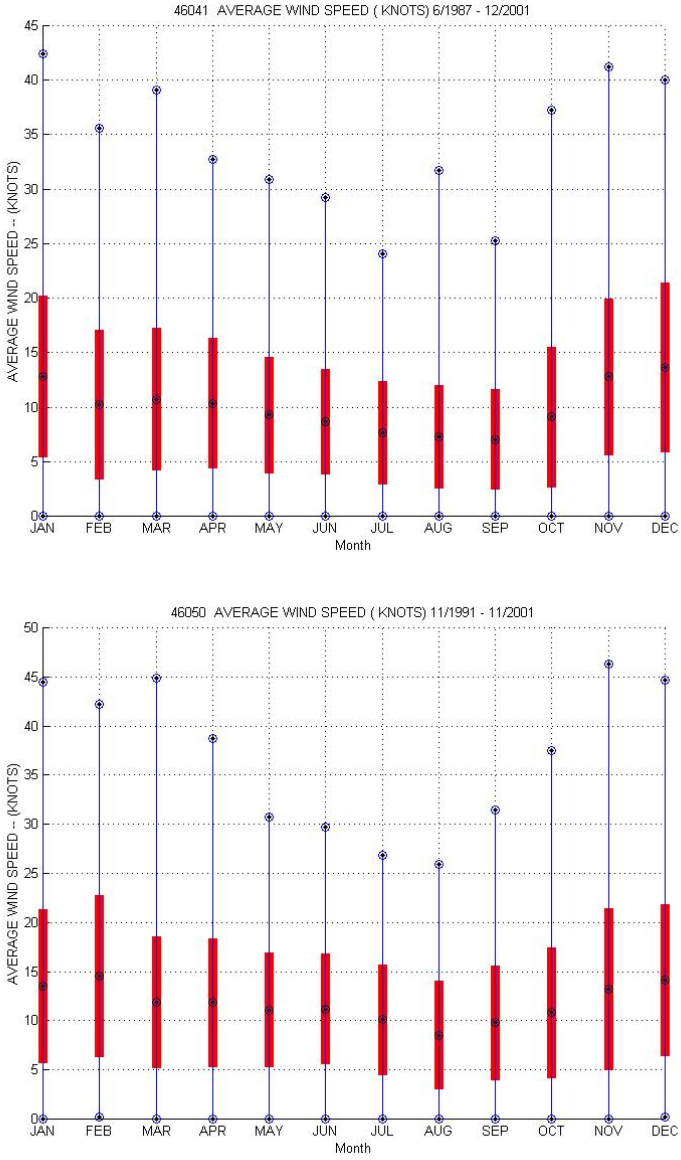

Figure 14. Monthly means, standard deviations, and extremes of hourly average wind speeds measured at NDBC Station 46029 (top) and 46050 (bottom). [Figure reproduced from http://www.ndbc.noaa.gov]

The distributions of hourly average wind speeds and maximum gust speeds at NDBC Stations 46041 and 46050 are plotted in Figure 15. The y-axes are scaled logarithmically to more accurately display the frequency of occurrence of rare high-wind-speed events.

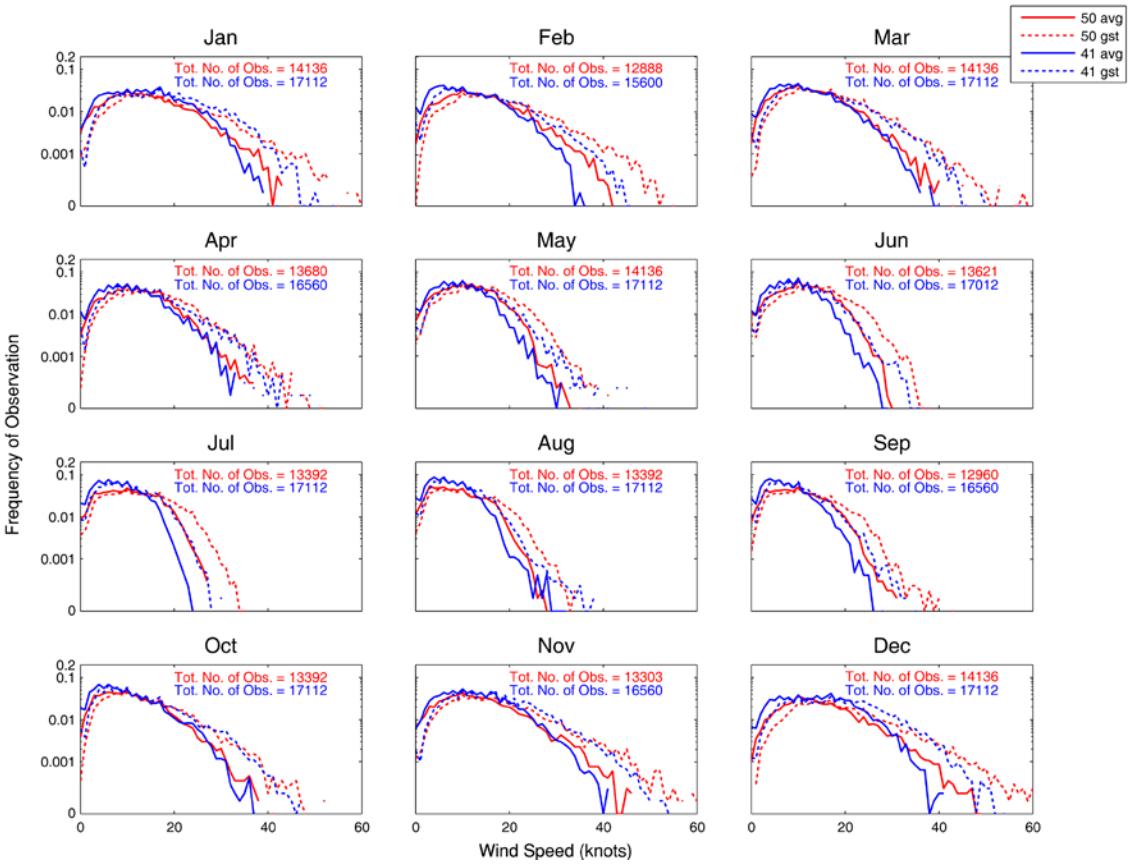

Figure 15. Monthly distributions of wind speed measurements made at NDBC Stations 46041 (blue) and 46050 (red). The distributions of hourly averages are plotted as solid lines, and the distributions of hourly maximum 5-second gust speeds are plotted as dashed lines.

3.2.2 Historical Wave Data

Records of wave height, direction, dominant period, and average period are available at hourly resolution from NDBC Stations 46050, and 46041. Monthly means, standard deviations, and extremes of significant wave height (average height of the highest one-third of all waves) are shown in Figure 17. Mean significant wave height shows a distinct seasonal cycle, increasing from 1.5 m in July to about 3.5-4 m in December. Significant wave height extremes are more variable. Extremes of 6 to 9 m are found in all months except May, July and August. A notable extreme of 14 m was recorded at 46050 in March.

Recent analyses of deep-water wave buoy data published by Ruggiero et al. (2010) argue that significant wave heights have increased off the Pacific Northwest increased at a rate of approximately 0.015 m yr^{-1} since the mid-1970s, while averages of the five highest SWHs per year have increased at the appreciably greater rate of 0.071 m yr^{-1} (Figure 16).

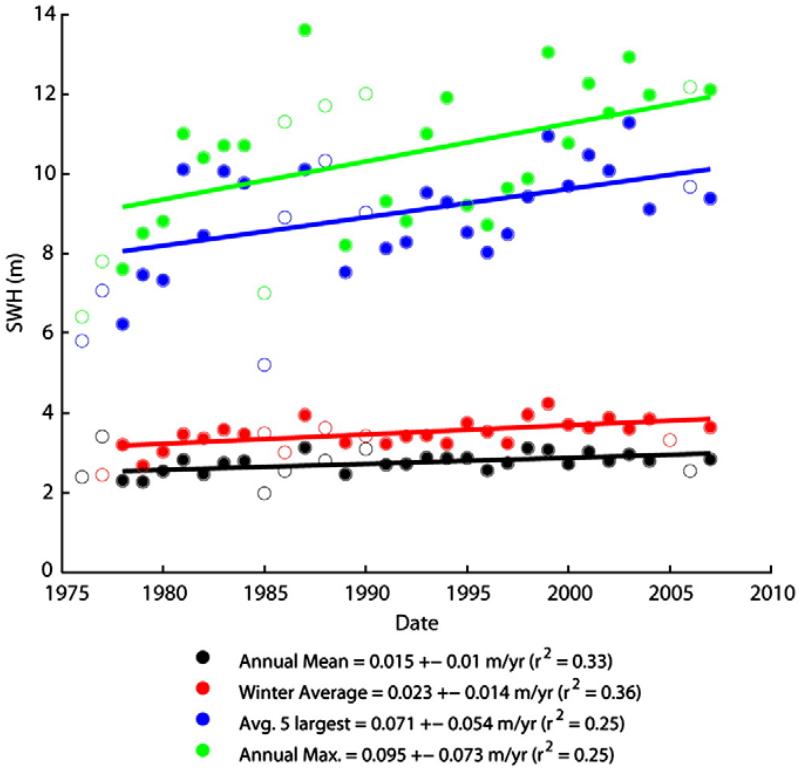

Figure 16. Decadal increases in annual mean, winter average, average of the five largest per year, and annual maxima SWHs measured by NDBC Buoy 46005. The regression slopes and their ± uncertainties are given along with the r^2 values. Each of the regressions is statistically significant at the 95% confidence level. Open circles represent years that did not satisfy the criterion for inclusion and have not been included in the regressions. Figure reproduced from Ruggiero et al. [2010].

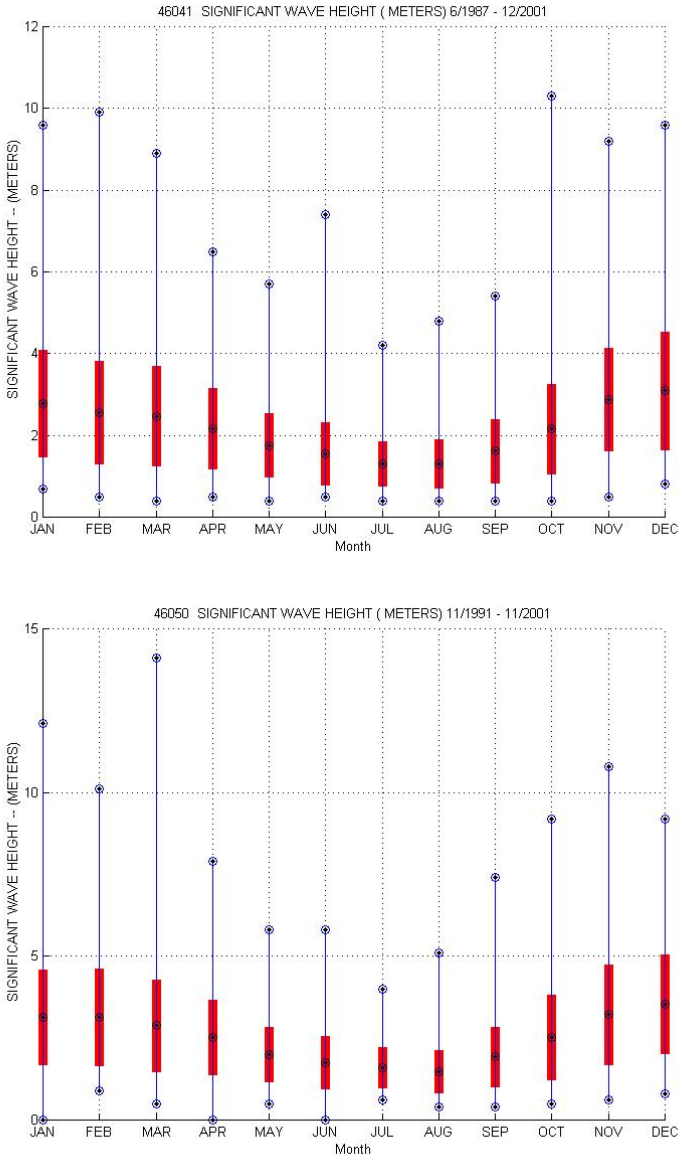

Figure 17. Monthly means, standard deviations, and extremes of significant wave height at NDBC Station 46041 (top) and 46050 (bottom). [Figure reproduced from http://www.ndbc.noaa.gov]

3.2.3 Solar Radiation

NASA provides a large number of satellite-derived data products relating to "Surface meteorology and Solar Energy". Daily average insolation on a horizontal surface is available at a horizontal resolution of 1° in latitude and longitude during the period Jul 1983 – Jun 2006. Histograms of average daily insolation reported for 44.5°N, 124.5°W are shown by month in Figure 18. Winter months (Nov-Feb) show relatively compact distributions, with mean insolation near 75 W/m^2. Distributions are qualitatively different in spring and summer (Apr-Sep), when

long tails are seen on the low end of the distribution. Peaks in the spring and summer distributions occur at values between about 200 W/m^2 and 250 W/m^2.

Radiometer measurements were collected at NDBC Station 44089 for a one-year period from April 2005 through April 2006. The LI-COR LI-200 pyranometer sensor measured shortwave radiation only, while the NASA product depicted in Figure 19 describes total insolation across the entire spectrum; however during the 12-month period when the two datasets overlap, the agreement is reasonable (Figure 19). The seasonal cycle of insolation, with maxima near 250 W/m^2 in summer and minima near 75 W/m^2 in winter, is clearly seen.

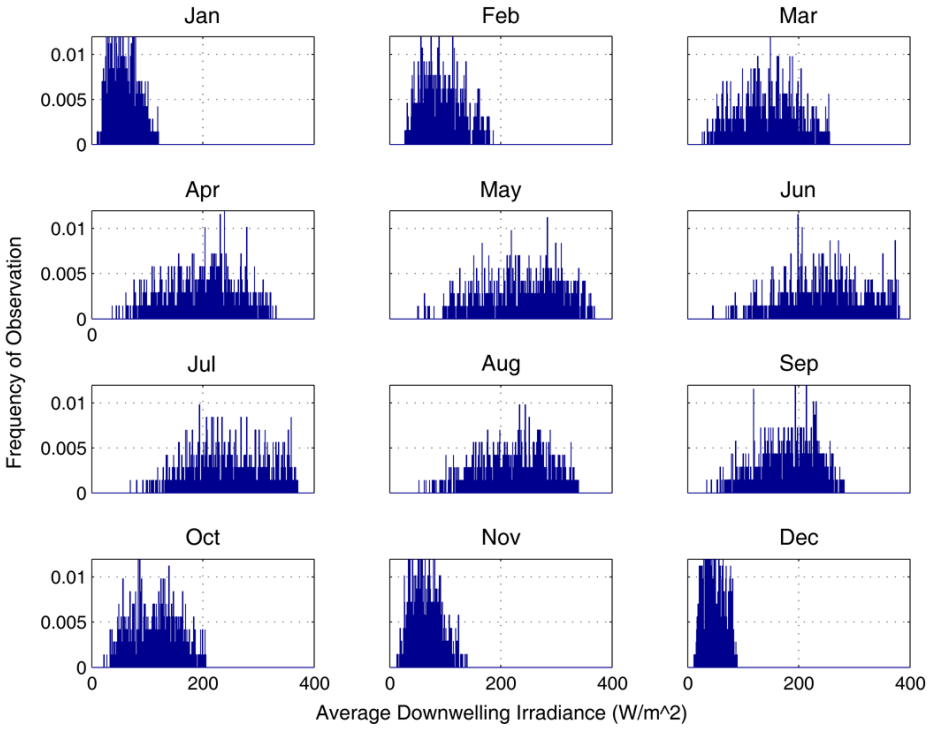

Figure 18. Monthly distributions of daily average insolation on a horizontal surface at 44.5°N, 124.5°W calculated from a NASA satellite-derived data product spanning 23 years.

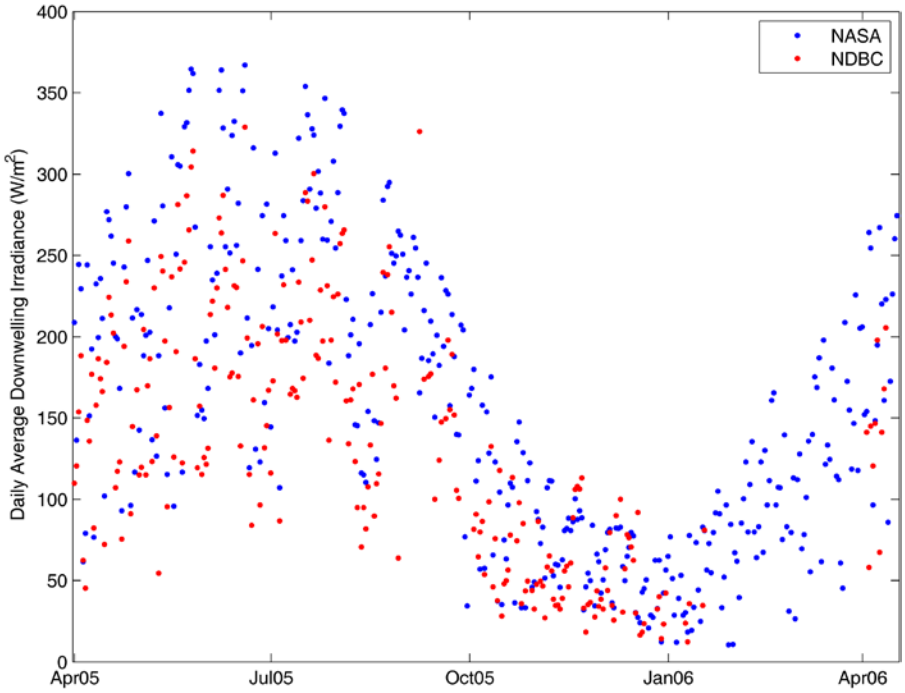

Figure 19. NASA daily average insolation and shortwave radiation measured at NDBC Station 44089. A daily average has been applied to the NDBC data.

3.3. Environmental Extremes

3.3.1 Extra-tropical Cyclones

Extra-tropical cyclones are the dominant cause of midlatitude high-frequency variability. Over the north Pacific most cyclones originate in the western Pacific basin and move northeastward across the north Pacific basin (Raible and Blender, 2004). When approaching the land, these cyclones can bring hurricane-force winds, heavy precipitation (Deng, 2009) and maximum wave heights that exceed 14 meters (Allan and Komar, 2002) to the coastal areas.

An extreme example of such storm activity is the Great Coastal Gale of 2007, which refers to a series of extra-tropical cyclones that affected Oregon, Washington and British Columbia between December 1 and December 3, 2007. The storms arrived in four waves (Figure 20). The first developed off the coast of Washington on 1 December and brought high winds and cold temperatures. The second wave arrived late on 2 December and reached its peak intensity just before striking the northern coast of Washington. A wave associated with the last low pressure system arrived early on 3 December and helped to maintain the strong pressure gradient before the arrival of the strongest system late on 3 December (Read, 2007).

The storms on December 2 and 3 produced an extreme, long-duration wind event with hurricane-force wind gusts of up to 220 km/h at Holy Cross, Washington on the Washington coast and 208 km/h at Bay City, Oregon on the Oregon coast (Read, 2007). The Great Coastal Gale of 2007 resulted in two NOAA NDBC buoys (46050 and 46029) and the NANOOS NH-10 mooring being torn from their anchors. On December 3, 2007 when 46050 and 46029 reported being adrift they were reporting wind gusts in excess of 108 km/hr and significant wave heights

of approximately 13 m (NDBC, 2008). Figure 21 shows the condition of 46050 and 46029 upon recovery.

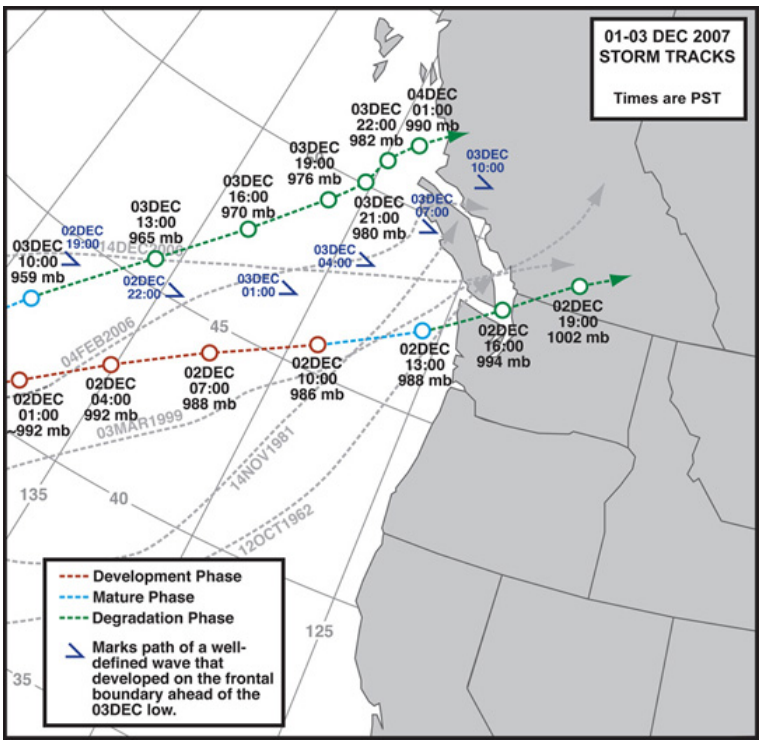

Figure 20. The storm tracks of lows and waves that were associated with the Great Coastal Gale of 2007 (Figure reproduced from Read, 2007).

Figure 21. NDBC Buoy 46029 (Left) and 46050 (Right) after they broke free during the Great Coastal Gale of 2007 (Figure reproduced from NDBC, 2008).

While the Great Coastal Gale of 2007 ranks as one of the most extreme storm events to hit the Pacific Northwest in the last century it is not a unique event. For example, the Columbus Day Storm of 1962 was associated with higher wind speeds than the Great Coastal Gale of 2007. Gusts of 222 km/hr were recorded at Newport, OR, but it was shorter in duration (Lynott and

Cramer, 1966; Read, 2005). Another example of a powerful storm event occurred between 6 and 8 December 2004. During this event both 46029 and 46050, which recorded wind gusts of 94 km/hr and significant wave heights of 5.5 m, broke free from their moorings (NDBC, 2008). Descriptions of other significant Pacific Northwest storm events are available at http://www.climate.washington.edu/stormking.

3.3.2 Phytoplankton Blooms / HABS

Harmful Algal Blooms (HABs) are a common occurrence in the coastal waters of the Pacific Northwest. Of particular concern are HABs that are attributed to *Pseudo-nitzschia* species, a group of diatoms that produce the neurotoxin domoic acid (Trainer et al., 2002). Domoic acid (DA) causes permanent short-term memory loss in victims and is associated with the syndrome commonly referred to as amnesic shellfish poisoning. Domoic acid has also been documented to cause seabird and marine mammal deaths (Trainer et al. 2000). In addition to health implications for humans and animals, HAB events along the Washington coast have an economic impact and are of particular concern to U.S. state agencies, coastal Native tribes and businesses that rely on shellfish harvests. The total estimated impact of a coastwide seasonal closure of the Washington State recreational razor clam fishery for 2008 is estimated to be $20.42 million (Dyson and Huppert, 2010). In Oregon, DA contamination events in 1998, 2003, 2004, and 2005 led to spatially large and prolonged closures of Oregon razor clam and mussel beds to harvesting. Oregon's Department of Fish and Wildlife estimates that the 2003-2004 closure resulted in a $4.8 million loss to Oregon's shelfish industry (Tweddle et al., 2010).

Trainer et al. (2002) emphasized the importance of the Juan de Fuca eddy, located offshore of northern Washington State and southern Vancouver Island, British Columbia, as an initiation site for toxic *Pseudo-nitzschia* blooms (Figure 22). These authors hypothesize that the eddy acts as an "incubator", whereby blooms are maintained offshore in the eddy throughout the summer, then brought onshore by changes in the wind field associated with either episodic wind reversal events during the upwelling season, or the transition from summer upwelling to winter downwelling in September/October. Modeling studies (MacFadyen et al., 2005) and analyses of ocean color satellite data (Sackmann and Perry, 2006) have confirmed the importance of the Juan de Fuca eddy as a source for Washington shelf waters. In addition to the Juan de Fuca eddy, Heceta Bank, located off the central Oregon coast, has been recognized as a potential "hot-spot" for toxic *Pseudo-nitzschia* bloom development (Figure 22) (Trainer et al., 2001) as flow–topography interactions in this region can lead to enhanced surface plankton retention (Hickey and Banas, 2003).

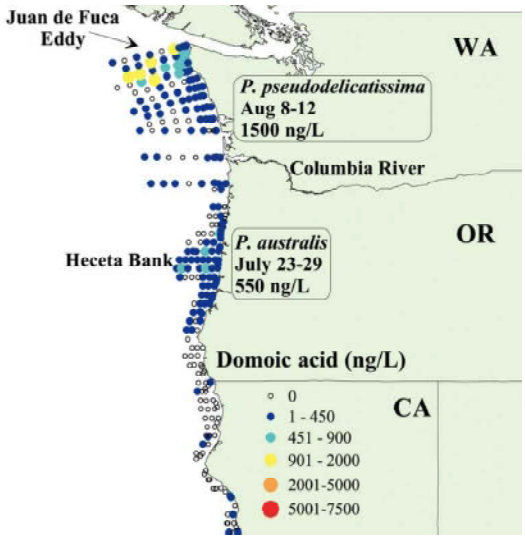

Figure 22. Domoic acid concentrations in *Pseudo-nitzschia* species along the Pacific Northwest Coast in 1998. Areas of persistent high domoic acid concentrations are associated with retentive circulation patterns such as the Juan de Fuca eddy and Heceta Bank. Figure reproduced and edited from Hickey and Banas [2003].

Trainer et al. (2009) describe a large, nearly monospecific diatom bloom of toxigenic *Pseudo-nitzschia cuspidata* off the coasts of Washington State and British Columbia. These authors found that during this September 2004 bloom event cell concentrations reached 6.1 x 10^6 cells L^{-1}, and that cellular DA was highest in and just south of the Juan de Fuca eddy region, where levels ranging from 13 to 35 pg $cell^{-1}$ were observed. These DA values are greater than those measured during a coastal bloom of *P. cf. pseudodelicatissima* (maximum abundance of 15 x 10^6 cells L^{-1}) in 1998, when maximum cellular DA was estimated at 0.5 pg $cell^{-1}$ (Adams et al. 2000). Another example of a significant HAB event, which resulted in the mass mortality and stranding of thousands of sea birds, occurred along the Oregon and Washington coasts in late October 2009. This event was attributed to the dinoflagellate *Akashiwo sanguinea*, which while ostensibly nontoxic, produces a proteinaceous foam that strips the natural oils from the weather proofing of a bird's plumage, causing them to die of hypothermia (Jessup et al., 2009).

3.3.3 Hypoxia / Anoxia

Globally, dissolved oxygen concentrations are decreasing both near the coast and in the open ocean (Gilbert et al., 2010; Díaz and Rosenberg, 2008). These trends are consistent with the findings of Bograd et al. (2008), Chan et al. (2008) and Connolly et al. (2010) who show long-term declines in dissolved oxygen in the southern and northern regions of the California Current System (Figure 23). Particularly severe seasonal hypoxic events observed off the Oregon coast in 2002 and 2006 are described in Grantham et al. (2004) and Chan et al. (2008), respectively.

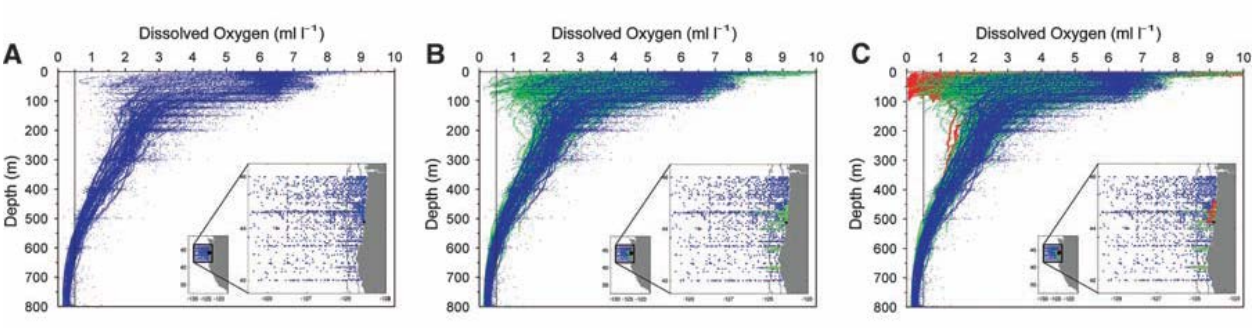

Figure 23. Dissolved oxygen profiles during the upwelling season (mid-April to mid-October) in the upper 800 m of the continental shelf and slope of Oregon (42.00°N to 46.00°N). (A) 1950 to 1999 from the World Ocean Database and Oregon State University archives (n = 3101 hydrocasts, blue). (B) (A) with additional data for 2000 to 2005 (n = 834 hydrocasts, green). (C) (A) and (B) plus data for 2006 (n = 220 hydrocasts, red). The black vertical line denotes the 0.5 ml l−1 threshold. (Insets) Overlapping locations of hydrographic (blue, green, and red) and remotely operated vehicle (black) stations through time and the 100-m and 1000-m isobaths. Figure reproduced from Chan et al. (2008).

Grantham et al. (2004) investigate, using cross-shelf transects, a severe inner-shelf hypoxia, defined to be dissolved oxygen concentrations < 1.43 ml l^{-1} (Díaz and Rosenberg, 1995), event that occurred along the Oregon shelf (44–44.65°N) between July and September 2002. During this event, which was driven in part by an anomalous invasion of nutrient-rich, subarctic water into the California Current System (Freeland et al., 2003; Wheeler et al., 2003) and large-scale wind stress anomalies over the northeast Pacific (Murphree et al., 2003), bottom dissolved-oxygen concentrations of 0.21–1.57 ml l^{-1} were found to extend from the shelf break to nearshore stations (2–5 km offshore) along the Newport, Strawberry Hill (SH) and Heceta Head hydrographic lines (Figure 24). Inner-shelf cruises along the SH line recorded bottom dissolved-oxygen concentrations of 1.0 ml l^{-1} within 700m of the surf zone. Grantham et al. (2004) report that at the observed height of the 2002 hypoxia event, dissolved-oxygen-deficient bottom waters occupied up to 40m of the water column and that hypoxic conditions covered at least 820 km^2 of shelf area inshore of the 70-m isobath. The 2002 hypoxic event had a profound impact on benthic fish and invertebrate communities. Video from remotely operated vehicle (ROV) surveys for this period showed only dead fish and dead or moribund invertebrates on patch reefs adjacent to the SH line. In contrast, annual ROV surveys in 2000–02 showed no invertebrate die-offs and average rockfish densities of 12.8 per 100 m^2. In addition, 2002 commercial fishery data revealed crab (*Metacarcinus magister*) mortality to be > 75% in crab pots compared with the normal 0%.

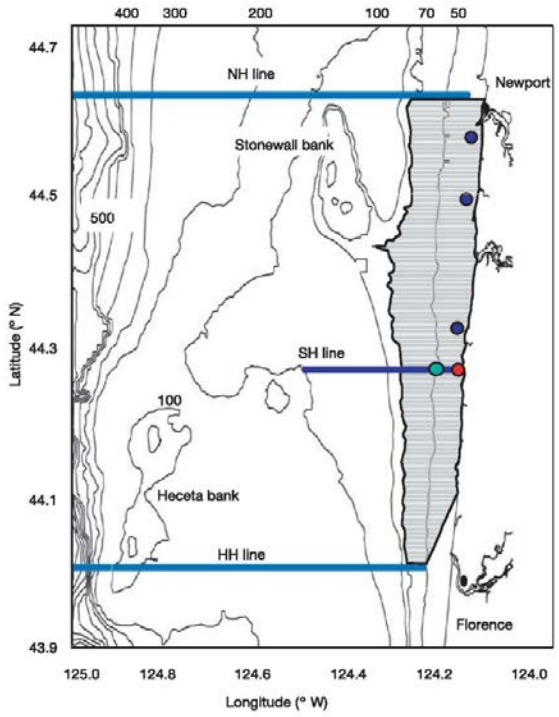

Figure 24. Location of the 2002 hypoxic zone and hydrographic transects off Oregon. Annual ROV patch reef surveys (green circle). Additional hydrographic stations (blue circles) and an acoustic Doppler current profiler (ADCP) location (red) are indicated. The minimum estimated spatial extent of the severe hypoxic zone over the inner shelf (820 km^2) is shown (grey). Figure reproduced and edited from Grantham et al. (2004).

Chan et al. (2008) describe a 2006 hypoxic event off the Oregon coast during which anoxia, defined to be dissolved oxygen = 0 ml l^{-1}, was measured for the first time over the continental shelf along the central Oregon coast. These authors found that the onset of anoxia was accompanied by the expansion of severe hypoxia, defined to be dissolved oxygen < 0.5 ml l^{-1}, across broad sections of the central Oregon shelf. At its peak, hypoxia was recorded along all cross-shelf transect lines between 44.25°N and 45.00°N, extending from the shelf break to the inner shelf and covering at least 3000 km^2. The 2006 hypoxic event was also exceptional in its vertical and temporal extents, occupying up to 80% of the water column in shallow (60 m) shelf waters and persisting over mid- and inner-shelf waters from June to October. Like the 2002 hypoxic event described in Grantham et al. (2004), the 2006 event had a devastating impact on rockfish and macroscopic benthic invertebrate communities (Chan et al., 2008). Oregon Department of Fish and Wildlife ROV surveys, conducted during August 2006, revealed the complete absence of all fish from rocky reefs that normally serve as habitats for diverse rockfish communities. These surveys also revealed the near-complete mortality of macroscopic benthic invertebrates and an accompanying rise of putative sulfide-oxidizing bacterial mats in shallow (50 m) waters (Chan et al., 2008). During the summer of 2006, hypoxia was also observed off the coast of Washington with dissolved oxygen concentrations < 0.5 ml l^{-1} along the inner shelf (Connolly et al., 2010). Connolly et al. (2010) estimate that during late summer 2006 hypoxic waters covered approximately 5000 km^2 of the Washington continental shelf (Figure 25).

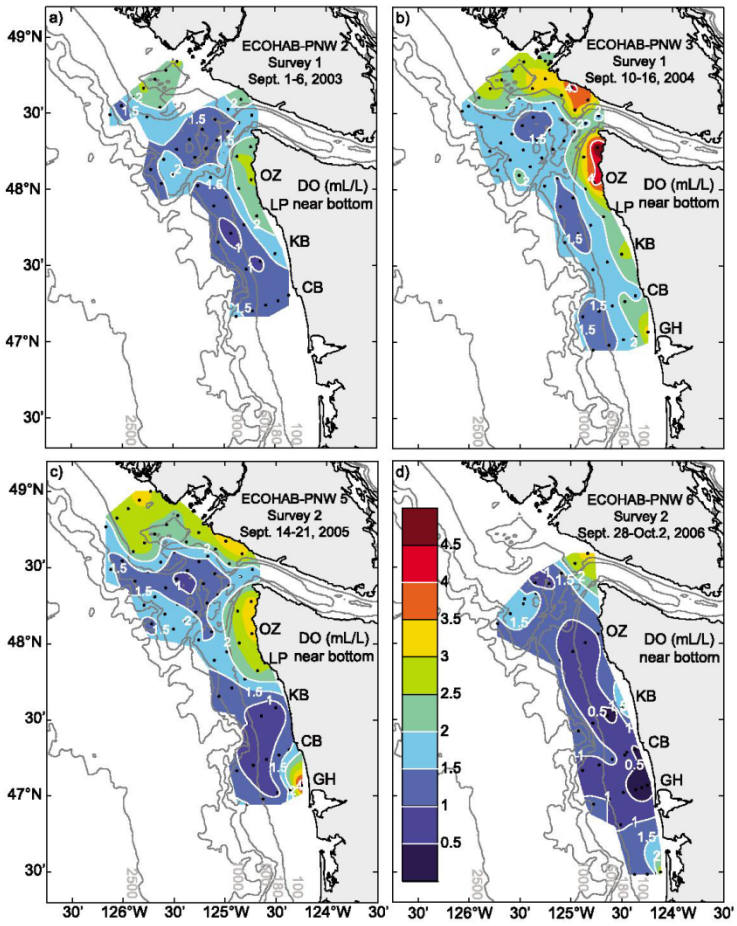

Figure 25. Near-bottom dissolved oxygen during late summer/early fall from 4 different years: (a) 2003, (b) 2004, (c) 2005, and (d) 2006. DO contours, shown in the color bar in Figure 23d, represent increments of 0.5 ml l^{-1}. Isobaths are indicated by gray contour lines. Station locations are shown as black dots. Abbreviations of selected transect names are shown along the Washington coast. Figure reproduced and edited from Connolly et al. (2010).

3.3.4 10, 30 and 100 Wind and Wave Return Periods

Wind and wave time series data were obtained from nearshore and offshore NDBC Buoys. Offshore NDBC buoy 46050 (Oregon) had the most severe conditions. Offshore NDBC buoy 46041 (Southern Washington) and nearshore Scripps/NDBC Buoy 46211 (Grays Harbor) had similar conditions.

The significant wave height and sustained wind for 10 year, 30 year, and 100 year events is estimated from wave and wind records from offshore NDBC buoy 46050 (see Appendix A for details of extreme event analysis).

Table 3. Wind and wave extremes using Weibull distributions

	Significant Wave Height (m)	Peak Period (s)	Wind Speed (m/s)
10 Year Return Period	13.06	15.9	25.4
30 Year Return Period	14.04	16.5	26.7
100 Year Return Period	15.12	17.2	28.0

Table 4. Wind and wave extremes using Pareto distributions

	Significant Wave Height (m)	Peak Period (s)	Wind Speed (m/s)
10 Year Return Period	12.45	15.6	25.1
30 Year Return Period	13.84	16.4	26.2
100 Year Return Period	15.37	17.3	27.1

Waves were determined using Weibull distributions for all sea states and Pareto distribution for peaks-over-threshold method. Both methods have been previously described. The 100-year events seem big and perhaps unrealistic but this is due to the small amount of data. There were only 10 full years measured from July 1-June 30 where there wasn't appreciable drop out. During that 10 years the maximum sea state was 14.04 m and maximum wind speed was 23.9 m/s.

3.4. Other Constraints

3.4.1 Shipping Lanes

Relative to shipping routes in other parts of the world, the US west coast is one of the busiest (Figure 26). This ship traffic includes ocean-going tugs and barges that travel between ports along the Oregon and Washington coasts. In the early 1970's conflicts developed between these vessel operators and commercial crab fishermen as the crab pots were fouling the vessels. These altercations resulted in lost fishing gear and significant vessel repair costs. Out of this conflict grew the Crabber/Towboat Lane Negotiation Project. This project, which is still in existence today, works to bring tug and barge operators and commercial crab fishermen together to agree on areas, tow lanes, where crab gear will not be set. The Navigable towboat and barge lanes through the crabbing grounds between Cape Flattery and San Francisco are described in Harbell (2010). The tow lanes off Grays Harbor, WA and Newport, OR are shown in Figure 27 and Figure 28, respectively and are accessible online at http://www.wsg.washington.edu/mas/pdfs/2010TowlaneCharts.pdf.

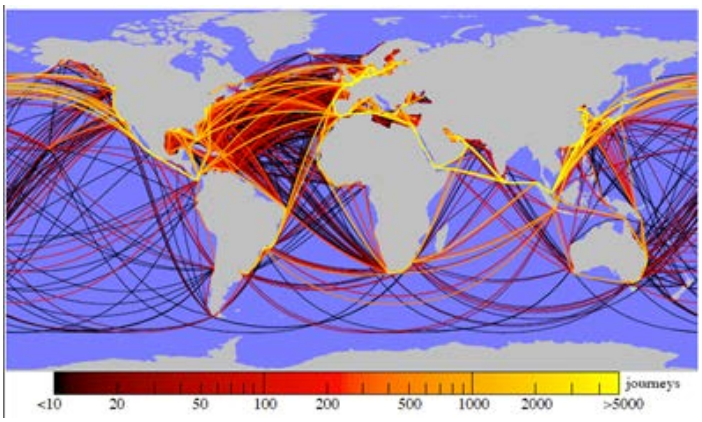

Figure 26. The trajectories of all cargo ships larger than 10,000 GT during 2007. The color scale indicates the number of journeys along each route. Figure reproduced and edited from Kaluza et al. (2010).

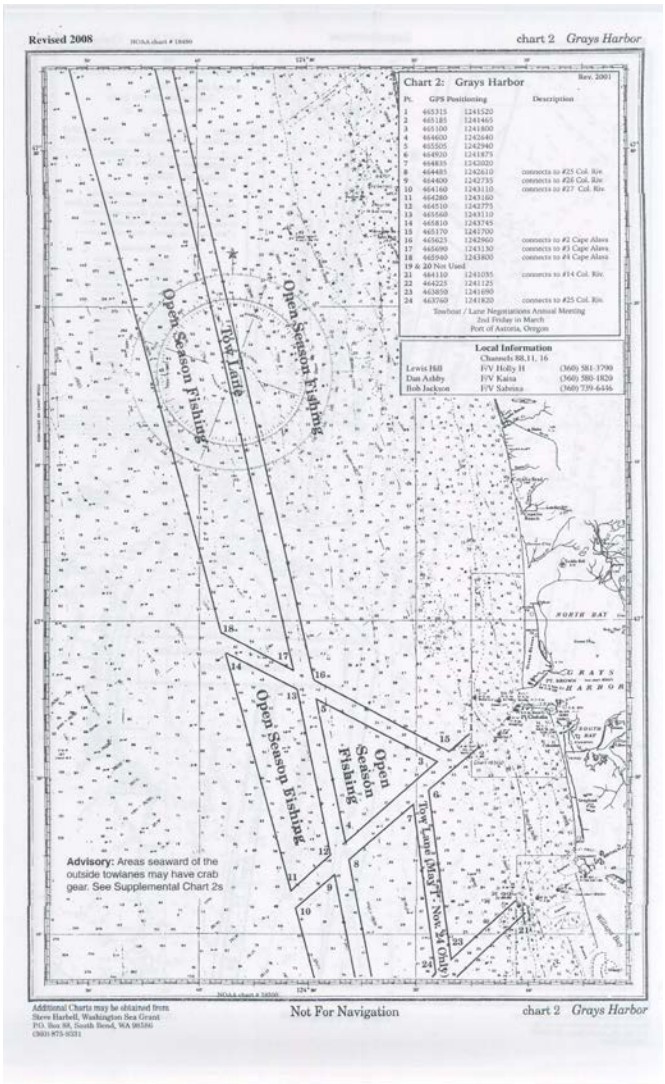

Figure 27. Navigable towboat and barge lanes off Grays Harbor, WA.

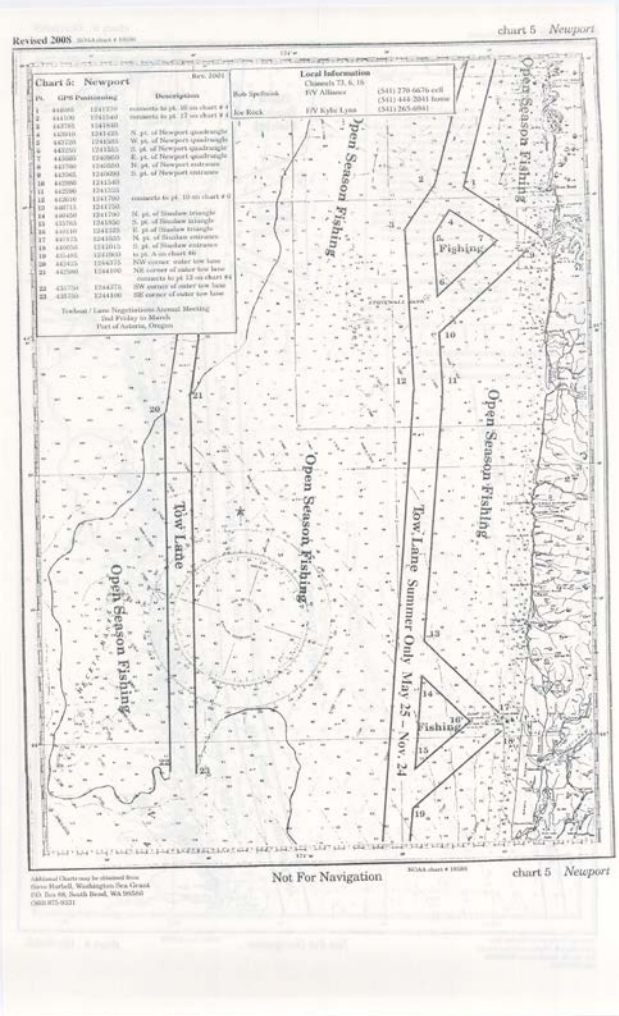

Figure 28. Navigable towboat and barge lanes off Newport, OR.

3.4.2 Fishing Areas

The main socioeconomic activities along the Oregon and Washington coasts are commercial fishing and shellfish farming. Fishing typically occurs from the shoreline to approximately 1,850 m depth and most effort takes place between January and September, with less from October through December. There are 4 main gear types used along the Oregon and Washington coasts: bottom trawl, near-bottom trawl, longlines, and pot gear. Scallop dredges are also used, but rarely as there are very few scallop areas remaining off of Oregon and Washington (Natural Resources Consultants [NRC] 2007).

In an effort to characterize the distribution and spatial extent of commercial, charter, and recreational fisheries along the Oregon coast Ecotrust and its partners collected geo-referenced information about the extent and relative importance of Oregon marine waters (Steinback et al., 2010). Data collection occurred between March-May 2009 and December 2009-September 2010. 244 commercial fishermen, 63 charter operators/owners, and 237 recreational fishermen participated in this project. 144 of these respondents were commercial, charter, and recreational

fishermen from the port of Newport (Table 5). The results of the Newport survey are represented in Figure 29. Figure 29 shows the combined aggregate fishing grounds for the commercial, charter, and recreational sectors for Newport. The commercial fishing ground aggregates that were combined were Dungeness crab (trap), salmon (troll), rockfish (fixed gear), and shelf bottom (trawl). The charter fishing ground aggregates that were combined were Dungeness crab, Pacific halibut, rockfish, and salmon. The recreational sport boat fishing ground aggregates that were combined were Dungeness crab, flatfish, Pacific halibut, rockfish, and salmon. Percent volume contours are depicted at 25, 50 and 75 percent intervals. These results are publically available at http://oregon.marinemap.org/.

Table 5. Number of fishermen interviewed by home port and fishery. From Steinback et al. (2010).

Fishery	Astoria	Garibaldi	Depoe Bay	Newport	Florence	Winchester Bay	Coos Bay/ Charleston	Port Orford	Gold Beach	Brookings	Oregon
Dungeness Crab - Trap	26	8	3	30	5	10	37	15	3	22	**159**
Hagfish - Trap	–	1	–	2	1	1	3	1	–	–	**9**
Pacific Halibut - Longline	5	4	3	11	1	5	10	5	–	1	**45**
Petrale Sole - Bottom Trawl	9	–	–	8	–	–	10	–	–	3	**30**
Pink Shrimp - Trawl	9	2	–	9	–	2	10	–	–	5	**37**
Rockfish - Hook and Line (dead)	–	1	3	4	–	–	16	13	2	7	**46**
Rockfish - Hook and Line (live)	–	1	2	1	–	–	2	15	4	7	**32**
Rockfish - Longline (dead)	–	1	–	–	–	–	2	8	–	1	**12**
Rockfish - Longline (live)	–	–	–	–	–	–	–	13	2	1	**16**
Rockfish - Trap	–	1	–	–	–	–	–	–	–	–	1
Sablefish - Longline	5	–	–	8	1	5	18	15	–	4	**56**
Sablefish - Trap	2	2	–	5	2	1	1	–	–	1	**14**
Salmon - Troll	8	6	3	16	4	9	39	10	3	15	**113**
Sardine - Net (Seine)	–	–	–	1	–	–	–	–	–	–	1
Seaward RCA - Trawl	12	–	–	10	–	–	8	–	–	4	**34**
Shelf Bottom - Trawl	9	–	–	6	–	–	4	–	–	–	**19**
Tuna - Troll	8	1	–	25	2	10	34	11	5	13	109
Urchin - Dive	–	–	–	–	–	–	1	2	1	–	4
Whiting - Midwater Trawl	3	–	–	8	–	–	2	–	–	1	14
Total[6]	**96**	**28**	**14**	**144**	**16**	**43**	**197**	**108**	**20**	**85**	**751**

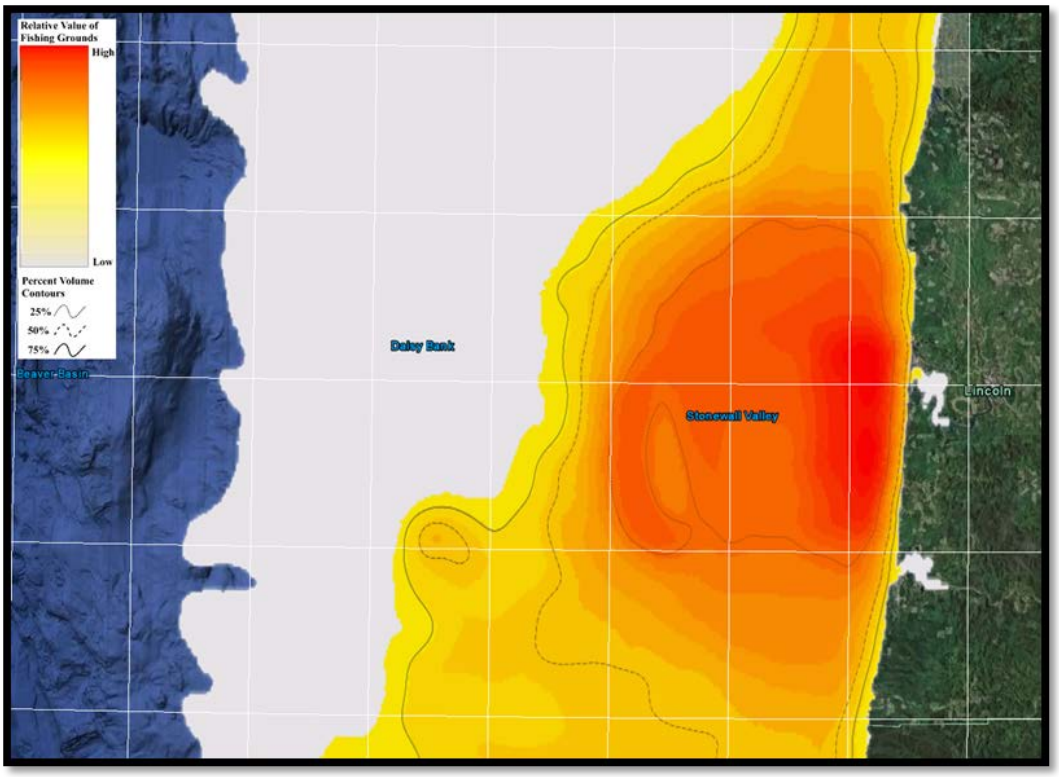

Figure 29. Relative value of combined aggregate fishing grounds for the commercial, charter, and recreational sectors for the port of Newport, OR. Percent volume contours are depicted at 25, 50 and 75 percent intervals. The grid depicts 10 minute lines of latitude and longitude.

Data similar to those collected for the Ecotrust report (Steinback et al., 2010), described above, are not available for the Washington Coast. Similar fisheries are, however, found off the coast of Washington with the most common fishing method being that of bottom trawling. Trawling typically occurs outside of the 3-nm state boundary out to about the 800 m isobath (SSEA 2011 Figure 3-2 pg 98). Most trawling effort for shrimp occurs during the summer months between 100-200 m depths near Tillamook Bay (NRC 2007). Along the Washington coast between the Columbia River and Destruction Island crab fishing occurs out to the 90 m isobath (Joe Schumacker, personal communication), with the majority of activity occurring inshore of the 40 m isobath (SSEA, 2011). Crab fishing effort decreases with increasing latitude north of Destruction Island. Troll fishing, primarily for salmon, typically occurs between inshore of the 55 m isobath between the Columbia River and Westport WA. Longline fishing for halibut and sablefish occurs in the vicinity of Grays Canyon, a submarine canyon which lies 35 nautical miles due west from the mouth of Grays Harbor (Joe Schumacker, personal communication). A detailed description of fishing activity along the Oregon and Washington coasts is presented in Section 3.2.6 of the SSEA report (SSEA, 2011).

3.4.3 Protected/Dangerous Areas and Seafloor Cables

Several submarine cable systems have been previously installed off the coasts of Oregon and Washington; some are in-service, some have been retired and left in place. Active systems crossed by the RSN cable include: Videsh Sanchar Nigam Limited cables (VSNL, 3 crossings); Southern Cross (1 crossing); Pacific Crossing 1 (1 crossing), and AKORN (1 crossing). Further

information on these and some of the out-of-service cables which would also be crossed by the RSN cable (4 crossings) is available at http://www.iscpc.org. The locations of these seafloor cables are described in NOAA Charts 18500, 18580, and 18520. NOAA chart 18500 details naval operating areas.

3.4.4 Marine Cultural Artifacts

As part of the National Science Foundation's Site-specific Environmental Assessment (SSEA, 2011) site-specific surveys were conducted to determine if any undiscovered resources fall within the immediate vicinity of the proposed RSN cable and Endurance Array moorings. Based on these surveys, neither archeological resources, nor historic resources (e.g., historic shipwrecks, aircraft wrecks) occur within the vicinity of the proposed Endurance Array moorings. In addition, communications with the Quinault Nation (―Nation) revealed that installation of the Grays Harbor Line within the area described in SSEA (2011) is not likely to impact any Quinault cultural, archeological, or historic resources.

The Nation and NSF have, however, acknowledged that components of the Grays Harbor Line may, through the micro-siting process, ultimately be located within the Nation's Usual and Accustomed fishing areas. The NSF and the Nation are in the final stages of negotiating a Memorandum of Agreement to address such issues.

3.4.5 Other Moorings and Glider Operations

Nine other moorings are known to be maintained within the Endurance Array region. Four NDBC Stations, 46050, 46029, 46089, and 46041 are indicated in Figure 4. These are 3-meter discus buoys with published watch circles of 257 m, 257 m, 1843 m, and 154 m, respectively. The locations of three Coastal Data Information Program (CDIP) Waverider and two NANOOS buoys as well as the NDBC buoys are listed in Table 6.

Table 6. Existing mooring locations.

Mooring Name	Latitude (N)	Longitude (W)
NDBC 46050	44.641	124.500
NDBC 46029	46.144	124.510
NDBC 46089	45.908	125.760
NDBC 46041	47.353	124.731
CDIP 036	46.857	124.244
CDIP 162	46.2155	124.128
CDIP 139	43.769	124.551
NANOOS NH-10	44.633	124.304
NANOOS Ćháʔba	47.9662	124.9499

Figure 30 shows the approximate glider lines operated by the University of Washington (UW), the Center for Coastal Margin Observation & Prediction (CMOP) and Oregon State University (OSU). The UW Seaglider line extends from 47 N, 127 W in the south to 48 N, 124,95 W in the north. The CMOP Slocum sampling grid runs north-south between 47 and 46.85 N and extends out to 125 W. The OSU Slocum line follows the Newport Hydrographic line at 44.65 N and extends out to 125 W.

Figure 30. Approximate glider lines operated by the University of Washington (UW), the Center for Coastal Margin Observation & Prediction (CMOP) and Oregon State University (OSU).

Sources and References

Data sources

NGDC coastal bathymetric database:
Divins, D.L., and D. Metzger, NGDC Coastal Relief Model,
http://www.ngdc.noaa.gov/mgg/coastal/coastal.html

ETOPO-1 global bathymetric database:
Amante, C. and B. W. Eakins, ETOPO1 1 Arc-Minute Global Relief Model: Procedures, Data Sources and Analysis. NOAA Technical Memorandum NESDIS NGDC-24, 19 pp, March 2009,
http://www.ngdc.noaa.gov/mgg/global/global.html

NOAA nautical charts:
http://www.charts.noaa.gov/
http://ocsdata.ncd.noaa.gov/BookletChart/PacificCoastBookletCharts.htm

World Ocean Atlas climatological hydrographic data:
http://www.esrl.noaa.gov/psd/data/gridded/data.nodc.woa98.html

QuikSCAT wind data from Climatology of Global Ocean Winds:
http://cioss.coas.oregonstate.edu/cogow/

NASA solar radiation data products:
http://eosweb.larc.nasa.gov/sse/

National Data Buoy Center meteorological data:
http://www.ndbc.noaa.gov/

Satlantic - Land/Ocean Biogeochemical Observatory (LOBO):
http://yaquina.satlantic.com/

Washington Sea Grant Tow Lane Charts:
http://www.wsg.washington.edu/mas/pdfs/2010TowlaneCharts.pdf

Appendix A

Methodology for determining extreme events

10, 30, and 100-Year Sea States

Historical records for significant wave heights comes mostly from reanalysis of wind data collected by satellites. The wind data is used as input into numerical models that calculate significant wave height. Since winds are averaged over a fairly course grid, the significant wave heights typically underestimate short-term events as measured by surface buoys. In one instance (***Station Papa***), we are able to compare 35-year results from GROW data reanalysis to overlapping 25-year measurements from an NDBC surface buoy (46001). The GROW data reanalysis underestimates 10,30, and 100-year sea states by about 10%.

Extreme events (10, 30, and 100-year sea states) are estimated using Peak-Over-Threshold method. We catalogue the peaks above a given threshold (typically 0.5 to 0.75 of the maximum significant wave height of the given time record). The peaks we choose must be separated by at least 48 hours (this is our subjective criteria to insure independent storm events). If there are two peaks within a ±48-hour window, then we only retain the largest peak within the window. We calculate the cumulative probability distribution for the peaks above our threshold such that $Pr(H_s \leq H_t) = 0$ where H_s is the significant wave height and H_t is the threshold and $Pr(H_s \leq H_m) = 1 - 1/(N+1)$ where H_m is the maximum peak and N is the total number of peaks above the threshold. Generalized Pareto Distributions are fitted to the measured distributions corresponding to different thresholds. Goodness of fit criteria is applied to the different threshold distributions, and this used to determine the parameters for the Generalized Pareto Distribution to use in estimating 10, 30, and 100-year sea states. The input cumulative probability for a N-year sea state is given by 1-1/(N*m) where m is the average number of peaks per year above the given threshold.

Recent analyses published by Ruggiero et al. (2010) argue that significant wave heights have increased off the Pacific NW when viewed using different statistics. Buoy data have been analyzed to assess this response in the wave climate by employing various time-dependent extreme value models that directly compute the progressive increases in the 25- to 100-year projections. The results depend somewhat on the assumptions made in the statistical procedures, on the numbers of storm-generated SWHs included, and on the threshold value for inclusion in the analyses, but the results are consistent with the linear regressions of annual averages and the observed shifts in the histograms. (P. Ruggiero et al. / Coastal Engineering 57 (2010) 539–552)

10, 30, and 100-Year Wind

Extreme wind events are determined in the same manner using Peak-Over-Threshold method. The wind data comes from satellite reanalysis studies and from surface buoy measurements.

Appendix B

Science Document from NE Pacific RFA

2. Scientific Objectives

This section is organized into scientific themes spanning the spatial and temporal scales of interdisciplinary ocean science. The emphasis is on experiments and objectives targeted at water-column processes over the continental margin forced by air-sea interactions, freshwater buoyancy inputs and through interaction with North Pacific circulation. In the following section on experimental design and observing requirements, we propose a set of observatory elements to address the scientific objectives that arise from the three thematic topics listed above.

2.1 Large-scale Transport of Water and Biogeochemical Properties

The regional oceanography of the PNW continental margin is influenced by the bifurcation of the North Pacific Current, and by the seasonally varying, strong north-south boundary currents: the California Current, the California Undercurrent and the Davidson Current (**Fig. 1**). The California Current is a surface-intensified, equatorward current that can reach speeds of 0.5–1.0 m s^{-1} and extends into the water column down to 500–1000 m. The California Undercurrent is a subsurface poleward current with a core at 200 m and an average speed of 0.15 m s^{-1}. The Davidson Current is a strong (up to 1 m s^{-1}) poleward, surface-intensified flow found over the continental shelf and slope in winter. These currents transport heat, salt, nutrients, dissolved oxygen, plankton, and invertebrate larvae north and south and are crucial to the ecosystem response in this region. The eastern boundary currents exhibit variability on a variety of time scales from the 2–5-day event time scale, through the seasonal time scale to interannual (El Niño/La Niña) and interdecadal [Pacific Decadal Oscillation (PDO)] variability.

The California Undercurrent extends along the upper continental slope of the entire US west coast and is relatively difficult to observe given its subsurface nature. This large-scale feature transports nutrient, salt, heat and plankton and larvae hundreds to thousands of kilometers along the coast. The undercurrent transport responds to interannual variability (Huyer et al., 2002) and provides a portion of the high-nutrient source water that is upwelled seasonally onto the continental shelves. In contrast to the US east coast, very few nutrients (iron being an exception) are provided to the PNW coastal ocean by river plumes. The undercurrent has been invoked as a possible mechanism for transporting phytoplankton seed stock as well as fish larvae throughout the region. On the other hand, because the flow in the undercurrent is oppositely directed from surface flows, it has been suggested that vertically migrating zooplankton may use the undercurrent to maintain a regional location (Swartzman et al, 2005). In spite of these important attributes, long term (> a few months) measurements in the undercurrent are almost nonexistent.

Besides being influenced by advective fluxes, PNW waters are affected by interannual changes originating in the tropical Pacific and communicated northward by coastally trapped waves. One example is deepening of the pycnocline and hence nutricline during El Nino years. We propose to combine observations from the PNW region (see section 3) with those from farther south (Pacific Coast RFA response) to examine this process.

A multi-faceted approach will be used to obtain the necessary in-situ measurements of the control volume encompassing the northeast Pacific continental margin. Within the control volume in deep water, acoustic tomography will be used to measure the low-wavenumber

synoptic flow and temperature fields. A set of east-west and north-south lines forming a control volume encompassing the northeast Pacific continental margin will be sampled with autonomous underwater vehicle gliders to obtain long-term, repeated measurements of upper-ocean volume transport and water property flux. Two heavily instrumented, multi-parameter east-west Endurance Lines of moorings will provide unprecedented, year-round, long-term time series. The combination of these three methodologies will allow us to address scientific questions related to large-scale eastern boundary current transport.

Important questions include:

- What is the spatial and temporal variability of the meridional transport of physical and biogeochemical properties (from the 2–20-day weather band to interannual and interdecadal)?
- What is the relationship between meridional transport and large-scale forcing by the wind and/or alongshore pressure gradients?
- How do the depth of the nutricline and its concentration of macronutrients affect coastal primary productivity?
- Is the California Undercurrent important for maintenance and/or spread of biological populations?
- What influences the time variability of the bifurcation of the North Pacific Current and how does its variability affect ecosystem response in PNW waters?

2.2 Large-Scale Along-Coast Gradients in Productivity and Community Structure

The general patterns of productivity and community succession in upwelling systems are well-known. Upwelling characteristics include an onshore to offshore progression from phytoplankton-poor newly upwelled water, to a highly productive diatom bloom, followed by nutrient exhaustion and smaller phytoplankton better suited to stratified conditions (Margalef, 1978). Sustained relaxation and downwelling conditions are typified by lower productivity and dominance by non-diatom phytoplankton. Superimposed on this simplified pattern, however are complex hydrographic and event scale changes which affect plankton community structure, trophic pathways, and carbon export in ways that are poorly known for most upwelling systems. For instance, under El Nino conditions, upwelled water off the Oregon coast is dominated by small pico (<2 um) and nanophytoplankton (Hood et al. 1992; Corwith and Wheeler, 2002), rather than large diatoms. Species and size-structure of the phytoplankton largely determine trophic pathways and carbon export (e.g. Michaels and Silver, 1988), which can change on times scales of days to weeks. At present, our knowledge of how the ecosystem responds to changes (seasonal, event, decadal) in the PNW system is limited by the sparseness of species-level observations with adequate temporal and spatial resolution.

Although both are upwelling systems, the productivity regimes on the Washington and Oregon coasts have many apparent, but not well understood, differences. For instance, chlorophyll is generally higher toward the north, as shown by seasonal time series of vertically integrated chlorophyll (Landry et al., 1989), satellite-derived ocean color (Strub et al., 1990; Thomas and Strub, 2001) and a dozen recent surveys of this region (Peterson, pers. comm.). The limited data available suggest that primary productivity follows the same spatial pattern, and is particularly surprising because the alongshore wind stress responsible for macronutrient supply (Huyer, 1983) increases in the opposite direction to the productivity. Nevertheless, the seasonal

variation in macronutrient supply to the mid-shelf does not differ substantially between the two regions (Landry et al., 1989), a possible consequence of enhanced upwelling from submarine canyons that indent the Washington shelf edge (Hickey, 1997). Model studies (Allen et al., 1995) show that a wider, gently sloping shelf results in slower circulation (i.e., possibly greater retention) and that the upwelling flow tends to be more concentrated in the bottom boundary layer than in steeper regions (hence more inflow from the richest layers and more bottom contact for micro-nutrient supply). Thus, the fact that the width of the shallow nearshore (<100 m deep) widens by more than a factor of two north of the Columbia mouth might contribute to the apparently similar levels of macronutrients across the region. However, it would not readily explain the higher primary productivity to the north.

Greater secondary productivity (e.g., in euphausiids and copepods; Landry and Lorenzen, 1989) is also observed off the northern WA coast and near the Columbia plume. Recent studies show that the abundance of euphausiid eggs is always higher (~700%) on the Washington shelf compared to the Oregon shelf (Peterson, pers. comm.) although zooplankton communities are similar on the two shelves (Peterson et al., 1979; Landry and Lorenzen, 1989). Juvenile salmon are more abundant on the northern coast and in the plume (Pearcy, 1992). Information on microzooplankton in the region is not yet sufficient to discern along-coast gradients, but substantial biomass of ciliates and heterotrophic dinoflagellates have been recorded on both the Washington coast (Chester, 1978; Landry and Hassett, 1982; Landry and Lorenzen, 1989; Lessard, unpubl.) and in upwelling waters off Oregon (Neuer and Cowles, 1994; Sherr and Sherr, 2002). As microzooplankton are the dominant herbivores in most coastal planktonic food webs (e.g., Neuer and Cowles, 1994; Strom et al., 2001), their biomass and grazing activities are key components to understanding trophic consequences of variations in phytoplankton structure and productivity.

Important questions include:

- Is phytoplankton community structure and productivity similar over the entire PNW?
- How does phytoplankton community structure change with event, season, year, and decades? Why does it change?
- How do bacteria, micro- and macrozooplankton biomass and community structure change over time/space? How are changes related to phytoplankton community structure?
- Are water property changes caused by local variation in forcing, changes from along the coast, or imposed from offshore by basin-scale effects?

2.3 Mesoscale Ecosystem Response in Two Contrasting Coastal Regions

The PNW coastline is relatively straight—thus jets, eddies and meanders that commonly occur off California are relatively less common (Hickey, 1998). Nevertheless two mesoscale features in the region have been shown to be of critical importance to the regional ecosystem. Both of these features – Heceta Bank off central Oregon and the JdF Eddy off northern Washington and southern Vancouver Island – modify circulation and local nutrient supply and enhance local productivity in their vicinity. The JdF eddy, located off the mouth of the Strait of JdF, is a seasonal feature caused by the interaction of flow exiting the Strait, the shelf edge coastal jet and the underlying topography (Tully, 1942; MacFadyen et al., 2005). Water transiting this eddy is ejected into the large-scale southward coastal jet system under upwelling conditions, subsequently moving southward.

2.3.1 Flow-Topography Interaction and Ecosystem Response over Heceta Bank, Oregon.

Recent studies off Oregon have revealed the importance of flow-topography interaction between the wind-driven coastal upwelling jet and a large submarine bank, Heceta Bank (Oke et al., 2002b; Castelao and Barth, 2005a; Barth et al., 2005a,b). Hydrographic and velocity observations and numerical modeling results show that the wind-driven coastal upwelling jet increases its separation from the continental shelf downstream of Heceta Bank as the spring-summer upwelling season progresses (**Fig. 8**). This occurs because the cumulative seasonal input of wind energy has made the upwelling jet more inertial and less able to follow alongshore changes in bottom topography. Separation also occurs more readily when the intrinsic length scale of the flow (the Rossby radius of deformation) is close to the bank width as it is for flow over Heceta Bank (Castelao and Barth, 2006). As the equatorward upwelling jet follows the mid-shelf isobaths around Heceta Bank, it leaves a "lee" or shadow region on the inshore side where currents are weaker and retention times are greater (Barth et al., 2005a,b; Castelao and Barth, 2005a; Kosro, 2005). This allows local primary production to outpace advective loss so that intense phytoplankton blooms are found in this region (**Figs. 8 & 11**). Respiration of organic matter exported to depth is a likely contributor to hypoxia in bottom water over Heceta Bank (see section 2.4). The increased residence times may also allow blooms to persist, possibly depleting certain micronutrients or leading to physiological stress that may cause domoic acid production in some diatoms (see section 2.5).

The separated jet downstream of the Bank creates considerable cross-shelf transport of heat, salt and chlorophyll (carbon) and contributes significantly to the properties of the California Current System (CCS) (Barth et al., 2000; 2002; Strub and James, 2002). In contrast to the spring/summer upwelling condition, wintertime shelf flow is to the north in the Davidson Current and little is known about its interaction with bottom topographic features. It is, therefore, critical to understand the time-dependent flow-topography interaction that leads to cross-margin transport and the connection between the continental shelf and the adjacent deep ocean.

Important questions include:

- How does the flow field over a mesoscale bank depend on wind-forcing, flow strength, seasonality (i.e., flow direction) and ocean climate variability?
- What are the consequences of this variability in forcing for the coastal ecosystem (e.g., productivity, community structure, development of hypoxia)?
- What are the along- and cross-shelf fluxes of heat, salt and carbon created by flow interaction with a mesoscale bank region throughout the year?
- How are cross-shelf property fluxes partitioned between the bottom boundary layer and the geostrophic interior?
- How predictable are coastal circulation and ecosystem response on a mesoscale bank? What does this imply about observing system requirements for coastal forecasting?

2.3.2 River-Influenced Coastal Ocean Dynamics and Ecosystem Response

The PNW shelf has two primary sources of freshwater—the Strait of JdF to the north, and the Columbia River, in the center. Neither the Fraser nor the Columbia are significant sources of macro nutrients to the coastal ecosystem. Nevertheless both features are responsible for delivery of large amounts of nutrients to the coast—in both cases via mixing and entrainment of upwelled coastal waters. The nutrients fuel high plankton growth in the region offshore of the strait (MacFadyen et al., 2005) as well as off the mouth of the Columbia (**Fig. 4**). Much of the water exported from the Strait of JdF is entrained in the southward flowing coastal jet influencing the Washington shelf. The plume from the Columbia River is a dominant feature in the hydrography of the U.S. West Coast, transporting dissolved and particulate matter, phyto- and zooplankton, larvae, and contaminants hundreds of kilometers along and across the continental margin (Barnes et al., 1972; Grimes and Kingsford, 1996) (**Fig. 3**). The Columbia plume flows northward over the shelf in fall and winter, and southward offshore of the shelf in spring and summer. However, the plume also changes direction, thickness and width with every change in local wind stress magnitude or direction (Hickey et al., 1998, Garcia-Berdeal et al., 2002). Recent studies have shown that the Washington shelf is rarely without some remnant freshwater even in summer—the plume is frequently bi-directional (Hickey et al., 2005) (**Fig. 9**). At such times, upwelling is inhibited on the Washington coast (**Fig. 10**). Thus, the Washington shelf is influenced by two freshwater sources in summer; in contrast, the central Oregon shelf is influenced solely by the Columbia River although local river input of freshwater and macro- and micro-nutrients is likely important off Oregon in winter.

The Columbia River plume is turbid, providing better refuge from grazing for higher trophic levels. Deep mixing is inhibited by high stratification at the base of the plume, thus tending to keep plankton within the euphotic zone. Plumes alter regional near-surface current patterns, providing along-plume jets for rapid transport, and convergences and trapping at frontal boundaries on the edges. For juvenile salmonids, the strength of the river flow and plume size appear critical as they move from freshwater to saltwater (Pearcy, 1992).

The exchange and eventual fate of terrestrial freshwater input has an important influence on the coastal ocean and the adjacent ocean basin. The cross-margin exchange of fresh water injects a wide range of scalar properties to the shelf system, and adds buoyant water dynamics. Freshwater input also impacts global climate by changing upper-ocean stratification, which in turn affects heat and momentum fluxes between atmosphere and ocean. Our lack of understanding of these processes is reflected in the very crude methods used in GCMs to study climate and ocean-atmosphere interaction in response to the introduction of terrestrial freshwater to the open ocean (Lee et al., 2006).

Important questions include:

- How does a large point source of freshwater affect the dynamics of shelf circulation?
- What is the role of time varying freshwater input in structuring the ecosystem?
- How does the presence of a river plume affect cross-shelf transfer of plankton, local upwelling, grazing, HABs occurrence and nutrient supply?
- What is the fate of freshwater delivered to the PNW shelf on event to decadal time scales? To what extent does it impact the stratification and freshwater content of the greater ocean basins?

2.4 Hypoxia in the Pacific Northwest

A previously unappreciated form of interannual variability occurred off the US west coast during 2002 when an anomalous water mass of Subarctic origin "invaded" the region from the north (**Fig. 7**, right panel; **Fig. 11**, upper panels) (Freeland et al., 2003). These large-scale, interannual signals have profound influence on the upwelling source waters (from 50-150 m depth) for the central Oregon shelf. Changes in shelf water properties and circulation, from event scale to interannual, have significant impact on coastal ocean ecosystems. The upwelling of nutrient-rich water into the euphotic zone over the shelf results in high phytoplankton productivity (Small and Menzies, 1981) and flow-topography interaction can result in regions with intense, concentrated productivity (Barth et al., 2005a,b). The combination of anomalous low-oxygen, nutrient-rich source waters in 2002 led to enhanced phytoplankton production over Heceta Bank (**Fig. 11**, lower left) (Wheeler et al., 2004; Thomas et al., 2004). The anomalously strong Subarctic water signal entering the northern California Current was traced to anomalous atmospheric forcing in the Gulf of Alaska using Argo float and ship CTD data (Crawford et al., 2005).

The combination of low-oxygen source water and microbial respiration of sinking phytoplankton material led to hypoxic conditions in the lower water column off central Oregon (**Fig. 11**, lower right panel) (Grantham et al., 2004). The hypoxia event lasted at least 60 days and there was significant die-off of Dungeness crabs and rockfish (Grantham et al., 2004). Time series on the Washington shelf indicate that near-bottom waters also were likely hypoxic during this event. Similar hypoxic conditions were observed off the central Oregon coast during summer 2004 with significant crab die-offs but relatively little impact on fish (F. Chan, H. Weeks, pers. comm.). In 2004, source water characteristics were statistically indistinguishable from average conditions, hinting at the increased importance of local respiration and retention versus anomalous source waters in creating low-oxygen shelf water. Having year-round, nearly continuous, long-term measurements of subsurface water properties, including chlorophyll fluorescence and dissolved oxygen, will allow us to more definitively assess the role of physical, chemical and biological processes in these important ecosystem changes.

Important questions include:

- What is the alongshore and temporal variability of coastal hypoxia in the PNW?
- What drives the invasion of anomalous Subarctic Water into the northern CCS?
- What are the relative contributions of low-oxygen, nutrient-rich source water versus local respiration in driving shelf waters hypoxic in the northern CCS?
- What wind conditions are optimal for retention of productive waters over Heceta Bank and subsequent intense phytoplankton blooms and hypoxia?

2.5 Harmful Algal Blooms

During the past decade the economic consequences of harmful algal blooms on fisheries and ecosystem health have been severe along the U.S. west coast. For example, the closure of Washington State beaches in 1991 to recreational and commercial shellfish harvesting due to high domoic acid concentrations in shellfish resulted in a $15-20 million revenue loss to local fishing communities (Horner and Postel, 1993). Domoic acid (DA), which is produced by several species of the diatom *Pseudo-nitzschia,* causes amnesic shellfish poisoning in mammals, including humans, resulting in severe neurological effects and even death. The commercial

Dungeness crab industry on which the Quileute Indian tribe depends for employment lost 50% of their income in 1998 due to harvest closures. The entire razor clam harvest of the Quinault tribe, on which they depend for both subsistence and commercial revenue, was again lost in the fall of 1998 (Trainer and Wekell, 2000). A survey of domoic acid along the entire U.S. west coast continental shelf in summer 1998 suggests a strong relationship between DA concentration and mesoscale topographic features (**Fig. 12**). Off northern California where large coastal promontories and hence rapid offshore transport occur, DA levels are low. Offshore of the Strait of JdF, over Heceta/Stonewall bank in Oregon, offshore of Monterey Bay (inshore of the Farallone Islands) and near the Santa Barbara Channel, DA levels are higher. One common characteristic of high DA regions is their capacity to have longer retention times than other coastal regions. The seasonal JdF eddy has been shown to be an initiation site for toxic blooms of *Pseudo-nitzschia* (Trainer et al., 2002). These toxic blooms are advected south of the eddy in the coastal jet and are transported onto the coast during periods of downwelling (MacFadyen et al., 2005). Incidents of paralytic shellfish poisoning, caused by the dinoflagellate *Alexandrium*, also leads to frequent shellfish closures in the PNW. Outbreaks of HABs have been increasing in frequency worldwide as well as in the PNW (Anderson, 1995), reinforcing the public health needs for sustained observations of these phenomena and the conditions that initiate them.

Important questions include:

- Are HABs increasing in time over the open shelf, or is it simply that transport to shore (where we see its impacts) is increasing?
- Are HABs tied to specific geographic sites and if so, why?
- What aspects of ecosystem variability lead to onset of HABs?

2.6 Carbon Dynamics and Cross-Margin Flux

It has long been recognized that the upwelling margins of the North East Pacific (NEP) are highly productive regions. What had not been recognized until recently, however, is how important these regions might be to air-sea CO_2 exchange and deep ocean carbon sequestration. In fact, the carbon dynamics of the margins of the North American continent are poorly understood and are under sampled to the point that it is uncertain whether or not the margins are a net source or sink of atmospheric CO_2. Some studies have suggested that the “continental shelf pump” could be responsible for as much as 1 Pg C yr^{-1} sink globally. A recent analysis using satellite data suggests that the margins may be responsible for more than 40% of carbon sequestration in the ocean [*Muller-Karger et al.*, 2005]

On much of the west coast, summer-time upwelling brings high-pCO_2 water as well as abundant pre-formed nutrients to the surface. As a result, photosynthetic uptake often depletes upwelled nutrients and drives surface–water pCO_2 to very low levels. This can make such regions large local net sinks for atmospheric CO_2, as observed by Hales et al. (2005). In other cases (Friederich et al., 2002) biological demand is insufficient to take up the excess CO_2 in upwelled waters and such areas are net sources of CO_2 to the atmosphere. The relative importance of upwelling of high-pCO_2 waters versus rapid biological consumption of excess nutrients, and the resulting effect on air-sea CO_2 exchange has been shown to affect the chemistry of marine airmasses impinging on the North American continent (Lueker et al., 2003). The degree to which these same upwelled waters carry and exchange methane from benthic

sources on the shelf and upper slope is also unknown but this process might constitute a significant source of methane to the atmosphere (Heeschen et al. 2005; Collier and Lilley, 2005).

More recently, using budgets of oxygen and particulate organic carbon (POC) in the same region, Hales et al (2006) showed that essentially all of this newly-produced carbon appears to be exported from the shelf, probably to the deep ocean where it is sequestered for centuries or longer. Hales et al. (2006) suggested a mechanism whereby modulation of the frequency and intensity of upwelling-favorable conditions on timescales of several days could lead to frequent events where POC suspended in the bottom-boundary-layer was transported to the shelfbreak and subsequently sunk into the deep ocean. In summary, carbon is just one of many water properties (others include nutrients, fresh water, dissolved oxygen, plankton) for which we require a more quantitative understanding of its cross-margin flux.

Important questions include:

- Is the coastal margin of the NEP ocean a net sink or source of atmospheric CO_2?
- Within the PNW, how does carbon export vary with shelf width, river influences, nutrient supply and shelf break topography?
- How does carbon export to the sediments change over time?
- What are the carbon export mechanisms from the shelf to the deep sea and how do they change over time?

2.7 Tidally Generated Internal Bores and Nonlinear Internal Wave Packets

Tidal forcing provides a continuous source of energy to the coastal ocean. With improved modeling capability and increased bathymetric resolution the prediction of barotropic tidal elevation and currents off Oregon are becoming increasingly more accurate. However, the internal tide is more complicated and will require in situ observations in order to make advances in a predictive capability. Internal tides are internal waves generated in a stratified ocean by the interaction of tidal driven flow with topography. The continental slope serves as an effective generator of internal tide propagating cross-shelf. As it propagates and shoals, the internal tide becomes nonlinear, and often develops into an internal bore accompanied by an energetic packet of high-frequency oscillations (sometimes called solitons, solitary waves or solibores) (e.g., Liu 1988; Sandstrom and Oakey 1995; Henyey and Hoering 1997) (**Fig. 13**). As the bore and nonlinear wave packet continue to shoal, energy is dissipated and vertical mixing occurs. This mixing may play an important role in the circulation of the coastal ocean and is currently not included in regional modeling efforts. The nonlinear wave packets may also serve as an important mechanism for cross-shelf transport – onshore advection of particles in the upper water column and the simultaneous offshore advection at depth (e.g., Lamb 1997). This process may be important in both larval recruitment and sediment transport (e.g., Bogucki and Redekopp 1999, Shanks 1988). The internal tide is not as predictable as the barotropic tide as it is sensitive to the vertical and horizontal stratification which varies at low frequencies. The presence of jets and eddies will also affect the propagation and evolution of the internal tide. In winter when shelf waters are more mixed than in summer and the foot of the downwelling front is on the outer shelf, nonlinear internal wave of elevation can propagate along the near-bottom density interface (**Fig. 14**). Observations of summertime nonlinear internal waves of depression have been limited to short-term ship (several days) and moored (tens to 100 days) measurements, while wintertime bottom wave packets have rarely been documented (Klymak and Moum 2003).

Important questions include:

- What are the background and tidal conditions that lead to the generation of internal bores and nonlinear internal wave packets?
- How do these features evolve as they propagate across the shelf?
- What is their contribution to cross-shelf transport, sediment resuspension and mixing?

2.8 Flow Interaction with Hydrate Ridge Methane Source

The Newport Hydrographic Line (44.6N), occupied since the early 1960s, is located just to the south of Hydrate Ridge, an offshore topographic feature with well-characterized seafloor gas hydrates and methane seeps (eg.Suess et al., 2001, Torres et al. 2004, Trehu et al., 2004). When methane enters the water column at 600-800 m, it is subject to transport by the local circulation (Heeschen et al., 2005) (**Fig. 15**). This opens the possibility for some very synergistic experiments, namely the use of methane to trace water circulation and the predictions of the methane's fate based on knowledge of local circulation processes. For example, Rehder et al. (2002) show how out-gassed methane is brought to the surface by wind-driven coastal circulation. This accelerates the transport of methane from the seafloor to the atmosphere where methane plays a strong role as a greenhouse gas. It has also been recognized that shallower, active methane sources on the Heceta Bank complex provide methane fluxes that may be greater or equivalent to those from the deeper hydrate system (Collier and Lilley, 2005). While Rehder et al. (2002) demonstrated the existence of this process, long-term, year-round measurements are needed to quantitatively assess the importance of this link between a sub-seafloor process and ocean-atmosphere dynamics.

We propose to link our Endurance Array off Newport, Oregon, to biogeochemical studies proposed for Hydrate Ridge (see RFA response by Trehu et al.). By using the same observatory elements, specifically a cable providing power and communications, we can fully observe both sub-seafloor and water column processes. Although gas hydrates are found in many places on the world's continental slopes and some locations have been well-studied from a geological and chemical point-of-view, Hydrate Ridge is unique in being collocated on a long-time hydrographic line anchoring a region with high ecological interest.

Figures

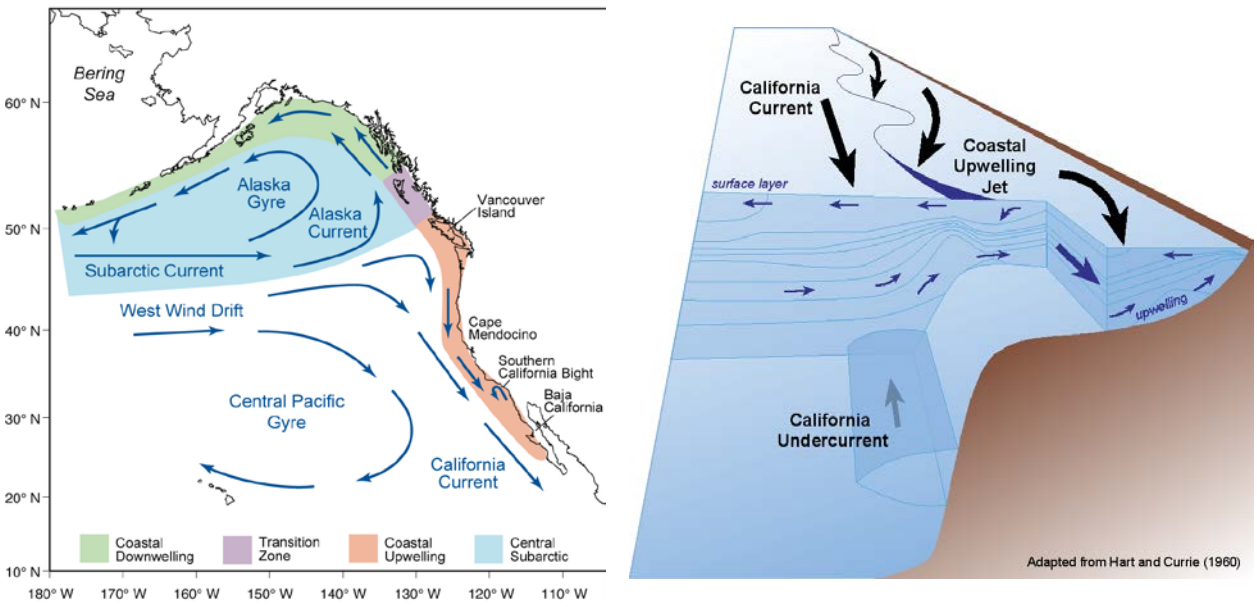

Figure 1: (left) Regional circulation in the northeast Pacific. (right) Eastern boundary current system of equatorward and poleward flows off the Pacific Northwest coast.

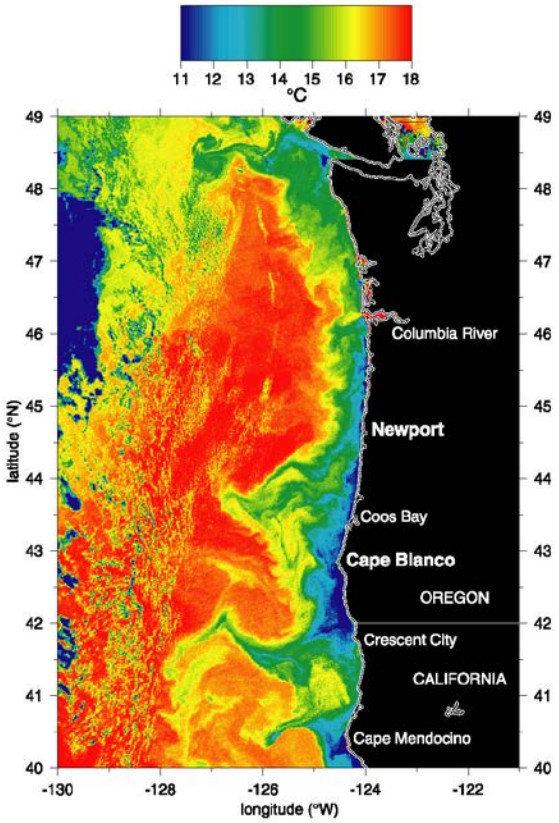

Figure 2: (left) Sea-surface temperature during summer showing cold upwelled water near the coast along the PNW coast. (right) Bottom bathymetry off the PNW.

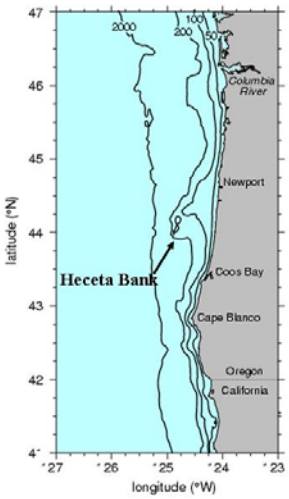

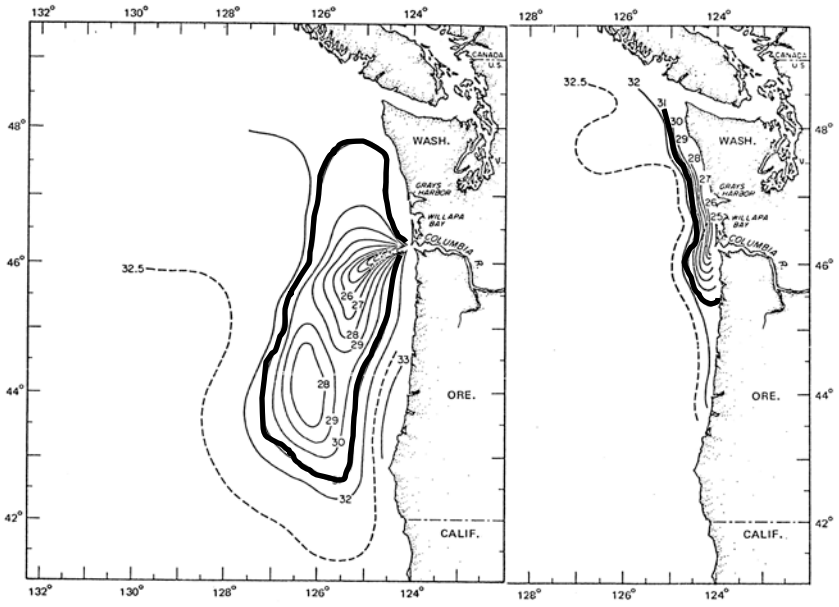

Figure 3: Sea-surface salinity during (left) summer and (right) winter showing the influence of the Columbia River outflow. The 31 isohaline is bold. (After Barnes et al., 1972)

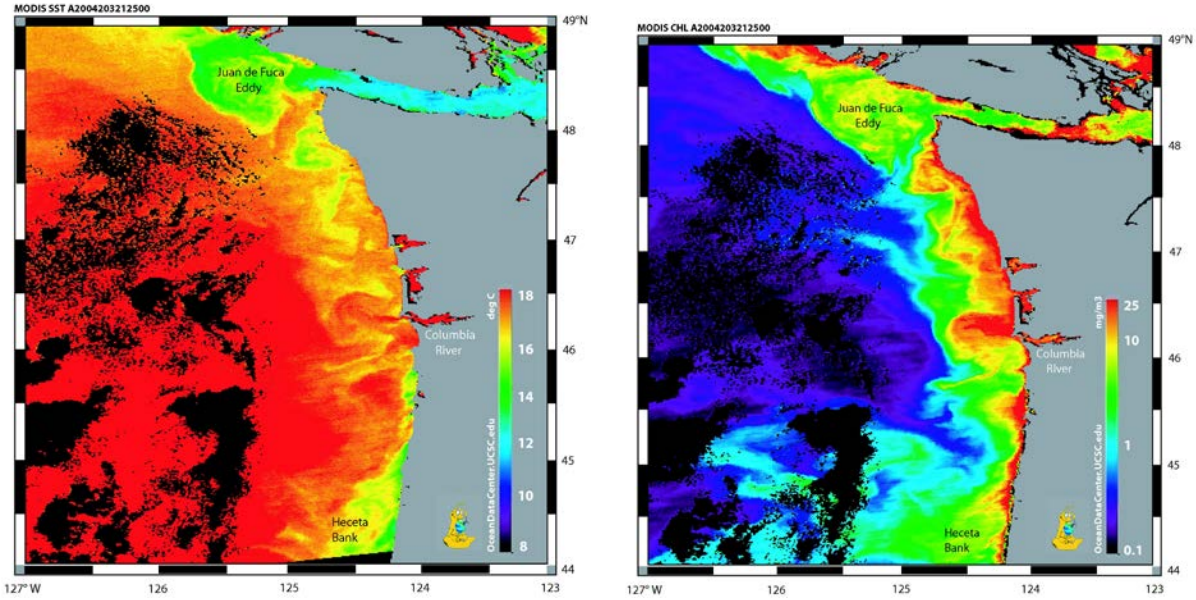

Figure 4: July 2004: Satellite SST from July 2004 showing upwelling in the south along the Oregon coast, the Juan de Fuca eddy off the Strait of Juan de Fuca and the Columbia River plume influences on the Washington shelf. (right) Satellite-based chlorophyll estimates showing large-scale gradients along the PNW coast and the Columbia River plume influence. (Courtesy of R. Kuedela.)

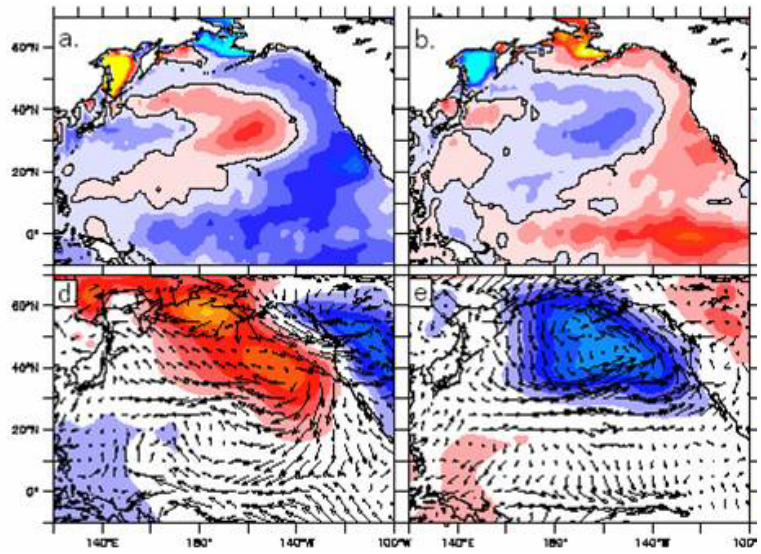

Figure 5: (top) Sea-surface temperature anomalies averaged over Nov-Feb from (left) cool (1970-1976) and (right) warm (1977-1983) phases of the Pacific Decadal Oscillation. (bottom) Anomalies of sea level pressure (color) and winds for the same time periods. (After Peterson and Schwing, 2003.)

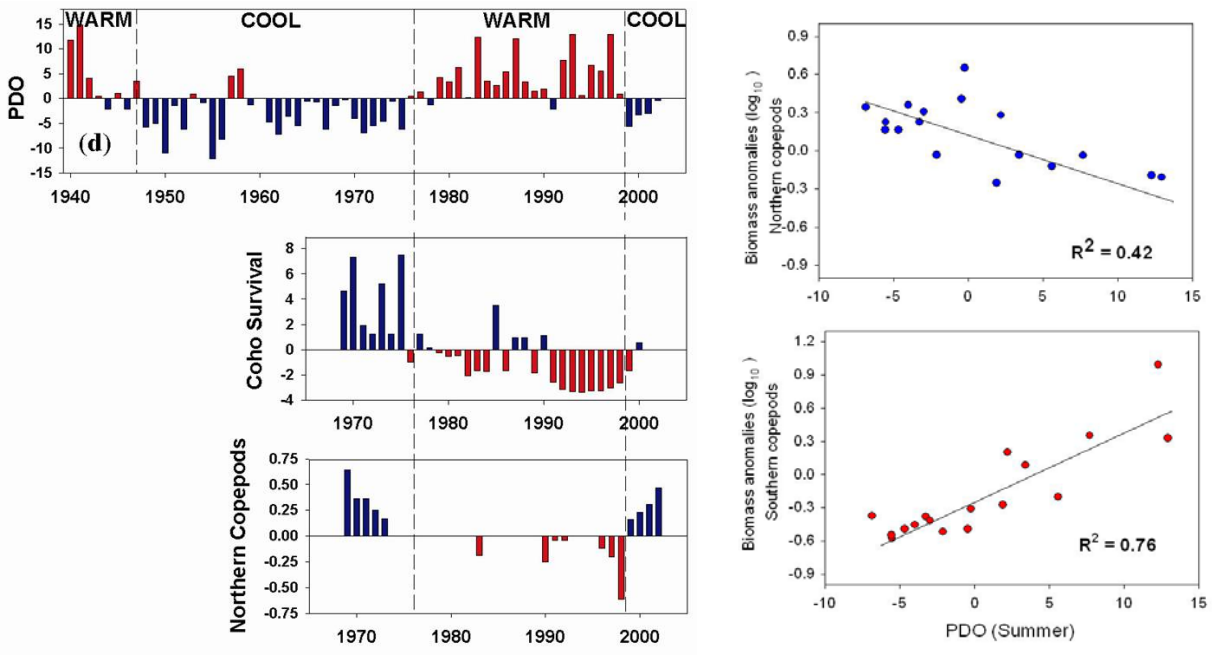

Figure 6: (left) Time series of (top) the PDO index summed annually over May-Sep, (middle) coho salmon survival and (bottom) biomass anomalies of cold-water copepod species. (right) Biomass anomalies of (top) northern and (bottom) southern copepod species versus the summer PDO index. (From Peterson and Schwing, 2003 and Peterson, unpublished data.)

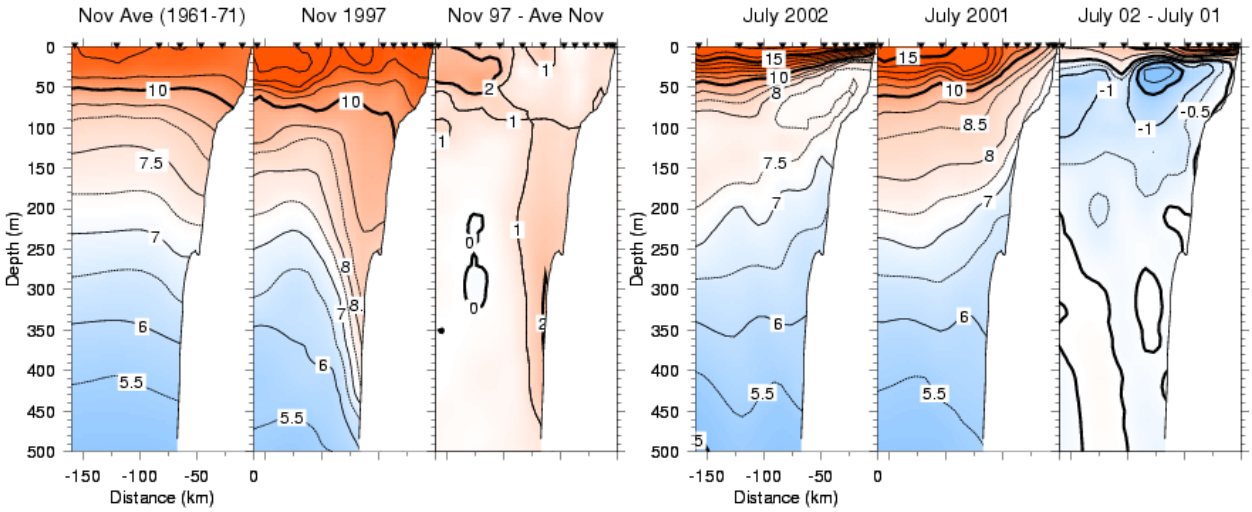

Figure 7: Vertical sections of temperature off Newport, Oregon during the (left) 1997 El Nino and the (right) 2002 Subarctic Invasion. (From Huyer et al., 2002 and Freeland et al., 2003.)

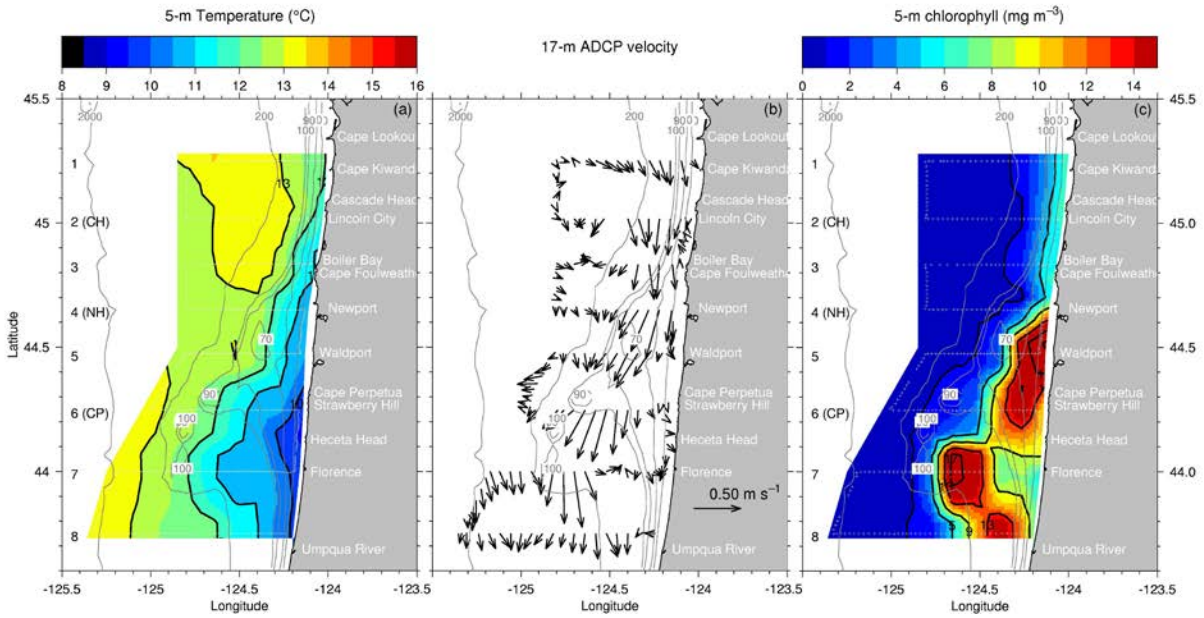

Figure 8: Maps of near-surface temperature, velocity and chlorophyll over Heceta Bank off central Oregon during spring 2001. (From Barth et al., 2005.)

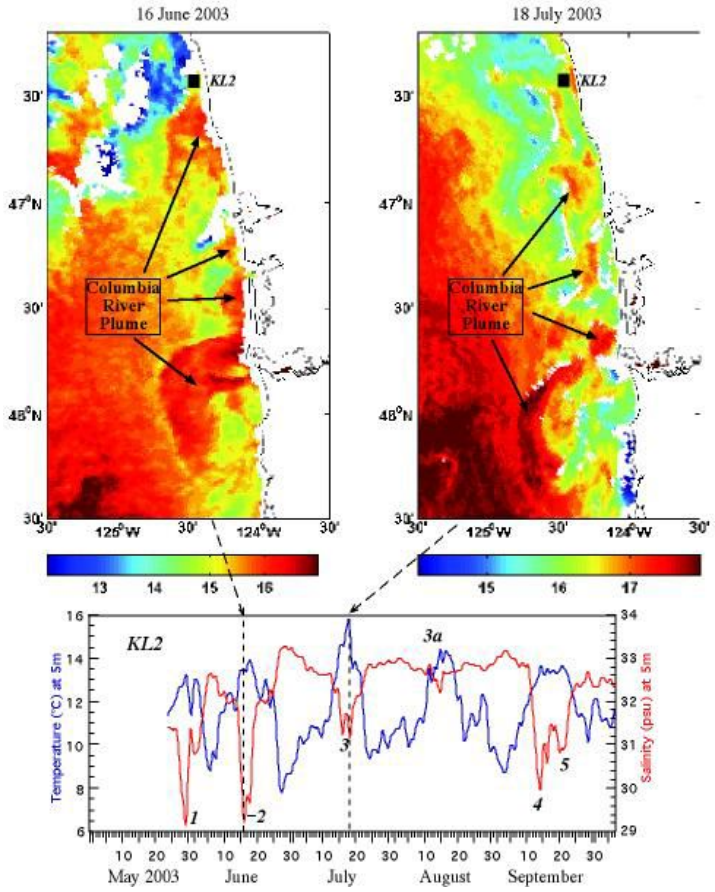

Figure 9: Example of summertime bi-directional Columbia plume as seen in satellite-derived sea surface temperature. This phenomenon occurs frequently in summer months, with new plumes developing off WA each time a storm passes through the region. The setting with respect to temperature and salinity at 5 m on the inner shelf at KL2 is shown in the lower panel. Mooring location is shown on the satellite images. (From Hickey et al., 2005.)

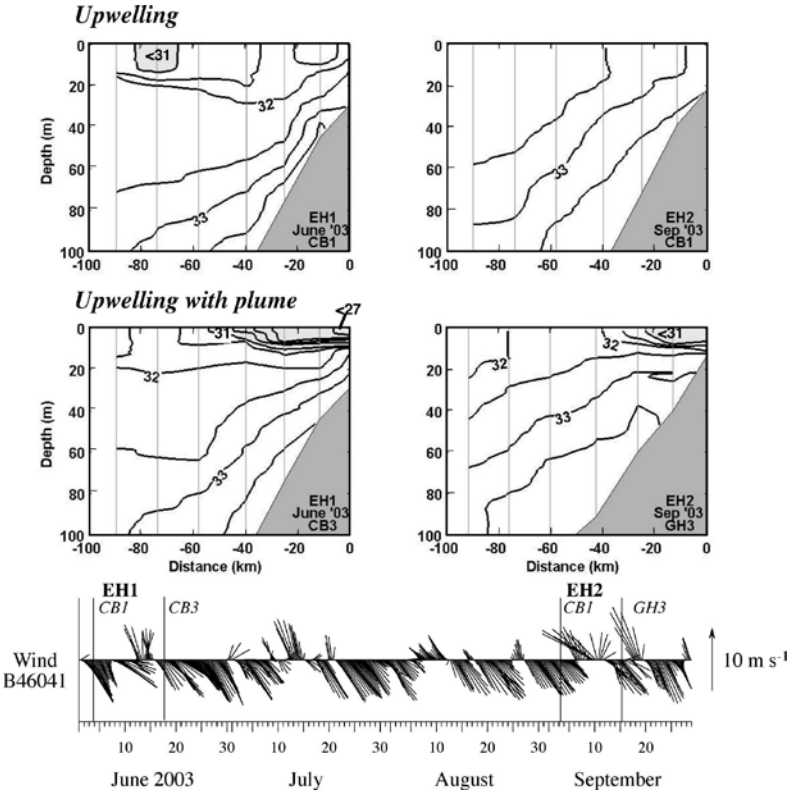

Figure 10: Contoured salinity sections across the central Washington shelf illustrating inhibition of upwelling by the Columbia plume. Data are shown at the end of several days of upwelling-favourable winds(upper panels) and during upwelling-favorable winds following a recent storm (lower panels) when a new plume has developed on the WA shelf. To provide the environmental setting, vector wind time series (N-S-E-W frame) are also shown. (From Hickey et al., 2005.)

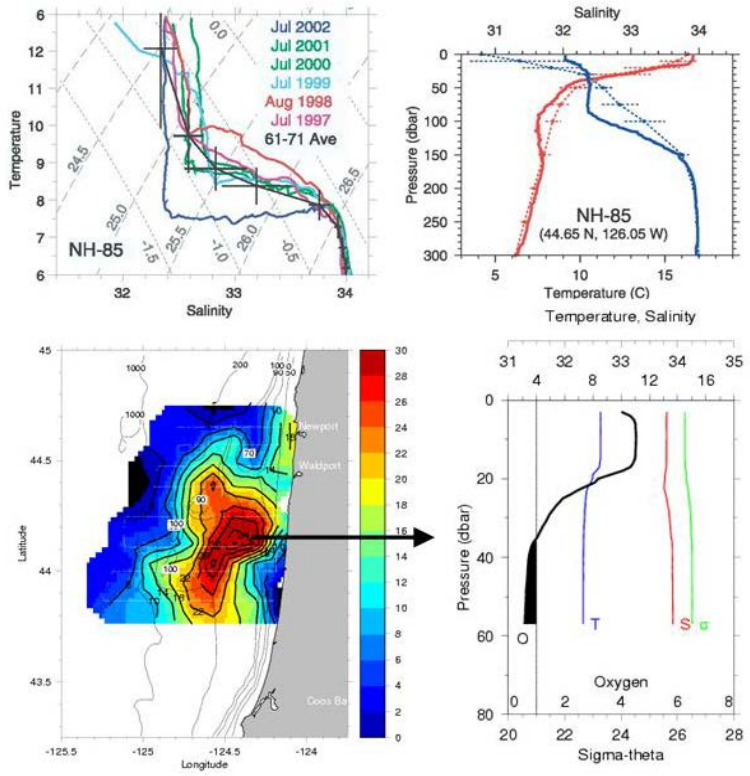

Figure 11: Subarctic water invasion and hypoxia over Heceta Bank in 2002: (upper left) T-S diagram on the Newport Hydrograhic (NH) line showing the anomalous, cold, fresh mid-depth water mass during summer 2002; (upper right) vertical profiles of temperature and salinity on the NH line showing anomalies between 25 and 150 m; (lower left) 5-m chlorophyll (mg m^{-3}) with maximum values in excess of 20 mg m^{-3} over Heceta Bank; and (lower right) vertical profiles at a station within the high chlorophyll feature over Heceta Bank showing hypoxic water within 20 m of the bottom (from Freeland et al., 2003 and Grantham et al., 2004).

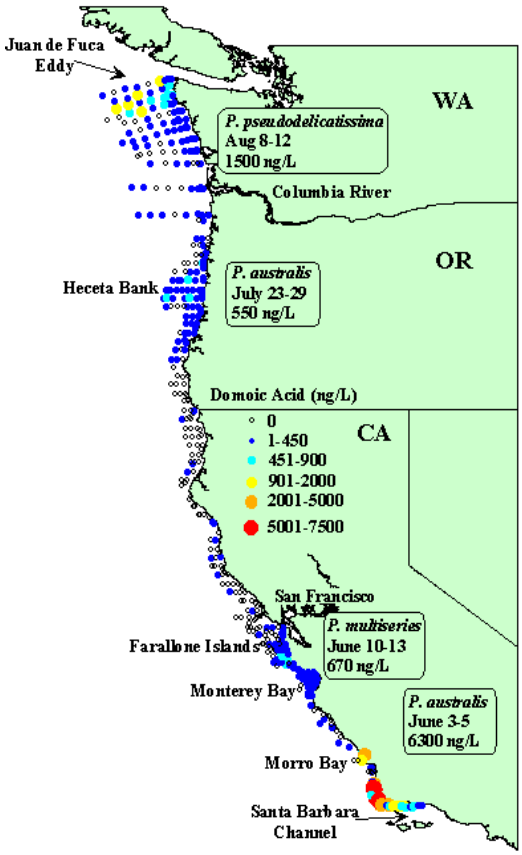

Figure 12. Particulate DA in *Pseudo-nitzschia* species on the U.S. West Coast in 1998. Maximum concentrations of DA and toxic species are indicated to the right of each area of high toxin. Each of these areas is associated with relatively retentive circulation patterns. (Hickey and Banas, 2003; data from Trainer et al., 2000, 2002).

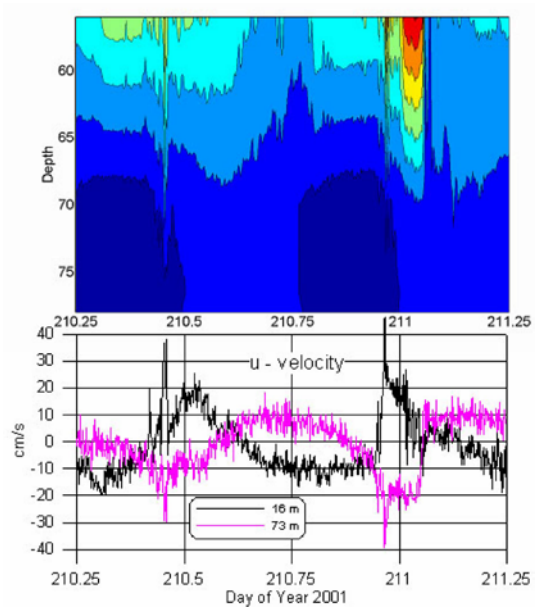

Figure 13: A one-day time series from an 80-m site on the Oregon shelf (45ºN). The cross-shelf component of velocity (u) shows a strong semidiurnal internal tide that is out of phase between 16 and 76 m (lower panel). The corresponding near-bottom temperature is also shown with 0.1ºC contour levels (upper panel). Sharp jumps in u and T indicate highly nonlinear internal waves (From Levine, unpublished data.)

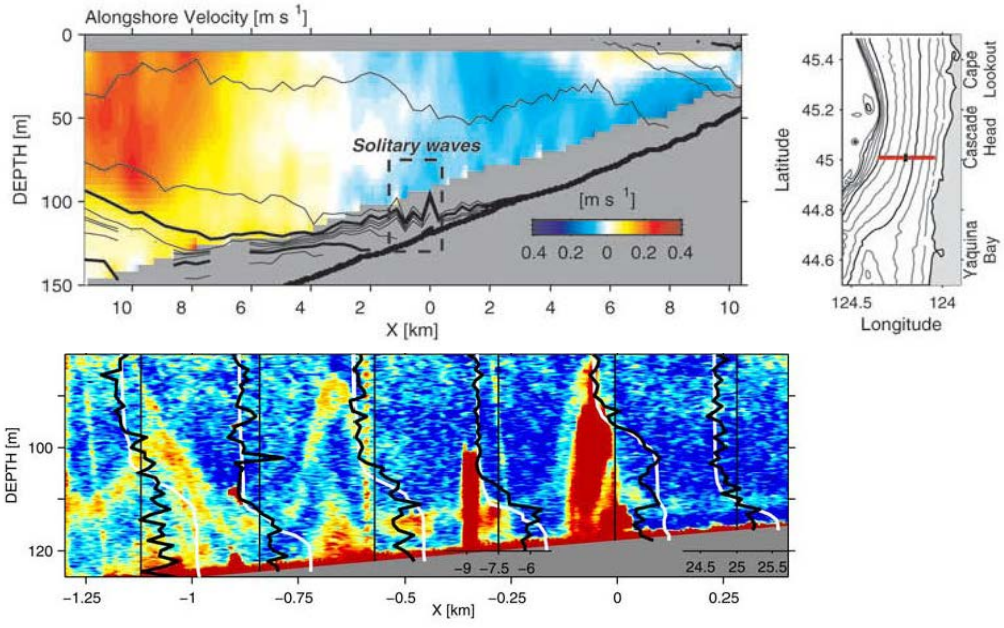

Figure 14: Near-bottom solitary waves observed during January 2003 off central Oregon. (top) Potential density and along-shelf velocity (color). (bottom) 120-kHz echosounder image (red is high intensity) with profiles of turbulent dissipation (black) and density. (From Klymak and Moum, 2003.)

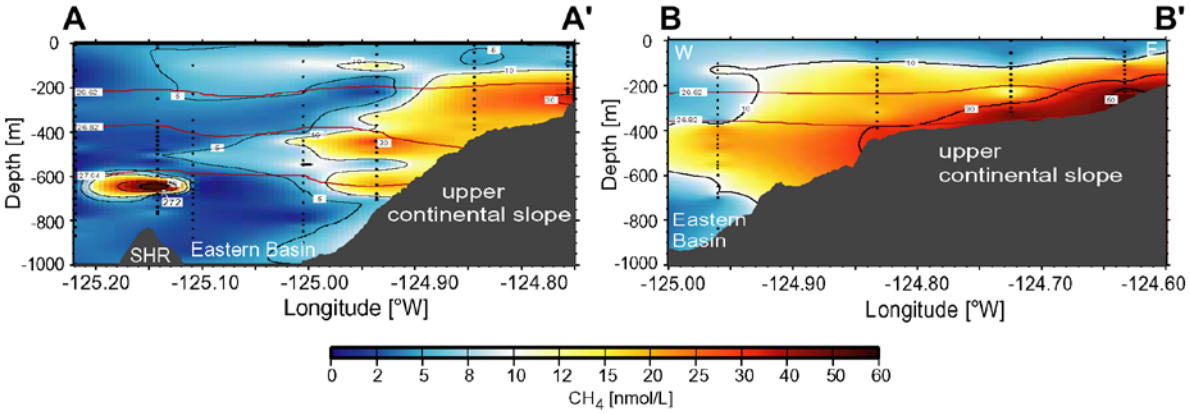

Figure 15: Methane concentrations along two hydrographic transects of the margin near the Newport Line (44.65N). Section A-A' spans from the upper continental slope out to Southern Hydrate Ridge (SHR) where intense deep plume associated with the hydrates can be seen. Section B-B' focuses on the upper slope and emphasizes the shallower sources, possibly associated with Heceta Bank and related slope seeps. (From Heeschen et al., 2005).

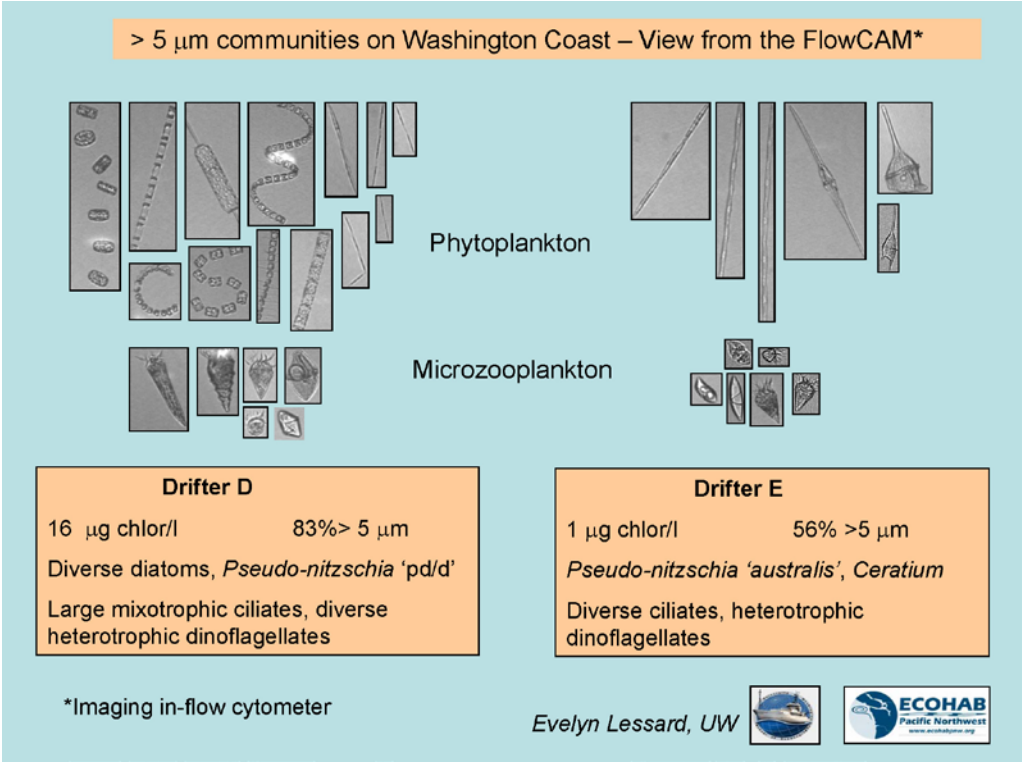

Figure 16: FlowCAM images showing representative phytoplankton and microzooplankton from two sites on the Washington coast, sampled one week apart in September, 2003. (Courtesy of E. Lessard, UW.)

References

Adams, N.G., M. Lesoing, and V.L. Trainer, 2000. Environmental conditions associated with domoic acid in razor clams on the Washington coast. J. Shellfish Res. 19: 1007–1015.

Allan J.C. and P.D. Komar, 2002. Extreme storms on the Pacific Northwest Coast during the 1997–98 El Niño and 1998–99 La Niña, *Journal of Coastal Research* 18, 175–193.

Allen, J.S., P.A. Newberger, and J. Federiuk, 1995. Upwelling circulation on the Oregon continental shelf 1. Response to idealized forcing. *J. Phys. Oceanogr., 25*, 1843-1866.

Anderson, D.M. (ed), 1995. ECOHAB. The ecology and oceanography of harmful algal blooms. A national research agenda. WHOI, Woods Hole, MA. 66pp.

Baptista, A.M**.**, Y. Zhang, A. Chawla, M. Zulauf, C. Seaton, E.P. Myers III, J. Kindle, M. Wilkin, M. Burla and P.J. Turner, 2005. A cross-scale model for 3D baroclinic circulation in estuary–plume–shelf systems: II. Application to the Columbia River. *Cont. Shelf Res.*, *25*(7–8)**,** *935–972.*

Barnes, C.A., A.C. Duxbury and B.-A. Morse, 1972. Circulation and selected properties of the Columbia River effluent at sea. Pp. 5–80 in "The Columbia River Estuary and Adjacent Ocean Waters," A.T. Pruter and D.L. Alverson (eds.), Univ. of Washington Press, Seattle, WA.

Barth, J.A., 1994. Short-wavelength instabilities on coastal jets and fronts. *J. Geophys. Res*., 99, 16095-16115.

Barth, J. A., S. D. Pierce and R. L. Smith, 2000. A separating coastal upwelling jet at Cape Blanco, Oregon and its connection to the California Current System. *Deep-Sea Res. II*, *47*, 783–810.

Barth, J.A., T.J. Cowles, P.M. Kosro, R.K. Shearman, A. Huyer and R.L. Smith, 2002. Injection of carbon from the shelf to offshore beneath the euphotic zone in the California Current. *J. Geophys. Res., 107(C6***),** doi:10.1029/2001/JC000956.

Barth, J. A., S.D. Pierce and T.J. Cowles, 2005a. Mesoscale structure and its seasonal evolution in the northern California Current System, *Deep-Sea Research II*, *52*, 5–28.

Barth, J.A., S.D. Pierce and R.M. Castelao, 2005b. Time-dependent, wind-driven flow over a shallow midshelf submarine bank. *J. Geophys., Res*, 110, C10S05, doi:10.1029/2004JC002761.

Batchelder, H.P., J.A. Barth, P.M. Kosro, P.T. Strub, R.D. Brodeur, W.T. Peterson, C.T. Tynan, M.D. Ohlman, L.W. Botsford, T.M. Powell, F.B. Schwing, D.G. Ainley, D.L. Mackas, B.M. Hickey and S.R. Ramp, 2002a. The GLOBEC Northeast Pacific California Current System program. *Oceanography*, 15(2), 36–47.

Batchelder, H.P., C.A. Edwards and T.M. Powell, 2002b. Individual-based models of copepod populations in coastal upwelling regions: implications of physiologically and environmentally influenced diel vertical migration on demographic success and nearshore retention. *Prog. Oceanogr*., *53*, 307–333.

Beardsley, R.C. and S. J. Lentz, 1987. The Coastal Ocean Dynamics Experiment collection: An introduction. *J. Geophys. Res., 92*(C2), 1455–1463.

Bograd, S.J., C.G. Castro, E. Di Lorenzo, D.M. Palacios, H. Bailey, W. Gilly, and F.P. Chavez, 2008. Oxygen declines and the shoaling of the hypoxic boundary in the California Current. *Geophys. Res. Lett.* 35: L12607, doi:10.1029/2008GL034185.

Bograd, S.J., and Lynn, R.J., 2001. Physical-biological coupling in the California Current during the 1997-99 El Niño – La Niña cycle, *Geophys. Res. Lett.*, 28, 275-278.

Bogucki, D. and L.G. Redekopp, 1999. A mechanism for sediment resuspension by internal solitary waves. *Geophys. Res. Let.*, 26, 1317–1320.

Brink, K.H., and T.J. Cowles, 1991. The coastal transition zone program, *J. Geophys. Res*., 96(C8), 14,637–14,647.

Castelao, R.M. and J.A. Barth, 2005a. Coastal ocean response to summer upwelling favorable winds in a region of alongshore bottom topography variations off Oregon. *J. Geophys. Res*., 110, C10S04, doi:10.1029/2004JC002409.

Castelao, R.M. and J.A. Barth, 2006. The relative importance of wind strength and along-shelf bathymetric variations on the separation of a coastal upwelling jet. *J. Phys. Oceanogr*., 36, 412-425.

Chan, F., J.A. Barth, J. Lubchenco, A. Kirincich, H. Weeks, W.T. Peterson, and B.A. Menge, 2008. Emergence of anoxia in the California Current large marine ecosystem, *Science*, 319, 920, doi:10.1126/science.1149016.

Chavez, F.P., Collins, C.A., Huyer, A., and Mackas, D.L., 2002. El Niño along the west coast of North America, *Prog. Oceanogr*., 54(1-4), 1-5.

Chelton, D.B., Bernal, P.A., and McGowan, J.A., 1982. Large-scale interannual and physical interaction in the California Current, *J. Mar. Res*., 30, 1095-1125.

Chester, A.J., 1978. Microzooplankton relative to a subsurface chlorophyll maximum layer. *Mar. Sci. Comm., 4*, 275-292

Chhak, K., and E. Di Lorenzo, 2007. Decadal variations in the California Current upwelling cells, *Geophys. Res. Lett*., 314, L14604, doi:10.1029/2007GL030203.

Chua, B.S. and A.F. Bennett, 2001. An inverse ocean modeling system, *Ocean Modeling*, 3, 137–165.

Collier, R. and M. Lilley, 2005. Composition of shelf methane seeps on the Cascadia continental margin, *Geophys. Res. Lett., 32,* L06609, doi:10.1029/2004GL022050.

Collins, C.A., N. Garfield, T.A. Rago, F.W. Rischmiller, and E. Carter, 2000. Mean structure of the inshore countercurrent and California undercurrent off Point Sur. *California. Deep-Sea Research II* **47**, pp. 765–782

Connolly, T. P., B. M. Hickey, S. L. Geier, and W. P. Cochlan, 2010. Processes influencing seasonal hypoxia in the northern California Current System, *J. Geophys. Res.*, 115, C03021, doi:10.1029/2009JC005283.

Corwith, H.L. and P.A.Wheeler, 2002. El Nino related variations in nutrient and chlorophyll distributions off Oregon. *Prog. in Oceanography, 54*, 361–380.

Crawford, W., P. Sutherland and P. van Hardenberg, 2005. Cold water intrusion in the eastern Gulf of Alaska in 2002. *Atmosphere-Ocean*, 43(2), 119–128.

Curchitser, E.N., D.B. Haidvogel, A.J. Hermann, E.L. Dobbins, T.M. Powell, and A. Kaplan, 2005. Multi-scale modeling of the North Pacific Ocean: Assessment and analysis of simulated basin-scale variability (1996–2003), *J. Geophys. Res.*, 110, C11021, doi:10.1029/2005JC002902.

Deng Y, 2009. Dominant Modes of Variability in the Western U.S. Coastal Cyclonic Activity: Dynamical Origins and Impacts on the Precipitation Characteristics Science and Technology Infusion Climate Bulletin. NOAA's National Weather Service 34th NOAA Annual Climate Diagnostics and Prediction Workshop, Monterey, CA, 26-30 October 2009.

Diaz, R.J. and R. Rosenberg, 1995. Marine benthic hypoxia: a review of its ecological effects and the behavioural responses of benthic macrofauna. Oceanogr. Mar. Biol. Ann. Rev. 33:245–303.

Díaz, R. and R. Rosenberg, 2008. Spreading dead zones and consequences for marine ecosystems, Science, 321, 926–929, doi:10.1126/science.1156401.

Dorman, C.E., and C.D. Winant, 1995: Buoy observations of the atmosphere along the west coast of the United States, 1981-1990, *J. Geophys. Res.*, 100, pp. 16,029-16,044.

Dushaw, B.D., P.F. Worcester, B.D. Cornuelle, B.M. Howe and D.S. Luther, 1995. Barotropic and baroclinic tides in the central North Pacific Ocean determined from long-range reciprocal acoustic transmissions, *J. Phys. Oceanogr*., 25, 631–647.

Dyson K., and D.D. Huppert, 2010. Regional economic impacts of razor clam beach closures due to harmful algal blooms (HABs) on the Pacific coast of Washington, Harmful Algae, 9(3), 264-271, DOI: 10.1016/j.hal.2009.11.003.

Egbert, G.D., A.F. Bennett and M.G.G. Foreman, 1994. TOPEX/POSEIDON tides estimated using a global inverse model. *J. Geophys. Res.*, 99(C12), 24821–24852.

Erofeeva, S.Y., G.D. Egbert and P.M. Kosro, 2003. Tidal currents on the central Oregon shelf: Models, data, and assimilation. *J. Geophys. Res.*, 108, 3148, doi:1029/2002JC001615.

Freeland H.J., G. Gatien, A. Huyer and R. L. Smith, 2003. Cold halocline in the northern California Current: An invasion of Subarctic water. *Geophys. Res. Lett*., *30(3),* 1131, doi:10.1029/2002GL016663.

Friederich, G.E., P.M.Walz, M.G. Burczynski and F.P. Chavez, 2002. Inorganic carbon in the central California upwelling system during the 1997–1999 El Niño–La Niña event. *Progress in Oceanography*, 54, 185–203

Gan, J. and J. S. Allen, 2002a. A modeling study of shelf circulation off northern California in the region of the Coastal Ocean Dynamics Experiment: Response to relaxation of upwelling winds. *J. Geophys. Res.*, 107(C9), 3123, doi:10.1029/2000Jc000768.

Gan, J. and J. S. Allen, 2002b. A modeling study of shelf circulation off northern California in the region of the Coastal Ocean Dynamics Experiment 2. Simulations and comparisons with observations. *J. Geophys. Res.*, 107(C11), 3184, doi:10.1029/2001JC001190.

Garcia-Berdeal, I., B. M. Hickey and M. Kawase, 2002. Influence of wind stress and ambient flow on a high discharge river plume. *J. Geophys. Res.*, *107*(C9), 3130-3154.

Gilbert, D., N.N. Rabalais, R.J. Díaz, and J. Zhang, 2010. Evidence for greater oxygen decline rates in the coastal ocean than in the open ocean, *Biogeosciences*, 7, 2283-2296, doi:10.5194/bg-7-2283-2010,

Grantham, B.A., F. Chan, K.J. Nielsen, D.S. Fox, J.A. Barth, A. Huyer, J. Lubchenco and B.A. Menge, 2004. Upwelling-driven nearshore hypoxia signals ecosystem and oceanographic changes in the northeast Pacific, *Nature*, 429, 749–754.

Grimes, C.B. and M.J. Kingsford, 1996. How do riverine plumes of different sizes influence fish larvae: Do they enhance recruitment? *Mar. Freshwater Res.*, *47*, 191–208.

Hales, B., T. Takahashi and L. Bandstra, 2005. Atmospheric CO_2 uptake by a coastal upwelling system *Global Biogeochem. Cycles*, 19, doi:10.1029/2004GB002295

Hales, B., L. Karp-Boss, A. Perlin, and P.A. Wheeler, 2006. Oxygen production and carbon sequestration in an upwelling coastal margin, *Global Biogeochem. Cycles*, 20, GB3001, doi:10.1029/2005GB002517.

Harbell, S., 2010. Towlane Charts, Cape Flattery to San Francisco: A Place to Tow/A Place to Fish, Year 2010 Edition. Available online at http://www.wsg.washington.edu/mas/pdfs/2010TowlaneCharts.pdf.

Hayes, S. P., and D. Halpern, 1976: Observations of internal waves and coastal upwelling off the Oregon coast. *J. Mar. Res*., 34, 247–267.

Heeschen, K.U., R.W. Collier, M.A. deAngelis, E. Suess, G. Rehder, P. Linke and G.P. Klinkhammer, 2005. Methane sources, distributions and fluxes from cold vent sites at Hydrate Ridge, Cascadia margin, *Global Geochem. Cycles*, 19, GB2016, doi:10.1029/2004GB002266.

Henyey, F. S. and A. Hoering, 1997. Energetics of borelike internal waves, *J. Geophys. Res.*, 102, 3323–3330.

Hickey, B. M., 1989: Patterns and processes of circulation over the shelf and slope. In *Coastal Oceanography of Washington and Oregon*, M. L. Landry and B. M. Hickey, eds. Elsevier, Amsterdam, pp. 41-115.

Hickey, B.M., 1997. Response of a narrow submarine canyon to strong wind forcing. *J. Phys. Oceanogr., 27*(5), 697–726.

Hickey, B. M., 1998. Coastal oceanography of western North America from the tip of Baja California to Vancouver Island. In *The Sea*, vol. 11, A. R. Robinson and K. H. Brink, eds., John Wiley & Sons, Inc.

Hickey, B.M. and N. Banas, 2003. Oceanography of the Pacific Northwest coastal ocean and estuaries with application to coastal ecosystems. *Estuaries*, 26(48), 1010–1031.

Hickey, B.M., L. Pietrafesa, D. Jay and W.C. Boicourt, 1998. The Columbia River Plume Study: subtidal variability of the velocity and salinity fields. *J. Geophys. Res.*, 103(C5): 10339–10368.

Hickey, B., S. Geier, N. Kachel, A. MacFadyen, 2005. A bi-directional river plume: The Columbia in summer. *Cont. Shelf Res*., 25 (14), 1631-1656, doi:10.1016/j.csr.2005.04.010.

Holladay, C.G., and J.J. O'Brien, 1975. Mesoscale variability of sea surface temperature, *J. Phys. Oceanogr*., 5, 761– 772.

Hood, R.R., S. Neuer and T.J. Cowles, 1992. Autotrophic production, biomass and species composition at two stations across an upwelling front. *Mar. Ecol. Prog. Ser.*, 83, 221–232.

Horner, R.A. and J.R. Postel, 1993. Toxic diatoms in western Washington waters (U. S. West coast). *Hyrdobiologica*, 269–270, 197–205.

Huyer, A., 1983. Coastal upwelling in the California current system. *Prog. Oceanogr., 12*, 259-284.

Huyer, A., 2003. Preface to special section on enhanced Subarctic influence in the California Current, 2002, *Geophys. Res. Lett.*, 30(15), 8019,doi:10.1029/2003GL017724.

Huyer, A., and R. L. Smith, 1985. The signature of El Niño of Oregon, 1982–1983, *J. Geophys. Res.*, 90, 7133– 7142

Huyer, A., R.L. Smith and J. Fleischbein, 2002. The coastal ocean off Oregon and northern California during the 1997–8 El Niño. *Progr. Oceanogr*., 54, 311–341.

Jessup, D. A., M. A. Miller, J. P. Ryan, H. M. Nevins, H. A. Kerkering, A. Mekebri, D. B. Crane, T. A. Johnson, and R. M. Kudela (2009), Mass stranding of marine birds caused by a surfactant producing red tide, PLoS ONE, 4(2), E4550, doi:10.1371/journal.pone.0004550.

Kahru, M., and Mitchell, B.G., 2000. Influence of the 1997-98 El Niño on the surface chlorophyll in the California Current, *Geophys. Res. Lett.*, 27, 2937-2940.

Kaluza, P., Kölzsch, A., Gastner, M.T. and Blasius, B., 2010. The complex network of global cargo ship movements. Journal Royal Society Interface 7: 1093-1103.

Keister, J. E., and P. T. Strub, 2008. Spatial and interannual variability in mesoscale circulation in the northern California Current System, *J. Geophys. Res*., doi:10.1029/2007JC004256.

Kilcher, L.F., and J.D. Nash, 2010. Structure and dynamics of the Columbia River tidal plume front, *J. Geophys. Res.*, 115, C05S90, doi:10.1029/2009JC006066.

Klymak, J.M., and J.N. Moum, 2003. Internal solitary waves of elevation advancing on a shoaling shelf, *Geophys. Res. Lett.*, 30, doi:10.1029/2003GL017706.

Kohut, J., S. Glenn, and D. Barrick, 1999. SeaSonde is integral to coastal flow model development, *Hydro Int.*, 3(3), 32–67, 4575900.

Kosro, P. M., 2005. On the spatial structure of coastal circulation off Newport, Oregon, during spring and summer 2001 in a region of varying shelf width. *J. Geophys. Res.*, 110, C10S06, doi:10.1029/2004JC002769.

Kosro, P.M., and J.D. Paduan, 2002. Shore-based mapping of ocean surface currents at long range using 5 MHz HF backscatter, *EOS, Trans. Am. Geophys. Union (abstract only), Paper OS21E-101, Ocean Sciences Meeting, Feb 2002*.

Kuebel Cervantes, B.T., and J.S. Allen, 2006. Numerical model simulations of continental shelf flows off northern California, *Deep Sea Res. Part II: Topical Studies in Oceanography*, 53 (25-26), 2956-2984, doi:10.1016/j.dsr2.2006.07.004.

Kurapov, A.L., G.D. Egbert, J.S. Allen, R.N. Miller, S.Y. Erofeeva and P.M. Kosro, 2003. The M2 internal tide off Oregon: Inferences from data assimilation. *J. Phys. Oceanogr.*, 33, 1733–1757.

Kurapov, A.L., J.S. Allen, G.D. Egbert, R.N. Miller, P.M. Kosro, M. Levine and T. Boyd, 2005a. Distant effect of assimilation of moored currents into a model of coastal wind-driven circulation off Oregon. *J. Geophys. Res.*, 110, C02022, doi:10.1029/2003JC002195.

Kurapov, A.L., J.S. Allen, G.D. Egbert, R.N. Miller, P.M. Kosro, M.D. Levine, T. Boyd, and J. A. Barth, 2005b. Assimilation of moored velocity data in a model of coastal wind-driven circulation off Oregon: Multivariate capabilities, *J. Geophys. Res.*, 110, C10S08, doi:10.1029/2004JC002493.

Kurapov, A.L., J.S. Allen, G.D. Egbert, R.N. Miller, 2005c. Modeling Bottom Mixed Layer Variability on the Mid-Oregon Shelf during Summer Upwelling. *J. Phys. Oceanogr.*, 35 (9), 1629-1649.

Lamb, K.G., 1997. Particle transport by nonbreaking, solitary internal waves, *J. Geophys. Res.* 102, 18641–18660.

Landry, M.R., and R.P. Hassett, 1982. Estimating the grazing impact of marine microzooplankton. *Mar. Biol., 67*, 283-288.

Landry, M. R. and B. M. Hickey, eds. 1989. *Coastal oceanography of Washington and Oregon*. Elsevier Oceanography Series 47, Elsevier, Amsterdam. 607 p.

Landry, M.R., J.R. Postel, W.K. Peterson and J. Newman, 1989. Broad-scale patterns in the distribution of hydrographic variables. In *Coastal Oceanography of Washington and Oregon*, M.R. Landry and B.M. Hickey (eds.), Elsevier Press, Amsterdam, pp. 1–41.

Lee, H-C., A. Rosati, and M.J. Spelman, 2006. Barotropic tidal mixing effects in a coupled climate model: Oceanic conditions in the Northern Atlantic. *Ocean Modelling*, 11, 464-477.

Legaard, K.R., and A.C. Thomas, 2006. Spatial patterns in seasonal and interannual variability of chlorophyll and sea surface temperature in the California Current, *J. Geophys. Res*., 111, C06032, doi:10.1029/2005JC003282.

Liu, A. K., 1988. Analysis of nonlinear internal waves in the New York Bight, *J. Geophys. Res.*, 93, 12317–12329.

Lueker, T.J., S.J. Walker, M.K. Vollmer, R.F. Keeling, C.D. Nevison, R.F. Weiss and H.E. Garcia, 2003. Coastal upwelling air-sea fluxes revealed in atmospheric observationsof O2/N2, CO2 and N2O. *Geophys. Res. Lett.*, doi:10.1029/2002GL016615.

Lynott, R. E. and O. P. Cramer, 1966: Detailed analysis of the 1962 Columbus Day windstorm in Oregon and Washington. *Monthly Weather Review*, **94**, 105-117. (Available online at http://docs.lib.noaa.gov/rescue/mwr/094/mwr-094-02-0105.pdf).

MacFadyen, A., B.M. Hickey and M.G.G. Foreman, 2005. Transport of surface waters from the Juan de Fuca eddy region to the Washington coast: Implications for HABs. *Cont. Shelf Res.,* 25, 2008-2021.

Mantua, N. J., S. R. Hare, Y. Zhang, J. M. Wallace, and R. C. Francis, 1997. A Pacific decadal climate oscillation with impacts on salmon, *Bull. Am. Meteorol. Soc*., 78, 1069–1079.

Marchesiello, P., J.C. McWilliams and A. Shchepetkin, 2003: Equilibrium structure and dynamics of the California Current System. *J. Phys. Oceanogr.*, 33, 753–783.

Margalef, R., 1978. Phytoplankton communities in upwelling areas. The example of NW Africa. *Oecologia Aquatica*, 3, 97–132.

McGowan, J. A., D. R. Cayan, and L. M. Dorman, 1998. Climate-ocean variability and ecosystem response in the northeast Pacific, *Science*, 281, 210–217.

McGowan, J. A., D. B. Chelton, and A. Conversi, 1996. Plankton pattern, climate and change in the California Current, Rep. 37, pp. 45–68, Calif. Coop. Ocean. Fish. Invest., Univ. of Calif., San Diego, Calif.

Michaels, A.F and M.W. Silver, 1988. Primary production, sinking fluxes and the microbial food web. *Deep-Sea Res. I,* 35, 473–490.

Muller-Karger, F.E., R. Varela, R. Thunell, R. Luerssen, C. Hu, and J.J. Walsh, 2005. The importance od continental margins in the global carbon cycle, *Geophysical Res. Lett., 32*, L01602, doi: 01029/02004GL021346.

Murphree, T., S.J. Bograd, F.B. Schwing, and B. Ford, 2003. Large-scale atmosphere–ocean anomalies in the northeast Pacific during 2002. *Geophys. Res. Lett.* 30, 8026. doi:10.1029/ 2003GL017303.

NDBC, 2008. NDBC 2007 Equipment Performance Summary**,** NDBC Technical Document 08-01. (Available online at https://www.fbo.gov/utils/view?id=7e1dccb040648bd090f657 1117538c9b)

NRC. 2007. Major Bottom Contact Fisheries in the Vicinity of the Regional Cabled Observatory off Oregon and Washington, Updated Report. Prepared by NRC, Seattle, WA for Fugro Seafloor Surveys, Inc., Seattle, WA. 18 April.

Neuer, S., and T.J. Cowles, 1994. Protist herbivory in the Oregon upwelling system. *Mar. Ecol. Prog. Ser., 113,* 147-162.

Oke, P., J.S. Allen, R.N. Miller, G.D. Egbert, and P.M. Kosro, 2002a. Assimilation of surface velocity data into primitive equation coastal ocean models, *J. Geophys. Res., 107*(C9), doi:10.1029/2000JC000511.

Oke, P.R., J.S. Allen, R.N. Miller, G.D. Egbert, J.A. Austin, J.A. Barth, T.J. Boyd, P.M. Kosro and M.D. Levine, 2002b. A modeling study of the three-dimensional continental shelf circulation off Oregon. Part I: Model-data comparisons. *J. Phys. Oceanogr., 32*, 1360–1382.

Oke, P.R., J.S. Allen, R.N. Miller and G.D. Egbert, 2002c. A modeling study of the three-dimensional continental shelf circulation off Oregon. Part II: Dynamical analysis. *J. Phys. Oceanogr.*, 32, 1383–1403.

Paduan, J.D. and I. Shulman, 2004. HF radar data assimilation in the Monterey Bay area, *J. Geophys. Res.*, 109(C7), doi:10.1029/2003JC001949.

Paduan, J.D., P.M. Kosro and S.M. Glenn, 2004. A national coastal ocean surface current mapping system for the United States, *Marine Technology Society Journal*, 38(2*)*, 102–108.

Pearcy, W.G., 1992. *Ocean Ecology of North Pacific Salmonids*. University of Washington Press, Seattle, WA, 179 pp.

Peterson, W. T. and F. B. Schwing, 2003. A new climate regime in northeast Pacific ecosystems. *Geophys. Res. Lett., 30*(17), 1896, doi:10.1029/2003GL017528.

Peterson, W.F., C.B. Miller, and A. Hutchinson, 1979. Zonation and maintenance of copepod populations in the Oregon upwelling zone. *Deep-Sea Res., 26*, 467-494.

Pinkel, R., W. Munk, P. Worcester, B.D. Cornuelle, D. Rudnick, J. Sherman, J.H. Filloux, B.D. Dushaw, B.M. Howe, T.B. Sanford, C.M. Lee, E. Kunze, M.C. Gregg, J.B. Miller, J.M. Moum, D.R. Caldwell, M.D. Levine, T. Boyd, G.D. Egbert, M.A. Merrifield, D.S. Luther, E. Firing, R. Brainard, P. Flament and A.D. Chave, 2000. Ocean mixing studied near Hawaiian Ridge, *Eos Trans. AGU*, 81, 545 and 553.

Pullen, J.D. and J.S. Allen, 2000. Modeling studies of the coastal circulation of Northern California: shelf response to a major Eel river flood event, *Cont. Shelf Res.*, 20, 2213–2238.

Pullen, J.D. and J.S. Allen, 2001. Modeling studies of the coastal circulation off northern California: Statistics and patterns of wintertime flow. *J. Geophys. Res.*, 106, 26959–26984.

Raible C.C., Blender R, 2004. North hemisphere midlatitude cyclone variability in GCM-simulations in different ocean representations. *Climate Dynamics* 22:239–248

Read, Wolf, “The Great Coastal Gale of Dec 1-3, 2007”, Journal Notes, 2007. (Available online at http://www.climate.washington.edu/stormking/December2007.html)

Read, Wolf, “The "Big Blow" of Columbus Day 1962”. (Available online at http://www.climate.washington.edu/stormking/October1962.html)

Rehder, G., R.W. Collier, K. Heeschen, P.M. Kosro, J. Barth and E. Suess, 2002. Enhanced marine CH4 emissions to the atmosphere off Oregon caused by coastal upwelling. *Global Biogeochemical Cycles*, 16(3), 1081, doi:10.1029/2000GB001391.

Rhodes, R.C., H.E. Hurlburt, A.J. Wallcraft, C.N. Barron, P.J. Martin, E.J. Metzger, J.F. Shriver, D.S. Ko, O.M. Smedstad, S.L. Cross and A.B. Kara, 2001. Navy real-time global modeling systems. *Oceanography*, 15(1), 29–43.

Risien, C.M., and D.B. Chelton, 2006. A satellite-derived climatology of global ocean winds, *Remote Sensing of Environment*, 105 (3), 221-236 doi:10.1016/j.rse.2006.06.017.

Ruggiero, P., P.D. Komar, J.C. Allan, 2010. Increasing wave heights and extreme value projections: The wave climate of the U.S. Pacific Northwest. *Coastal Engineering*, 57 (5), 539-552, DOI: 10.1016/j.coastaleng.2009.12.005.

Sackmann, B., and M.J. Perry, 2006. Ocean color observations of a surface water transport event: Implications for Pseudo-nitzschia on the Washington coast. *Harmful Algae* 5, 608-619.

Sandstrom, H. and N.S. Oakey, 1995. Dissipation in internal tides and solitary waves, *J. Phys. Oceanogr.*, 25, 604–614.

Schwing, F.B., D.M. Palacios, and S.J. Bograd. 2005. El Niño impacts on the California Current ecosystem. U.S. CLIVAR Newsletter, Vol. 3, No. 2, 5-8.

Shanks, A.L., 1988. Further support for the hypothesis that internal waves can transport larvae of invertebrates and fish onshore, *Fish. Bull. U.S.*, 86, 703–714.

Sherr, B.F., and E.B. Sherr, 2002. Microzooplankton distribution in relation to phytoplankton community succession in the upwelling ecosystems off Oregon and Northern California. *EOS, Trans. Am. Geophys. Union, 83*, 200.

Shulman I., J.C. Kindle, S. deRada, S.C. Anderson, B. Penta and P.J. Martin, 2004. Development of a hierarchy of nested models to study the California Current System. *Estuarine and Coastal Modeling*, Proceedings of the 8th International Conf., Edited by Malcom Spalding and H. Lee Butler, 74–88.

Small, L.F. and D.W. Menzies, 1981. Patterns of primary productivity and biomass in a coastal upwelling region. *Deep-Sea Res.*, 28, 123–149.

Smith, R.L., A. Huyer and J. Fleischbein, 2001. The coastal ocean off Oregon from 1961 to 2000: is there evidence of climate change or only of Los Niños? *Prog. Oceanogr., 49*, 63–93.

Spitz, Y.H., P.A. Newberger and J. S. Allen, 2003. Ecosystem response to upwelling off the Oregon coast: Behavior of three nitrogen-based models. *J. Geophys. Res.*, 108(C3), 3062, doi:10.1029/2001JC001181.

Spitz, Y.H., J.S. Allen, and J. Gan, 2005. Modeling of ecosystem processes on the Oregon shelf during the 2001 summer upwelling, *J. Geophys. Res.*, 110, C10S17, doi:10.1029/2005JC002870.

SSEA, 2011. Site-Specific Environmental Assessment for the National Science Foundation-Funded Ocean Observatories Initiative (OOI). Prepared by TEC Inc., Bainbridge Island, WA for the National Science Foundation. January 2011.

Steinback C., S. Kruse, C. Chen, J. Bonkoski, T. Hesselgrave, N. Lyman, L. Weiss, A. Scholz, and E. Backus, 2010. Supporting the Oregon Territorial Sea Plan Revision: Oregon Fishing Community Mapping Project. Prepared by Ecotrust, Portland, OR. 15 November 2010.

Strom, S.L., M.A. Brainard, J.L. Holmes, and M.B. Olson, 2001. Phytoplankton blooms are strongly impacted by microzooplankton grazing in coastal North Pacific waters. *Mar. Biol., 138*, 355-368.

Strub, P.T. and C. James, 2000. Altimiter-derived variability of surface velocities in the California Current System: 2. Seasonal circulation and eddy statistics. *Deep-Sea Res. II*, 47, 831–870.

Strub, P. T., and C. James, 2003. Altimeter estimates of anomalous transports into the northern California Current during 2000– 2002, *Geophys. Res. Lett.,* 30(15), 8025, doi:10.1029/2003GL017513.

Strub, P.T., C. James, A.C. Thomas, and M.R. Abbott, 1990. Seasonal and nonseasonal variability of satellite-derived surface pigment concentrations in the California Current. *J. Geophys. Res., 95*, 11501-11530.

Suess, E., and 19 others, 2001. Seafloor hydrates at Hydrate Ridge, Cascadia margin, in: Natural gas hydrates: occurrence, distribution, and detection, C. Paull and W. Dillon, eds, AGU monograph 91.

Swartzman, G., B. Hickey, M. Kosro and C. Wilson, 2005. Poleward and equatorward currents in the Pacific Eastern Boundary Current in summer 1995 and 1998 and their relationship to the distribution of euphausiids. *Deep Sea Res. II*, 52 (1-2), 73-88, doi: 10.1016/j.dsr2.2004.09.028

Thomas, A.C., P.T. Strub and P. Brickley, 2004: Anomalous satellite-measured chlorophyll concentrations in the northern California Current in 2001–2002. *Geophys. Res. Lett*., *30(15),* 8022, doi:10.1029/2003GL017409.
Torgrimson, G. M., and B. M. Hickey, 1979: Barotropic and baroclinic tides over the continental slope and shelf off Oregon. *J. Phys. Oceanogr*., 9, 945–961.

Torres, M.E., K. Wallmann, A.M. Trehu, G. Bohrmann, W.S. Borowski and H. Tomaru, 2004. Gas hydrate dynamics at the Hydrate Ridge southern summit based on dissolved chloride data, *Earth and Plan. Sci. Let.*, 226, p. 225–241.

Trainer, V.L. and J.C. Wekell. 2000. Red Tides Newletter: The cost of harmful algal blooms on the West Coast, autumn 2000. Northwest Fisheries Science Center and Washington Sea Grant (eds.), 8 pp.

Trainer, V.L., N.G. Adams, B.D. Bill, C.M. Stehr, J.C. Wekell, P. Moeller, M. Busman and D. Woodruff, 2000. Domoic acid production near California coastal upwelling zones, June 1998. *Limnology and Oceanography*, 45, 1818–1833.

Trainer, V.L., N.G. Adams, and J.C. Wekell, 2001. Domoic acid-producing *Pseudo-nitzschia* species off the U.S. west coast associated with toxification events. In: Hallegraeff G.M., Blackburn S.I., Bolch CJ, Lewis RJ (eds) Harmful algal blooms 2000. IOC-UNESCO, Paris, pp 46–48

Trainer, V.L., R. Horner and B. M. Hickey, 2002. Biological and physical dynamics of domoic acid production off the Washington USA coast. *Limnology and Oceanography*, 47(5), 1438–1446.

Trainer, V.L., M.L. Wells, W.P. Cochlan, C.G. Trick, B.D. Bill, K.A. Baugh, B. F. Beall, J. Herndon, and N. Lundholm, 2009. An ecological study of a massive bloom of toxigenic Pseudo-nitzschia cuspidata off the Washington State coast. Limnol. Oceanogr., 54(5), 2009, 1461-1474, DOI: 10.4319/lo.2009.54.5.1461

Trehu, A.M., Bohrman, G., Rack, F.R., Collett, T.S., D.S. Goldberg, P.E. Long, A.V. Milkov, M. Riedel, P. Schultheiss, M.E. Tores**,** N.L. Bangs, S.R. Barr, W.S. Borowski, G.E. Claypool, M.E. Delwiche, G.R. Dickens, E. Gracia, G. Guerin, M. Holland, J.E. Johnson, Y-J. Lee, C-S. Liu, X. Su, B. Teichert, H. Tomaru, M. Vanneste, M. Watanabe and J.L. Weinberger, 2004. Three-dimensional distribution of gas hydrate beneath southern Hydrate Ridge: constraints from ODP Leg 204, *Earth and Plan. Sci. Let.*, 222, p. 845–862.

Tully, J.P., 1942. Surface non-tidal currents in the approaches to Juan de Fuca strait. *Journal of the Fisheries Research Board of Canada, 5,* 398–409.

Tweddle J.F., P.G. Strutton, D.G. Foley, L. O'Higgins, and coauthors (2010) Relationships among upwelling, phytoplankton blooms, and phycotoxins in coastal Oregon shellfish. Mar Ecol Prog Ser 405:131-145

Wheeler. P.A., A. Huyer and J. Fleischbein, 2004. Cold halocline, increased nutrients and higher chlorophyll off Oregon in 2002. *Geophys. Res. Lett*., 30(15), 8021, doi:10.1029/GL017395.